A Knowledge Based Approach for Design Optimisation of Ultrasonic Transducers and Arrays

By

Sivaram Nishal Ramadas

In the fulfillment of the requirement
for the degree of Doctor of Philosophy.

Centre for Ultrasonic Engineering
Department of Electrical and Electronic Engineering
University of Strathclyde

Declaration

I declare that this thesis embodies my own research work and that it was composed by myself. Where appropriate, I have made acknowledgments to the work done by others.

Sivaram Nishal Ramadas

Copyright

Acknowledgement

There is a saying in my native language "Matha, Pitha, Guru, Theyvam", which literally translates to "Mother, Father, Teacher, and then God". My simple upbringing has taught me, to value the education and teaching I got, over even my religious faith.

On that note, I would like to thank my family, for their never ending support and encouragement, and my supervisor Professor. Gordon Hayward, Head of Centre for Ultrasonic Engineering (CUE) at University of Strathclyde for providing me with the opportunity to work within CUE, and specially his guidance, and support throught the duration of this work.

Thanks should also go to collegues at CUE who made this research not only possible but also worthwhile and enjoyable. A special note of appreciation to my other supervisor Dr. Richard O'Leary for helping me out during the crisis times; Dr. Tony Mulhollond for help with modelling; Tommy, Grant, and Alex for manufacturing devices for this research; Alexandre Troge for making all those matching layers; Victor Murray and David Robertson for their input for designing the expert system; Andy in modelling arrays; and; Dr. Gareth Pierce and Prof. Keith Worden for advise on optimisation techniques; Lynn and Sylvia for all their help and support.

This research was both supported and carried out using the excellent facilites provided by CUE, at the University of Strathclyde.

Dedicated to my parents

Table of Contents

Abstract

A new knowledge-based, interactive tool for design and optimisation of ultrasonic transducers and arrays is proposed. An intelligent rule based expert system front end is used to capture domain specific expert knowledge and guide the design and optimisation process. The design optimisation is carried out using a genetic algorithm based search procedure. A number of analytical models have been developed to simulate a variety of thickness mode transducer structures, including multi-layers incorporating inversion, parallel and independent configurations. Preliminary investigation is carried out to configure analytical models to be directly compatible with electronic simulation environments such as PSPICE, enabling design optimisation of signal to noise ratio, bandwidth and efficiency, with respect to transducer structure and constituent materials. A selection of design optimisation examples are provided to illustrate the usefulness of the proposed approach. The results are shown to compare very favourably with experiments and serve to demonstrate that the knowledge-based approach is a very efficient and attractive alternative. It may be implemented for design and optimisation of any kind of transducer system, subject to the availability of an appropriate simulator.

List of Symbols

The most common symbols and abbreviations used in this thesis are listed below. Less common or rarely occuring terms are defined within the text.

1-D	One dimensional
A_f	Particle displacement within a layer in forward direction
AI	Artificial intelligence
A_b	Particle displacement within a layer in backward direction
A_R	Area of the transducer surface
BFIL	Back face inversion layer
COMPD	In-house 1-3 piezoelectric composite modelling tool
C_0 or C_t	bulk or static capacitance of the transducer
C	Charge
D	Electrical displacement
E	Electrical field strength
$\hat{E}_t$	mean square voltage of thermal noise
$\hat{E}_n$	is the voltage noise spectral density
expert1	Open source rule based deduction engine
fb	Fractional bandwidth (3dB or 6 dB)
f1, f2	Lower and upper cutoff frequencies
fp	Peak frequency
F, B	Forward and backward travelling force component in a layer
FEA	Finite element analysis
FFT	Fast Fourier Transformation
FFIL	Front face inversion layer
F_{meq}, V_{eeq}	Voltage parameter used in Thevenin equivalent transducer model
GA	Genetic algorithm
gatool	Genetic algorithm optimisation toolbox in MATLAB
GUI	Graphical user interface
h	Piezoelectric constant relating the stress and charge,
IL(T)	Inversion layer (transducer)
IFFT	Inverse Fast Fourier Transformation
i	Imaginary unit in a complex number
I_{DC}	is the direct current in A
$\hat{I}_n$	is the current noise spectral density
I_{sh}	is the RMS value of Shot noise
j	Layer number

K_F	Front face reverberation factor
K_B	Back face reverberation factor
k	Boltzmann's constant $= 1.38 \times 10^{-23}$ J/K
K	wavenumber
KFI(s)	Reverberation factor in the forward loop
KBI(s)	Reverberation factor in the feedback loop
L	Transducer (overall) active layer thickness
l	Normal layer thickness in an IL device
l'	Inversion layer thickness in an IL device
LSM	Linear systems model
M	Mass
MATLAB,SIMULINK	Commercial programming environment
NDE	Non destructive evaluation
PSPICE,LTSPICE	Commercial circuit simulation softwares
PZT	Lead Zirconate Titanate
PVDF	Polyvinylidene Fluoride
q	is the electronic charge 1.59×10^{-19} C
Q	Net charge residing on either of the surfaces
Q(s)	the net charge residing on either of the surfaces
R	resistance or real part of the conductor's impedance
R(t,f)	distance from the transducer point t to f
$P_r(f)$	relative pressure at the field point f
SNR	the overall system signal to noise ratio
SLPS	A comerical interface to integrate MATLAB and PSPICE software
s	Complex Laplace domain variable
T	temperature of the conductor in degrees Kelvin (K)
T	time taken by the acoustic wave to travel across the transducer thickness
t	transit time to cross a normal layer in ILT
t'	transit time to cross the inversed layer in ILT
T_F, T_B	Transmission coefficient of waves of force stricking the front and back face of a transdcuer
U^F, U^B	Systems matrix describing the acoustic wave transmission in front face and backface layers (passive)
v	Wave velocity in thickness direction
V_t	Voltage across the transducer electrode
V_E	Transducer drive voltage source
V(s)	Overall voltage across the transducer
V_{O-C}	is the open circuit voltage response

X	additional term to include effect of an inversion layer in a systems model
$Y(s)$	the operational admitance of the equivalent
$\hat{Y}$	Elastic constant at constant electrical displacement or the electrical field and mechanical strain measured under constant electrical displacement
Y_E	Feedback admittance, resulting in current flow out of the transducer electrical circuit at the transducer input)
Z_E	Arbitrary electrical load across a transducer
Z	Acoustic impedance
Z_{meq}, Z_{eeq}	Impedance parameter used in Thevenin equivalent transducer model
Z_C or Z_T	Acoustic impedance of the transducer.
$Z_T(s)$	Electrical impedance funciton of a transducer
Z_{IN}	Device input impedance
Δf	noise bandwidth of the measuring system in hertz
Γ	Tensile or compressive stress
ρ	Material density
λ	wavelength
ξ	Mechanical displacement in any point x within the transducer
ϵ	Relative permittivity (measured under conditions of constant, or zero, strain)

Chapter 1

Introduction

This chapter describes the main motivation of the thesis, which is to create an advanced tool for design and optimisation of application specific ultrasonic transducers and arrays. A summary of state of the art and description of deficiencies in current design approaches is presented, along with a brief description and justification of the proposed approach. A clear statement of the aims, objectives and contributions arising from the thesis along with a brief summary of the thesis contents is also provided.

1.1 Existing modelling techniques and required improvements

Ultrasonic transducers and arrays are used routinely in a diverse range of applications, including biomedicine imaging and therapy, non-destructive testing, sonar and industrial process monitoring. Successful and cost effective design of a piezoelectric transducer or array can be problematic, for a variety of well established reasons, and is reliant traditionally on practical experience, supplemented by performance

evaluation via computer modelling. As technological requirements have advanced, transducer complexity has increased dramatically, making intuitive design very difficult. Consequently, new improved design optimisation approaches are essential to keep pace with the increasingly stringent technological requirements.

1.2 Aims and contributions of the thesis

1.2.1 Aims of thesis

The primary aim of the thesis is to build a tool to help design and optimisation of complex application specific ultrasonic transduction systems. To achieve the above aim, a knowledge based approach for design and optimisation of ultrasonic transducers and arrays is proposed. In implementing this new strategy, the objective is to overcome some of the main difficulties in designing ultrasonic systems. Particularly, the domain specific expertise required in design and manufacture of ultrasonic systems, and design optimisation issues, taking into account the uncertainties involved in a manufacturing process. Specifically, the project involves developing a software tool prototype, which can be divided into the following key areas:

- Develop a number of analytical models to simulate a variety of thickness mode transducer structures, including multi-layers incorporating inversion, parallel and independent configurations

- Designing a rule based expert system to capture expert knowledge and guide the design and optimisation process and also to form an intelligent front-end for the software program by permitting interactive and flexible user dialogue.

- Implement a suitable optimisation or search procedure for design optimisation of complex transducer systems

2

- Propose ways to integrate the transducer models with electronic simulation environments such as PSPICE and LTSPICE, enabling design optimisation of signal to noise ratio

- A graphical user interface to unify all the key aspects of the project

1.2.2 Contribution to the field of ultrasonics

The key novelty in this research is the implementation of a suite of "design friendly" simulation software, bringing together an expert knowledge, optimisation programs, mathematical transducer models, material database and external commercial circuit simulation programs in an efficient way. Such an approach is extremely valuable to tailor individual device performance characteristics to specific operational requirements for transducer systems operating across many different application areas. As the proposed transducer design software encompass many key modular sections, the contributions made by the work described in this thesis lie in these different areas.

1.2.2.1 Modelling ultrasonic transducers

During the course of this work, various computer programs were written to simulate a wide range of transducer configurations. This work has also resulted in a new type of device known as the back face inversion layer (BFIL) transducer, possessing an extremely wide bandwidth and for which the author formulated the fundamental theory of operation. Analytical models depicting various configurations, including the position of the inverted lattice layer and multiple matching layers were developed from first principles. These new inversion layer models are verified extensively during the course of this thesis using both computer simulation (using finite element modelling) and experimental comparison. Also, investigations were carried out to extend the linear transducer models used in the proposed software to account for

loss within both the active and passive layers in the device. The other notable contribution arising from the modelling section is the new dimensional analysis based approach, to improve the accuracy of the existing matrix inversion method, to simulate conventional thickness mode transducers with multiple active and passive layers in a thickness mode transducer configuration.

A method is presented which permits the development of a passive matching layer design module in the proposed design software based on analogue filter design techniques. This facilitates efficient design of thickness mode transducers with multiple passive layers at the front and/or back face, resulting in extremely desirable wide bandwidth characteristics. Also, a new experimental procedure was proposed to validate bond quality, during passive layer manufacture in a transducer system design.

1.2.2.2 Noise analysis applied to transducer system design

A preliminary investigation into various approaches to analyse the noise performance of a transducer and its associated electrical interface is presented. A computer program was also developed to automatically export transducer model as an electrical equivalent parameter, to be used within commercial circuit simulation software (such as PSPICE and LTSPICE). Such an approach is extremely valuable for designing electrical circuits that complement the transducer system.

1.2.2.3 Transducer design optimisation

An adaptive optimisation process, using precise component parameters (experimental and materials database) and a genetic algorithm based concept are formed as a basis of design optimisation in this thesis. Using such precise data, the optimisation process can be controlled more closely than trial-and-error which is based mostly on experience. In addition to an extensive materials database used in transducer design

optimisation, the proposed transducer design software is integrated to the material generator (which enables modelling passive layers made up of two constituent materials) and an existing in-house software program to model 1-3 composite piezoelectric material parameters.

1.2.2.4   Expert system interface

A significant innovation in the proposed tool is incorporating an expert system in the front end interface. This is particularly useful in capturing expertise from multiple sources, and in sharing the resulting expert knowledge to help non-experts to reach scientifically supportable conclusions.

1.3   A summary of the thesis contents

The thesis is grouped under several chapters:

- Chapter 2 consists of an overview of the proposed design tool.

- Chapter 3 presents a review of state of the art and description of the modelling system. In addition to existing modelling approaches, detailed descriptions of the new mathematical models developed along the duration of this thesis are also presented in this chapter.

- Details of the analogue filter design approach used to solve the mechanical impedance matching problem in a transducer system is presented in Chapter 4.

- Chapter 5 presents a detailed description of the major noise mechanisms within a transducer system and introduces some of the common terminology used in noise analysis. This is followed by a preliminary investigation of different strategies to interface commercial circuit simulation environments, such as

PSPICE and LTSPICE, with the proposed transducer design tool. A selection of simulation results are presented to highlight the feasibility of such an integrated approach.

- Chapter 6 is divided into two main sections. Firstly, a description of the design of the expert system and control of the optimisation process is presented. The second section details the genetic algorithm approach, employing the design optimisation.

- A selection of design examples are presented in Chapter 7, to demonstrate the feasibility of such an integrated design approach. Firstly, a straight forward conventional thickness mode transducer design is considered. This is followed by the design and manufacture of a more complex inversion layer transducer consisting of two opposing zones of polarisation along its thickness direction. Finally, an example of the optimisation of a 1D sparse array configuration, to achieve required field characteristics with a minimum number of elements, is presented.

- Chapter 8 presents the summary of the research carried out so far and suggestions for future work.

1.4   Publications arising from this thesis

Journal Publications:

1. Estanbouli Y, Hayward G, Ramadas S N and Barbenel J C, "A Block Diagram Model of the Thickness Mode Piezoelectric Transducer Containing Dual, Oppositely Polarised Piezoelectric Zones", *IEEE Trans. on Ultrasonics, Ferroelectrics and Frequency Control*, Volume 53, Issue 5, May 2006, Page(s):1028 - 1036

2. Mulholland A J, O'Leary R L., Ramadas S N., Parr A, Troge A, Pethrick R A and Hayward G, "A Theoretical Analysis of a Piezoelectric Ultrasound Device with an Active Matching Layer", *Journal of Ultrasonics*, Volume 47, 2007, Page(s): 102-110.

3. Mulholland A J, Ramadas S N, O'Leary R L, Parr A, Troge A, Pethrick R A and Hayward G, " Enhancing the performance of piezoelectric ultrasound transducers by the use of multiple matching layers", *IMA Journal of Applied Mathematics*, 73 , 936 - 949, 2008.

4. Ramadas S N, Tweedie A, and Hayward G; "A Rule Based Design Optimisation Tool for Ultrasonic Transducers and Arrays", *Ultrasonics Journal*, 2009 (in preparation)

Conference Publications:

1. Ramadas S N, O'Leary R L, Mulholland A J, MacKintosh A R, Troge A, Pethrick R A, and , Hayward G, " Efficient wideband piezoelectric transduction: methodologies, materials, and design", *Anglo-French Physical Acoustics Conference 2009*, 18 - 22 January 2010, UK. (submitted)

2. Ramadas S N, Dziewierz J, O'Leary R L, Gachagan A, " Ultrasonic sensor design for NDE application: design challenges and considerations", *NDE 2009*, 10-12 Dec 2009 Tiruchi, India. (accepted)

3. Ramadas S N, O'Leary R L, Mulholland A J, Hayward G, MacKintosh A R, Troge A, and Pethrick R A, "Tapered transmission line technique based graded matching layers for thickness mode piezoelectric transducers", *IEEE Ultrasonic Symposium 2009*, 20-23 Sep 2009, Italy.

4. Ramadas S N, Tweedie A, and Hayward G; "A Rule Based Design Optimisation Tool for Ultrasonic Transducers and Arrays", *International Congress on*

Ultrasonics, Vienna, 2007.

5. Ramadas S N, Hayward G, O' Leary R L, Murray V, McCunnie T, Robertson D, Murray V, Mulholland A J, and Trogé A; "A Three-Port Acoustic Lattice Model for Piezoelectric Transducers Containing Opposing Zones of Polarization", *Proceedings of IEEE Ultrasonic Symposium*, Vancouver, Canada, Oct 2006, Pages(s):1899 - 1902

6. Ramadas S N, and Hayward G; "Knowledge based approach for design optimization of ultrasonic transducers and arrays", *Proceedings of IEEE Ultrasonic Symposium*, Rotterdam, The Netherlands, 18-21 Sept. 2005, Page(s):2247 - 2250

7. Estanbouli Y, Hayward G, Ramadas S N, and Barbenel J C; "A linear systems model of the thickness mode piezoelectric transducer containing dual piezoelectric zones", *Proceedings of IEEE Ultrasonic Symposium*, Montreal, Canada, 23-27 Aug. 2004, Volume 3, Page(s):1938 - 1941

Chapter 2

The proposed software structure

This chapter presents an overview of the transducer design tool. The key areas in the software architecture are identified and their interdependent nature is highlighted. In addition, the need for a graphical user interface and how it is implemented in the present software is described. Finally, the selection of MATLAB as the core implementation tool is justified.

2.1   Overview of the software

Fig. 2.1 shows the high level overview of the design tool. The central components of the transducer design tool is the transducer models. A number of models have been developed to simulate a variety of thickness mode transducer structures, including multi-layers incorporating inversion, parallel and independent configurations, and these are presented in detail in Chapter 3. Each is configured to be directly compatible with electronic simulation environments such as PSPICE [78], enabling design optimisation of signal to noise ratio, bandwidth and efficiency, with respect to transducer structure and constituent materials. A rule based expert system is
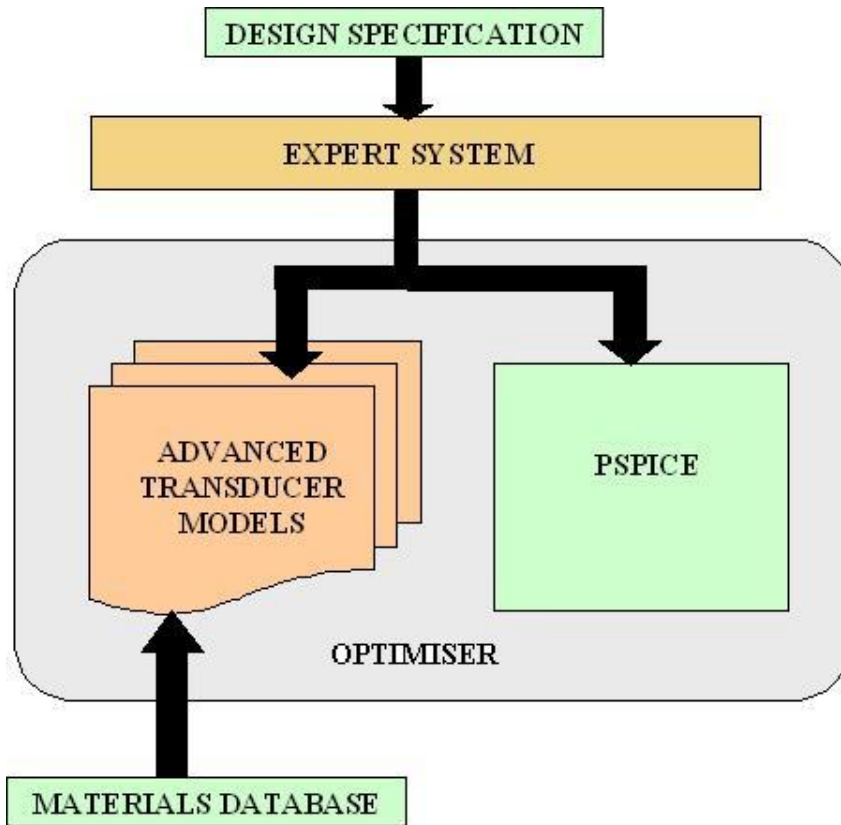
Figure 2.1: High level overview of the proposed transducer design tool

used to capture expert knowledge and guide the design and optimisation process. The expert system thus forms an intelligent front-end for the software program by permitting interactive and flexible user dialogue. The expert system also constrains the optimiser by identifying the key parameters. The optimiser works within this boundary to refine model parameters and improve system performance. The design optimisation is carried out using a genetic algorithm [1]–[6] based search procedure. The key areas in the software architecture are now introduced.

2.1.1 Advanced transducer modelling

The successful design of a piezoelectric transducer or array is often very difficult, owing to its complex interaction with the electrical load, mechanical load and many other influencing factors. For illustration purpose, mainly thickness mode devices are considered within the scope of this research. However, due to the modular nature of the software architecture, the software could be extended easily, subject to the availability of appropriate simulators, to include other types of transducer, such as electrostatic devices. Thickness mode ultrasonic transducers can be simulated in many ways, ranging from electro-mechanical equivalent circuits [7]–[9], one dimensional analytical models [11], systems block diagrams approach [14], through to relatively sophisticated finite element methods [16]. The details of some common modelling techniques and their merits will be discussed in detail in Chapter 3. In the software prototype, mostly linear systems models were considered over other models, as they offer rapid computational efficiency (allows fast calculation of system transfer function using vector operations in MATLAB), making them ideal for multiparameter optimisation problems. Also, new models are developed for a more complex inversion layer (IL) transducer, a multi layered device, having regions of opposite polarisation along the thickness direction [30], [31]. All the models employed in the design tool are based on the fundamental 1-D piezoelectric equations and the description of their mathematical formulation is presented in Chapter 3. Consequently, the central part of the software package is a collection of comprehensive thickness mode transducer models, which are capable of simulating the following:

- transmit, receive, and pulse-echo modes of operation

- complex transducer configurations including piezoelectric composites, stacked arrays, and inversion layer (IL) devices

- the effects of multiple matching and backing layers

11

- series, independent and parallel electrical excitation scenarios

- array transducer design and optimisation

Unlike conventional design tools, the key advantage of the proposed approach is that the transducer models receive input from a variety of sources. The knowledge base for application specific expert knowledge, design requirements from user input, materials properties from a database, electrical circuit information from an industry standard source, and finally the optimiser to work within this boundary to achieve or improve the required specification. Figure 2.2 shows the general structure.
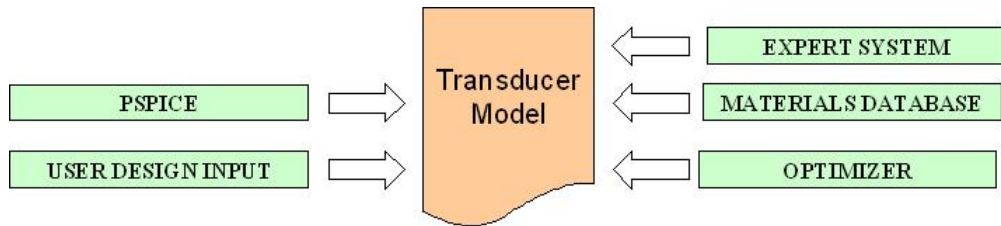
Figure 2.2: Schematic diagram of inputs for the transducer model

2.1.2 Design Optimisation Challenges and Knowledge Based User Interface

Ultrasonic transducer and array design optimisation is a multidimensional problem, involving many key parameters. The optimum setting of one parameter may depend on the exact setting of other parameters, making interactions between parameters equally important. This makes brute force, methodical search inefficient and almost impossible in many scenarios [2]-[6]. New approaches are needed to overcome key challenges faced by such optimisation problems. The proposed methodology uses an expert system [46]-[48] as a consultation system to provide recommendations during the design and optimsation process. Essentially, the expert system is used to constrain the optimisation process on the 'first cut' design for the desired application.

An expert system, also known as a knowledge based system, is a branch of Artificial Intelligence (AI) that uses human knowledge to solve problems [46]. The expert system program is used to give advice and reach decisions in the light of evidence provided in much the same way as human expert would be consulted. From a programming point of view, the problem-solving capability of an expert system program stems from its domain knowledge (i.e. rules and facts), combined with numerical calculation and reasoning strategies to arrive to a conclusion. Expert systems are particularly useful in applications where it is necessary to represent heuristics and uncertain information into a program, and by doing so be able to reason under uncertainty and explain their reasoning and results. The main advantages of using an expert system based approach include, but are not limited to the following:

- hold and maintain significant levels of information and centralise the decision making process in a software program

- increased distribution of expert knowledge from a wide range of sources (not necessarily multiple human experts, but also other sources such as books, and publications)

- provide reliable, fast and consistent results or advice for repetitive decisions, processes and tasks

Although significantly advantageous in many respects, limitations of expert systems may arise through the lack of human 'common sense' and creative responses needed in some decision making. Also, another key challenge is to capture a domain expert's knowledge, as in most cases the experts will not always be able to explain their logic and reasoning as a simple rule.

A modified version of expert1 [52], an open source, deduction engine code written in MATLAB, is used to build an intelligent rule based expert system front end to the

13

design tool. The primary task of the knowledge based user interface is to request information from the user, outputing intermediate and final results. Input to the expert system is also acquired from additional sources such as material databases and other simulation programs. Rule based programming allows knowledge to be represented as heuristics, or rules of thumb, which specify a set of actions to be performed for a given situation. A rule based knowledge representation is chosen primarily because of its similarity to human cognitive processes and its modular nature, which makes it easy to encapsulate knowledge and expand the expert system by incremental development.

A typical expert system has an architecture as shown in Fig. 2.3. Internally, it integrates a knowledge base that stores the encoded problem specific knowledge, and an inference engine that implements the reasoning mechanism and controls the interview process. The user supplies information (or facts) and receives expert advice in return. A detailed description of each sub-block in Fig. 2.3, their implementation, and knowledge engineering approach is presented in more detail in Chapter 6.

As previously mentioned, the majority of transducer engineering design problems are multidimensional in nature, often involving several parameters (some of which are highlighted in Figure 2.4) and a high degree of interaction between these parameters. To develop a full 'equation of state' to describe such a complex design process, to describe the cause and effect relationship of each component in a transducer assembly is often not possible. The optimisation problem is to choose the best values for all of these parameters, so that any desired performance is achieved. Some of the qualities of a piezoelectric transducer system, desirable for most applications, are listed below,

- improved operational bandwidth

- decrease ringing of impulse response

- increase peak amplitude of impulse response

- or optimally, all of the above
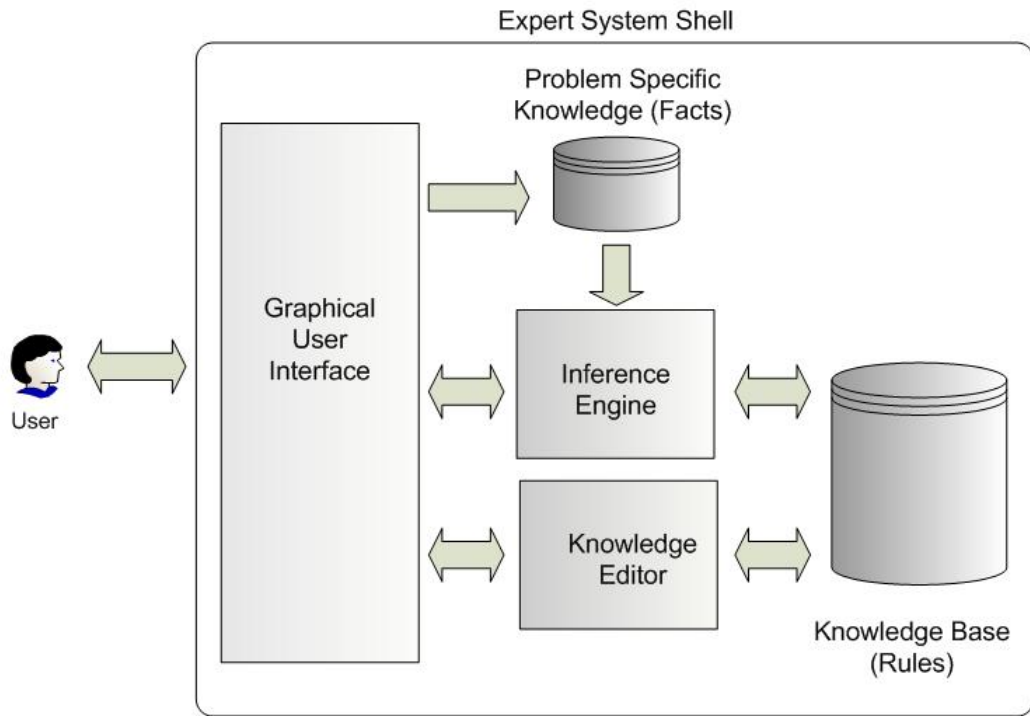
Figure 2.3: A typical expert system architecture

Consider a straightforward conventional thickness mode transducer design process. Typically, the specific acoustic impedance (product of material density and longitudinal wave velocity) of a PZT (Ferroperm, Kvistgard, Denmark), a common piezoelectric material, is approximately 33 MRayl. Ideally, the specific acoustic impedance of any backing block chosen should match with that of the ceramic, and also be very lossy in nature, so that there is no reflection returning from the backing block into the ceramic. However, if the transducer ceramic and backing have high impedance values compared to the mechanical load at the front face of the transducer, such as water or human tissue, the energy transmitted into the front medium is considerably less compared to that transmitted into the backing block, making the device less efficient. So, additional matching layers should be added between the
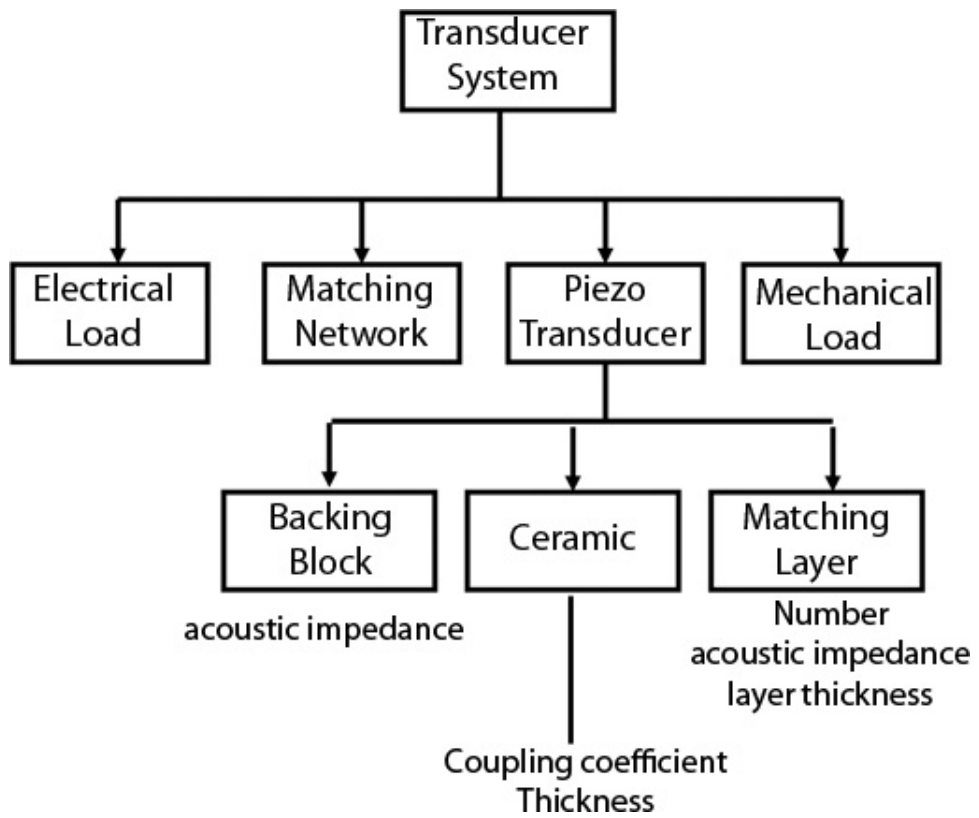
Figure 2.4: A sample design optimisation problem, highlighting key parameters that affect overall system performance

transducer and the mechanical load medium to improve the relative energy transfered into the load medium. The classical approach is to use one (or two) quarter wavelength matching layers, with acoustic impedance equivalent to the geometric mean of the acoustic impedance of the ceramic and the mechanical load medium [17]–[19]. However, such a quarter wavelength approach is not optimum, especially when the transducer is required to operate over a wide frequency range. Precaution should also be taken in selection of ceramic and matching layer geometry, undesirable aspect ratios can cause unwanted resonances in the matching layer and degrade the transducer performance considerably. Another important aspect that affects the design is the electrical impedance matching. Electrical tuning elements are typically placed between the coaxial cable and transducer to promote power transfer. Even in the case of designing a relatively straight forward thickness mode transducer, the design procedure is complex, especially over wider frequency bands. The design problem becomes more demanding in the case of complex transducer configurations such as stacked thickness mode devices and arrays, and clear strategies are required for reliable, fast and consistent design and manufacture of such devices. The proposed design software uses a genetic algorithm based search procedure to perform optimisation. The details of optimsation procedure is explained in Chapter 6.

2.1.3   Integration with commercial circuit design packages

PSpice A/D electric circuit simulator (hereafter abbreviated "PSPICE") from Cadence Design Systems, is now an industry standard for circuit simulation. It facilitates many forms of analysis in both the time and frequency domains. The availability of an extensive device library in PSPICE provides a very powerful platform for optimisation of the transducer electrical interface. Consequently, PSPICE can be employed in the efficient design of matching circuitry and critically, preamplifier electronics that maximize transducer signal to noise ratio. Also, PSPICE can

17

be used to investigate distortions in a system as effectively as a spectrum analyser. Accordingly, the transducer simulation sections of the software were constructed for compatibility with PSPICE. This facilitates the simulation of complex excitation and reception electronics and employs this knowledge in the overall transducer model, along with the transducer and its materials. Details of a commercially available interface (known as "SLPS") between PSPICE and the MATLAB/SIMULINK environment is presented in Chapter 3. The PSPICE SLPS interface could be unavailable for variety of reasons, including the version of MATLAB software in use, and cost, in which case, the transducer design tool is made to output device impedance and open circuit voltage in a format suitable to be simulated in PSPICE. The behavioural modelling capability of PSPICE, which allows definition of devices in terms of mathematical equations, lookup tables and Laplace transfer functions can be used to achieve this goal of integrating commercial circuit simulation tool with the proposed transducer design software. The possibility also exists to interface with other popular open source circuit simulators such as LTSPICE [79] and is also investigated. The detailed description of integration with commercial circuit simulation software is presented in Chapter 5.

2.1.4 Materials database and other useful utilities included in the proposed design tool

Material properties used in model based design and optimisation are critical and need to be accurate in order to get viable results. For this purpose the proposed design software is interfaced with a comprehensive database containing salient properties of materials used in transducer manufacture. A Microsoft Excel Spreadsheet database consisting of experimentally measured and verified materials properties (as shown in Table 2.1) was collated from a wide range of sources including [17] and [44]. A basic search capability is implemented in the software's user interface to

Material Name (Unique)	Impedance (Rayl)
Velocity Longitudinal (m/s)	Velocity Shear (m/s)
Density (kg/m3)	Poisson Ratio
Attenuation Longitudinal (dB/m)	Attenuation Shear (dB/m)
Relative Permittivity	Frequency (MHz)
Elastic Stiffness Constant (Pa)	

Table 2.1: List of key measured and verified material properties stored in the excel materials database

query for materials with specific properties. For example, while designing a front face matching layer profile for a thickness mode design, the designer could query the database for materials possessing certain acoustic impedance characteristics.

In addition to the extensive materials database, the proposed design tool has other useful utilities such as a material generator tool, and modelling capability to predict 1-3 composite piezoelectric material parameters (referred to as 'COMPD' hereafter). Figure 2.5 describes the material generator implemented in the proposed software, which aids creation of a new passive material by combining epoxy and particulate. This greatly helps to manufacture practical passive matching or backing layers for transducers with exact acoustic impedance profile predicted using the analogue filter design module (also included in the design software), and also is a valuable input to the design optimisation module.

Composites consisting of an active piezoelectric material (such as PZT-5A [45]) and a low acoustic impedance polymer (such as epoxy resin), are of great interest for ultrasonic transducer applications. Figure 2.6 shows a 1-3 composite arrangement often used in transducers, which corresponds to ceramic pillars in polyer matrix. The COMPD software enables modelling such 1-3 composite piezoelectric material parameters, in terms of an equivalent homogeneous medium [61]. This makes it possible to model piezoelectric composite materials (comprising of active ceramic and passive polymer phases that are widely used in biomedical and underwater applications), by using the resulting equivalent parameters in conjunction with a

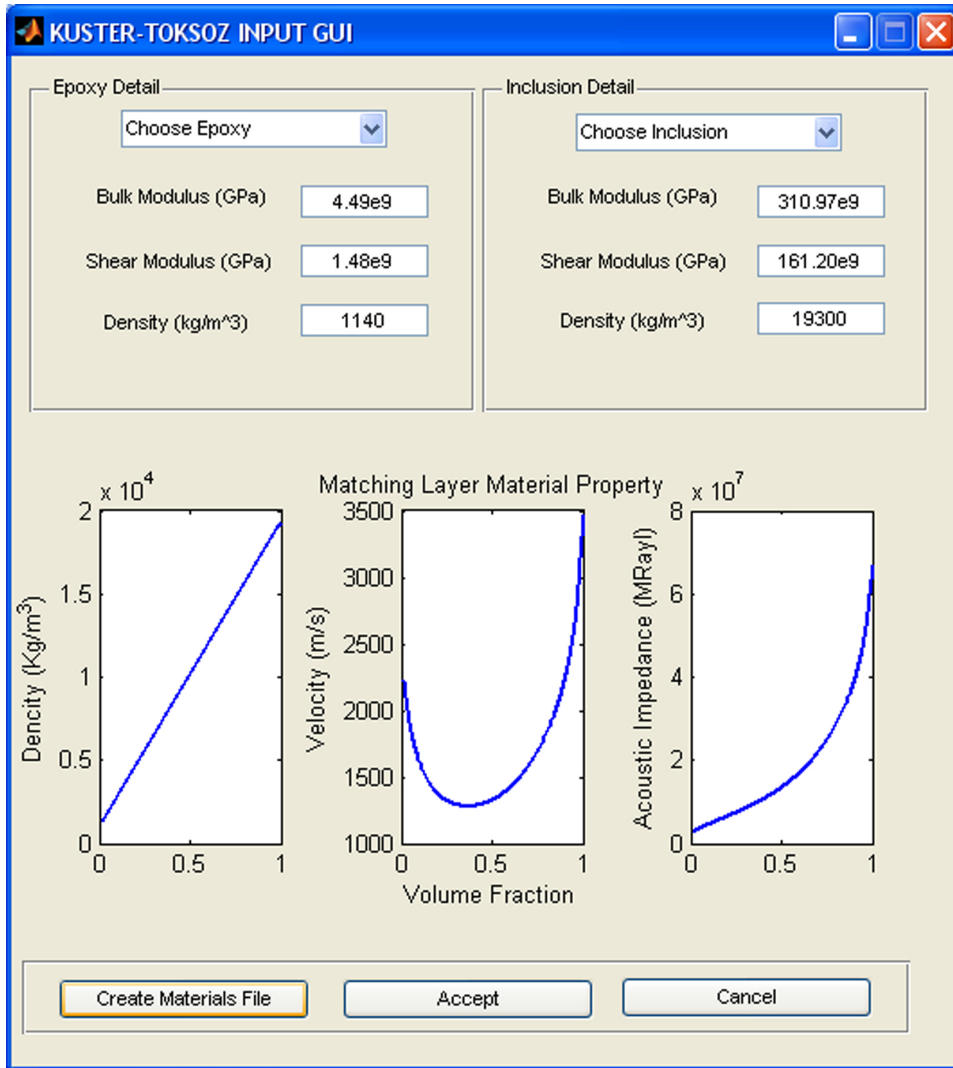wide variety of conventional modelling techniques.

Figure 2.5: Graphical User Interface (GUI) developed to generate composite material properties with two different phase (i.e. an epoxy and a particulate inclusion)
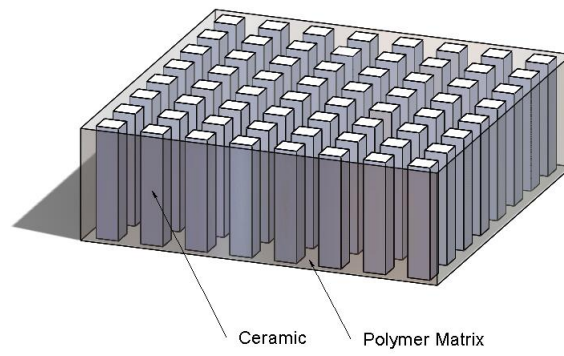
Ceramic   Polymer Matrix

Figure 2.6: Schematic representation of a 1-3 composite

2.2 Implementation of software as a toolbox in MATLAB

MATLAB [37], which is an abbreviation for MATRIX LABOROTARY, is primarily a tool for matrix computations. The MATLAB product family provides a high-level programming language, an interactive technical computing environment, and functions for algorithm development, numeric computation, data analysis and visualisation. Because MATLAB is a programming environment, its functional capabilities may be extended easily. In addition, MATLAB also supplies toolboxes with its core program for specialised applications, such as optimisation. A brief summary of MATLAB toolboxes used in the project and their key features are:

Optimisation, Genetic Algorithm and Direct Search Toolbox: The Optimisation Toolbox extends the MATLAB technical computing environment with tools and widely used algorithms for standard and large-scale optimisation. These algorithms can be used to solve a variety of problems, including constrained and unconstrained continuous and discrete situations. Using MATLAB and the Optimisation Toolbox, it is possible to easily define models, gather data, manage model formulations, and analyse results. They are ideal tools to find optimal solutions, perform trade-off analysis, balance multiple design alternatives, and quickly incorporate optimisation methods in algorithms and models. Also, optimisation capabilities in MATLAB are further extended by the availability of a toolbox for using the genetic and direct search algorithms. These algorithms are extremely useful for problems that are difficult to solve with traditional optimisation techniques, including problems that are not well defined or are difficult to model mathematically. Genetic Algorithms are particularly useful when computation of the objective function is discontinuous, highly nonlinear, stochastic, or has unreliable or undefined derivatives. All the Toolbox functions in MATLAB, which can be accessed through a

graphical user interface (GUI) or the MATLAB command line, are written in the open MATLAB language. This means that the user can inspect the algorithms, modify the source code, and create their own custom functions.

MATLAB Compiler: The MATLAB Compiler lets you automatically convert any MATLAB program into self-contained applications and software components (such as Excel add-ins and COM objects). Such stand alone applications and components created with the MATLAB compiler do not require MATLAB to run, making it ideal to share them with end-users. This significantly reduces application development time by eliminating the process of manually translating MATLAB programs into C or C++ code.

The MATLAB Compiler supports the full MATLAB language and most MATLAB based toolboxes. However it does not support any graphical user interface tools provided in MATLAB. For example, 'gatool', a graphical user interface to set and run genetic algorithm based optimisation problems, works within MATLAB, but cannot be packaged with any user program to form a stand alone executable program. However, most tools can be executed from a command line, making it possible to incorporate them into any user designed programs without the graphical user interface.

2.3 The Graphical User Interface

A Graphical User Interface, abbreviated GUI (pronounced GOO-ee), is a program interface that takes advantage of the computer's graphics capabilities to make the program more user friendly. Many users find that they work more effectively with a command-driven interface, especially if they already know the command language. On the other hand, a well-designed graphical user interfaces can free the user from

learning complex command languages, and make the program usable for all users with varied skill sets.

The first graphical user interface was designed by Xerox Corporation's Palo Alto Research Center in the 1973, for their personal computer 'Alto', featuring the world's first What-You-See-Is-What-You-Get (WYSIWYG) editor, a commercial mouse for input, a graphical user interface, and bit-mapped display [35]. But it was not until the 1980s and the emergence of the Apple Macintosh [36] that graphical user interfaces became popular. One reason for their slow acceptance was the fact that they require considerable CPU power and a high-quality monitor, which until this time were considered prohibitively expensive.

For the present purpose, the whole design and optimisation can be considered to be performed in three GUI stages.

- The first stage is a generic user interface, which prompts the user to enter a high level design specification. A high level design specification is a typical design specification, consisting of the main requirements such as bandwidth, sensitivity, and application, which the design process has to satisfy. Also the main options and flags for the simulation can be set at this level. For example, to switch the expert system OFF or ON can be done at this level. After inputing the high level design specification and the main simulation options are set, the program then brings up the second stage of the user interface.

- The second level of GUI accepts the low level specification, which specifies the complete design specification of the system to be designed. A typical low level design specification consist of details such as materials to be used, and device configuration. The user also has to specify the parameters to optimise at this stage. Once the low level specification is decided, then the user could simulate the system or choose to optimise the design.

- The final stage presents the user with results and design suggestions in a readable format.

A modular approach described so far was followed in implementing the GUI, to make it ideal for incremental development and add different models at later stages. Figure 2.7 describes the flow of control and different stages in an iterative design optimisation process.

2.4 Capabilities of the software

In summary, a new versatile tool for design and optimisation of ultrasonic transducers and arrays is proposed. The software capability includes

- expert system to store application specific knowledge and use this knowledge to guide design optimisation tasks

- contains a wide range of analytical transducer models to simulate variety of thickness mode configurations including stacked devices, arrays and hydrophones

- a graphical user interface for easy use for designers and engineers

- ability to interface with external programs such as PSpice for circuit simulation
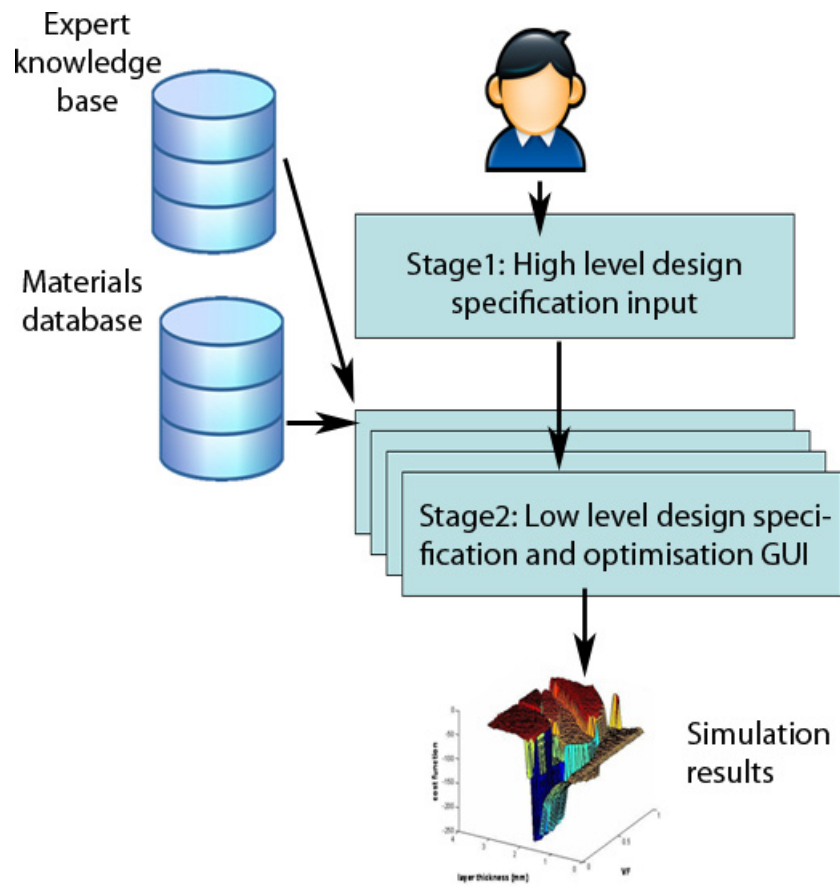
Figure 2.7: Graphical User Interface (GUI) flow

Chapter 3

Review of state of the art and description of the modelling system

This chapter presents an introduction into various approaches to modelling ultrasonic transducers. A brief review of the structure and analysis of the different modelling techniques such as the equivalent circuit approach, linear systems model, and finite element methods are discussed, together with their suitability for the current project. A detailed mathematical formulation of new models developed during the course of this thesis is also presented. A representative selection of results, including force output; received voltage; device operational impedance and signal to noise ratio is provided to illustrate the versatility and comprehensive coverage afforded by the approach.

3.1 Review of the transducer modelling techniques

Sensors are devices that convert one form of energy into another. Based on the principle and the type of measurand involved they can be classified into many types such as photoconductive, straingauges, and piezoelectric devices [65]. Even while considering a simple conventional thickness mode piezoelectric device, there is a wide variety of possible designs. Backing layers, matching layers, electrical load, and active element used are among the many parameters that could be varied, and successful design of a sensor device is often very difficult, owing to its complex interaction with these influencing factors. A comprehensive model, capable of predicting the device characteristics, is vital for designing complex systems involving such sensor elements. Only piezoelectric transducers (thickness mode piezoelectric transducer, stacked thickness devices, Inversion Layer Transducers), and arrays are included in the proposed software at the present stage. But, any other types of devices could be added later, provided there is a suitable analytical model available.

There are many ways to model piezoelectric transducers and arrays. The three main modelling techniques are the equivalent circuit approach, finite element analysis (FEA) and models based on Laplace transformation [17]. This section presents a review of some of the existing transducer models, mainly the ones that are based on Laplace domain techniques. The laplace domain models could be implemented in MATLAB using vector/matrix multiplications, and consequently offer the greatest scope for the development of a general transducer model suitable for optimisation purposes. The later part of this chapter also presents two new transducer models for inversion layer (IL) devices developed during the course of this research. Unless otherwise stated, only one-dimensional models are considered. That is, all electrical and mechanical quantities are assumed to vary only in the thickness dimension of the piezoelectric material and are satisfied by the one-dimensional wave equation. As will be seen, this is not an undue restriction and the so called thickness mode

family of transducers are appropriate for many practical applications.

3.1.1   Modelling conventional thickness mode piezoelectric transducers

Piezoelectric devices convert mechanical stress to electrical charge or voltage (direct effect), and vice versa (indirect effect). The piezoelectric property can be found in many materials (i.e. quartz, Lead Zirconate Titanate (PZT), and Polyvinylidene Fluoride (PVDF)...etc) and finds a wide range of application in fields including SONAR, bio-medicine, non destructive evaluation(NDE) and industrial process control. A typical thickness mode ultrasonic transducer is illustrated in Figure 3.1. These single element transducers are based on a piezoelectric plate (or disc) poled along the thickness direction. The transducer structure presented in Figure 3.1 is connected to an arbitrary electrical load (Z_E) in series with a Thevenin equivalent voltage source (V_E). When an electrical impulse is applied to the electrodes, an acoustic resonance (defined by the device thickness) is produced. Typically, piezoceramics (with high acoustic impedance around 30 MRayl) are often used as an active material in such transducers. Consequently, matching layers whose acoustic impedance is intermediate between the ceramic and the load medium, are used to improve device sensitivity, especially while operating into low acoustic impedance loads such as water (1.5 MRayl). On the rear face of the transducer a thick block (referred to as backing, often matched to the transducer active layer impedance) is used to act as a support and to attenuate acoustic radiation emitted from the back face of the transducer. Even though the presence of such backing blocks lowers device sensitivity, they are essential for achieving higher axial resolution. Each component of the probe assembly, described so far, has a specific function and has to be modelled thoroughly (often a trade-off of certain aspects based on each application requirement) prior to design of a transducer system to achieve desired performance.
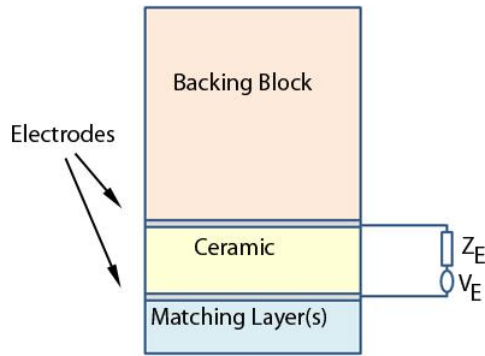
Figure 3.1: Conventional thickness mode piezoelectric transducer structure, configured as a transmit device

One of the popular ways to model such conventional thickness mode devices is using the well established acoustical-electrical analogies [7]–[9] of force-voltage and velocity-current. Martin and Sigelmann [8] represented a thickness mode piezoelectric transducer as a three-port 'black box' device, with one electrical and two mechanical ports, as illustrated in Figure 3.2(a). This three-port model can be reduced to a one-port model by considering a constant load Z2 at port 2 (backing block) and by considering a source generator at either of the remaining electrical (transmitter mode) or the mechanical (receiver mode) port which drives the system. They developed a model for the thickness mode piezoelectric transducer based on two Thevenin equivalent circuits, a mechanical equivalent circuit to represent the transmitting mode and an electrical Thevenin equivalent circuit to represent the reception mode. Figure. 3.2(b-c) shows the Thevenin equivalent models. Such electrical equivalents are useful for implementing transducer design in circuit simulation packages, such as PSPICE, which will enable us to perform noise analysis. However, they have to be developed specifically for each transducer configuration and cannot be used easily in conjunction with general purpose optimisers.
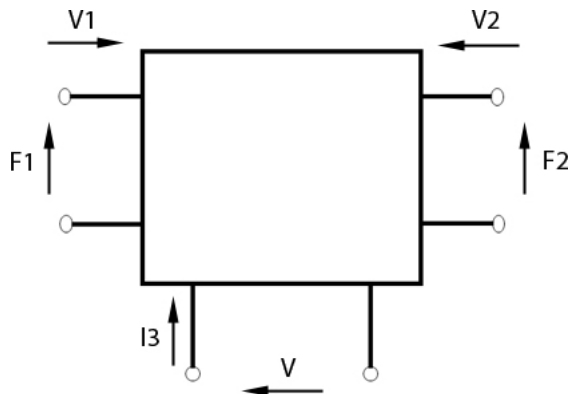
(a) Three-port 'Black Box' representation of thickness mode piezoelectric transducer
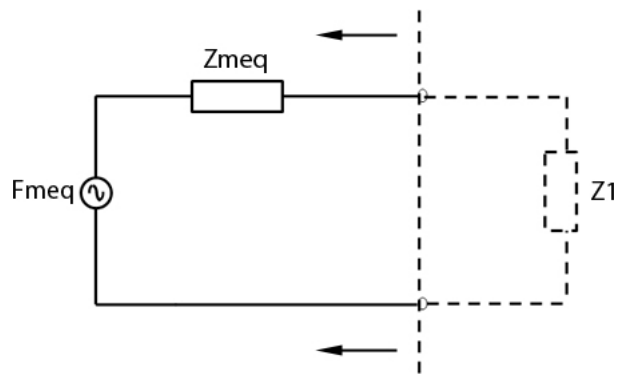
(b) Thevenin equivalent transmitter
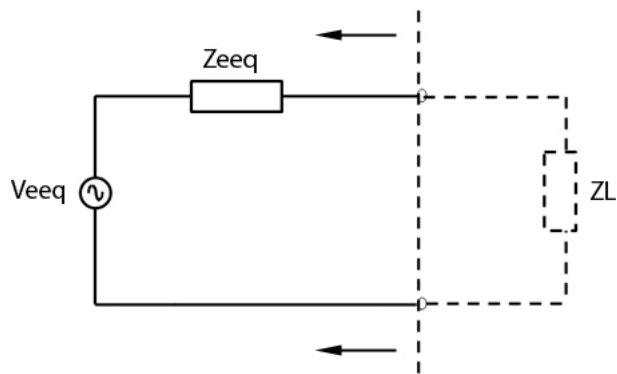
(c) Thevenin equivalent receiver

Figure 3.2: Thevenin equivalent transducer model

Following the analysis adopted by Mason, Redwood [10] provided a Laplace domain representation of a transducer in transmission and reception. Mason's fundamental equations used to describe a piezoelectric transduction sysetm is introduced later in Section . Lewis [11] extended Redwood's characterization of force and particle displacement within a layer in terms of their Laplace transforms, to model the effect of multiple matching and backing layers. By expressing the resulting system equations in a matrix form, and by using complex matrix inversion, the frequency response of the transducer system can be obtained. Utilising the Fast Fourier Transform (FFT), the actual transient response of the system can be modelled. One of the main problems with this technique is the size of the system matrix. The matrix order grows with the number of additional layers and matrix inversion tends to become singular and produce inaccurate results. The matrix inversion issue can be reduced by scaling the matrix before inverting it, and the details of this approach will be described later in this section. However, the process is design specific and cannot be generalised easily for optimisation problems.

Hayward [14] also extended Redwood's [10] technique to produce a feedback model for thickness mode piezoelectric devices. This Laplace model is superior in many ways to other analogies and helps to gain better understanding into the underlying physical working of thickness mode piezoelectric devices. Figure 3.3 shows a nominally 1MHz thickness mode transducer made of PZT-5A [44] active layer radiating directly into water simulated using a linear systems approach implemented in the proposed software. The device configuration used in the simulation is presented in Table 3.1. As indicated in Figure 3.3, conventional thickness mode transducers behave as mechanical cavity resonators, modified by the piezoelectric effect. Consequently, they demonstrate odd harmonic sensitivity, with nulls at the even harmonics. The results indicate clearly that device has around 95% fractional bandwidth,

32

calculated using the formula shown below:

$$\text{fb} = \frac{(\text{f2} - \text{f1}) * 100}{\text{fp}} \quad (3.1)$$

where f1,f2 are the 6dB cut off points and fp is the peak frequency.

Though the feedback technique used for simulation is not ideal for adding many additional matching or backing layers, it permits very simple, accurate and fast implementation, and hence has been added to the proposed design software to model relatively simple devices such as PVDF hydrophones and active thickness mode elements.

Electrical Load (ZE)	50 Ohm
Backing block Impedance	16 MRayl
Active Layer thickness	1.935 mm
Transducer geometry	Square (30 mm by 30 mm)
Piezoelectric constant h	2.215e9
Active Layer Material	PZT-5A (Impedance 30 MRayl approx.)

Table 3.1: Conventional thickness mode transducer parameters used in simulation

Jackson [63] developed a general three-port model for thickness mode transducers by extending the systems technique followed by Lewis and Hayward. One of the main advantages of this model is its capability to handle multiple matching and backing layers (as shown in Figure 3.4). Consider a system where the active ceramic is sandwiched between multiple passive layers at both its front and frear face, as shown in Figure 3.4. This system can be described using the lattice approach as described in the form shown in the Equation (3.2-STAGE 1), where the first equation represents the active layer (using the 3-port system matrix P), and the remaining equations describe wave propagation in the passive front and back face matching layers. All these three equations together describe the complete system and take the similar structure (i.e. the output is obtained by multiplying the system matrix with inputs). Alternatively, these three equations can be combined to represent the final

device (3.2-STAGE 2) as in [63]. This suggests a very good modular architecture for implementing in the proposed transducer design software, to model a wide variety of backing and matching configurations. F and B in the equations describe the force within a media travelling in opposite direction, V_t is the voltage across the transducer electrodes, Z_E is the electrical load and V_E is the drive voltage. The subscripts of F and B represent the layer number, negative meaning backing layer and postive meaning matching layer respectively.

$$\left\{ \begin{array}{c} \begin{bmatrix} F_{10} \\ B_{-10} \\ V_t \end{bmatrix} = [P] \begin{bmatrix} B_{10} \\ F_{-10} \\ V_E \end{bmatrix} \\ \begin{bmatrix} F_{(n+1)0} \\ B_{10} \end{bmatrix} = [U^F] \begin{bmatrix} F_{10} \\ B_{(n+1)0} \end{bmatrix} \\ \begin{bmatrix} B_{-(m+1)0} \\ F_{-10} \end{bmatrix} = [U^B] \begin{bmatrix} B_{-10} \\ B_{-(n+1)0} \end{bmatrix} \\ \textbf{STAGE 1} \end{array} \right\} \Rightarrow \left\{ \begin{array}{c} \begin{bmatrix} F_{(n+1)0} \\ B_{-(m+1)0} \\ V_t \end{bmatrix} = [W] \begin{bmatrix} B_{(n+1)0} \\ F_{-(m+1)0} \\ V_E \end{bmatrix} \\ \textbf{STAGE 2} \end{array} \right\} \quad (3.2)$$

Figure 3.5 shows the frequency spectrum simulation of the same transducer configuration detailed earlier in Table 3.1, but with an added front matching layer to reduce the impedance mismatch problem (i.e. matching an 30MRayl to 1.5 MRayl water load). The details of the matching layer parameters are provided in Table 3.2. The results indicate clearly that by incorporating an additional matching layer at the front face of the transducer has certainly helped efficient energy transfer between the two media (i.e. transducer and the water load). However, it has introduced additional ringing in the time domain response (as shown in Figure. 3.6), which effectively reduces the 6dB fractional bandwidth to approximately 70%, in this case. Often finding the best compromise between these two factors is the key to making the right transducer design for a specific requirement. The use of multiple matching layers based on the same principle, can further improve transducer performance (especially to produce high-efficiency, wide-band piezoelectric transducers) and this

34

is presented in detail later in Chapter 4.

Impedance (MRayl)	Layer thickness (mm)	Density Kg/m3	Longitudinal Velocity m/s
6.92E+06	3.3750e-04	5.14E+03	1.35E+03

Table 3.2: Matching layer parameters
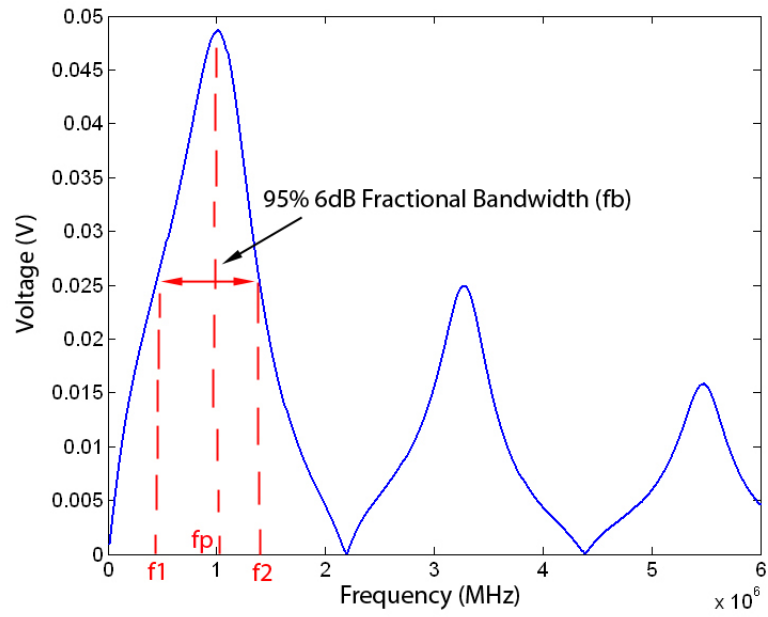
(a) Modulus frequency response
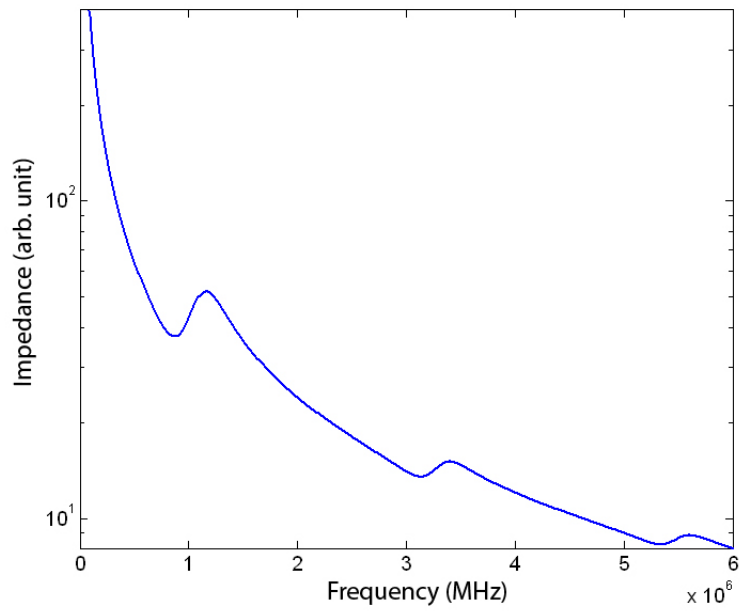
(b) Device operational impedance

Figure 3.3: Systems model [14] simulation of a 1MHz conventional thickness mode transducer (operating in reception mode)
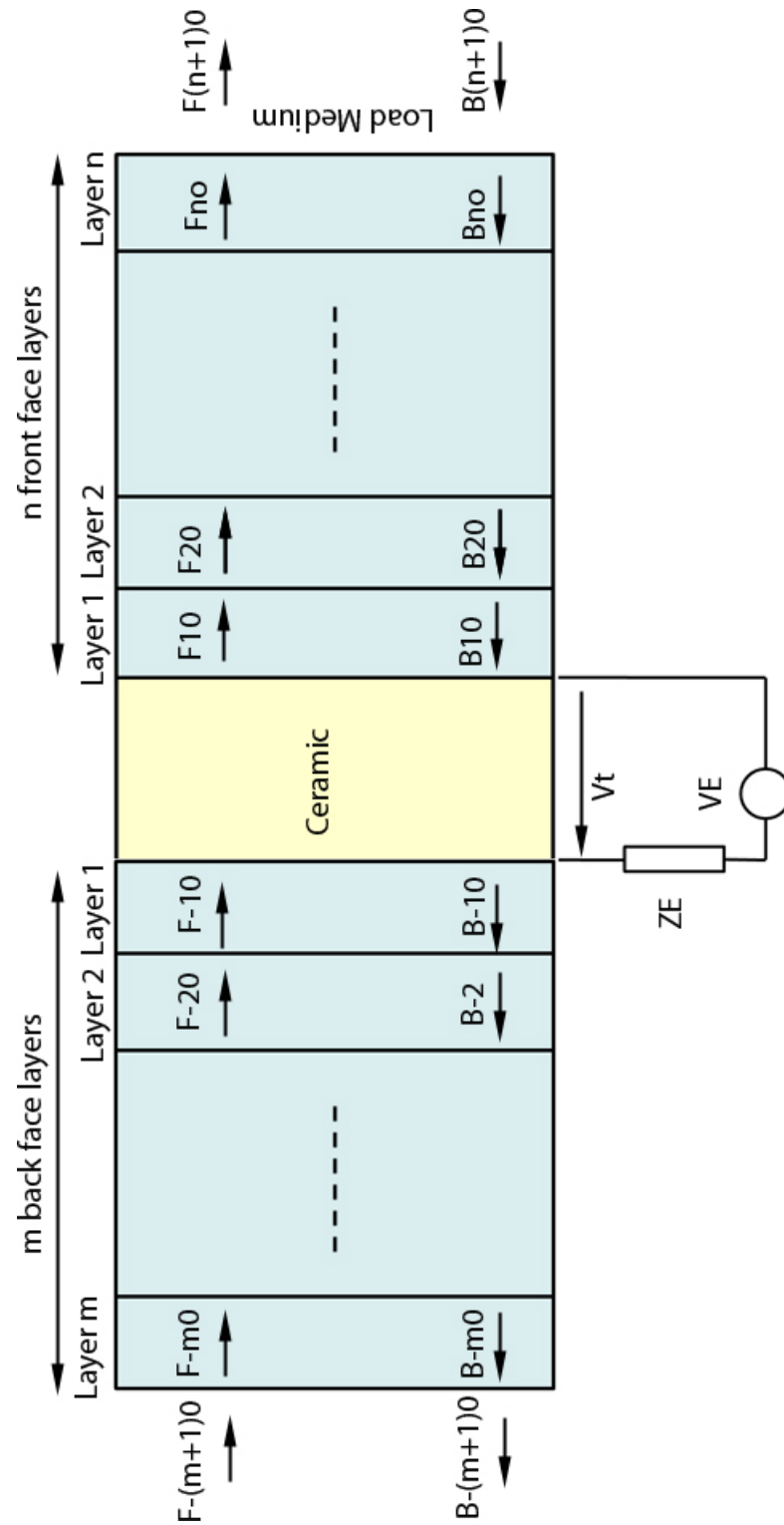
Figure 3.4: Transducer structure with multiple front and back layers, configured to operate as a transmitter, where F and B indicate forward and backward travelling force component in each layer, V_t is the voltage across the transducer electrodes, Z_E is the electrical load and V_E is the drive voltage
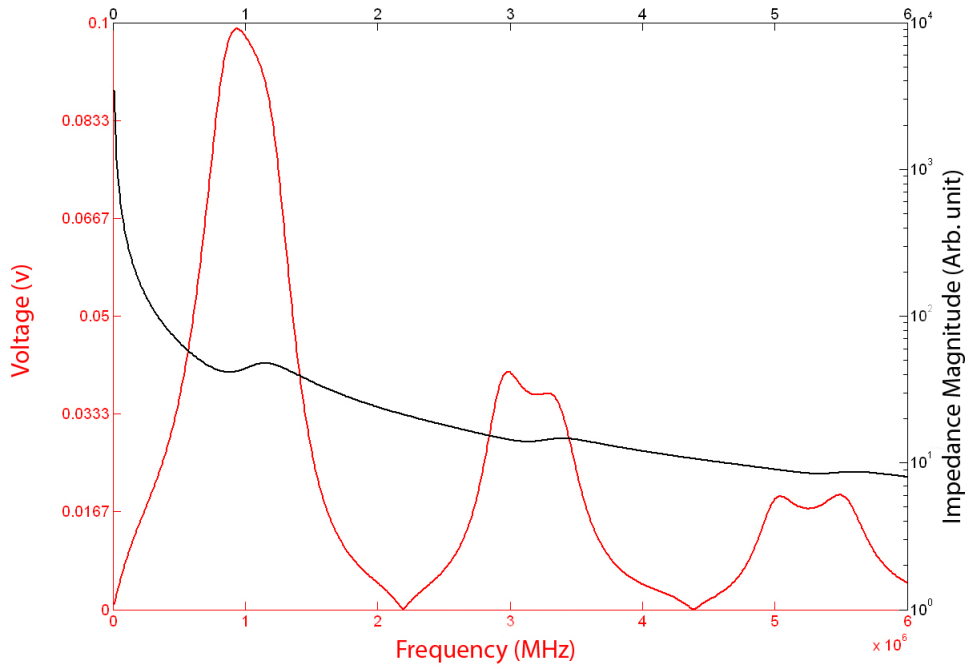
Figure 3.5: Time domain and modulus frequency response using a lattice model [62] for a 1MHz conventional thickness mode transducer, with a passive matching layers at the front face, operating in a water load
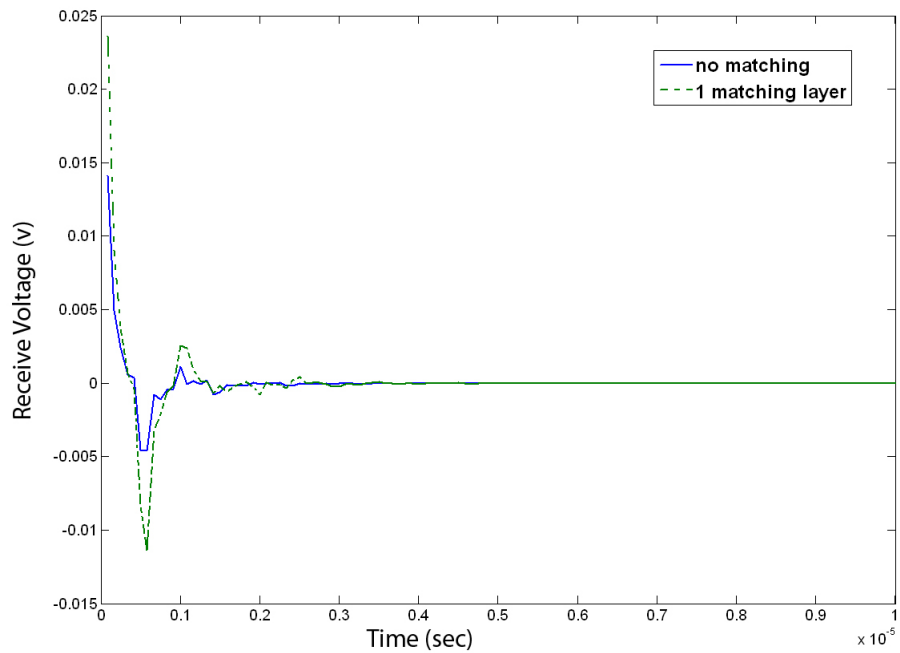
Figure 3.6: Time domain and modulus frequency response simulation for an unmatched and matched conventional transducer configuration operating in reception mode into a water load

38

3.1.2 Modelling inversion layer (IL) transducers

Inversion Layer (IL) transducers [27, 28, 29] are multi layered devices, having regions of opposite polarisation along their thickness direction. They have attracted the Biomedical and Non Destructive Evaluation (NDE) industrial community enormously because of mainly two reasons

1. Their potential for extended bandwidth and

2. Enhanced even harmonic sensitivity

A simple transducer configuration such as one shown earlier in Figure 3.1 in the previous section greatly restricts available bandwidth. However, it can be overcome through the IL structure, whereby an additional zone of polarisation can be created to operate efficiently at a desired even harmonic resonance. Figure 3.7 shows the structure of a transducer incorporating a front face inversion layer (abbreviated henceforth as FFIL). The transducer can be considered of two parts, i.e. the normal part (of thickness l, at the rear face of the transducer) and the inverted layer part at the front face of the transducer (thickness denoted by l'). In this case, the voltage on the transducer is the sum of the voltage across the normal and the inverted layer. The only difference between the inverted and the non inverted layer, is that the piezoelectric constant h will have opposite sign, and all the other parameters such as device acoustic impedance (Zc) and wave velocity in thickness direction (denoted by v_c) remain the same. Figure 3.8 shows the receive impulse response simulation of an inversion layer device performed for transducer configured as a receiver, with a 50 ohm electrical load connected across the device. The device operates directly into water with no matching layers and a backing block whose impedance is 50% the device acoustic impedance. The simulations were repeated for different thickness ratios of the front face layer. zero thickness ratio corresponds

to no front layer (i.e. a conventional thickness mode device) while 0.5 thickness ratio coressponds to two layers that have the same thickness. It is evident from the simulations that there is potential for wide bandwidth (from fundamental to third harmonic) as a result of harmonic sensitivity. Figure 3.9, illustares the concept where by incorporating an additional layer (polarised inversely to the original), along the thickness direction of the device, generates a peak at the even harmonic frequencies instead of a null. However, the various layer configurations need to be designed optimally to achieve wide useable bandwidth. Consequently, it is important that the proposed modelling package is able to simulate these devices effectively. This section details the development of a system model for a back face inversion layer (abbreviated henceforth as BFIL) transducer, where the inversed piezelectric layer is positioned at the back face of the transducer radiating into the backing block. The procedure followed here is the same used by [14] and [29]. This is an extremely fast model using vector multiplication and is useful for design and optimisation of the active element in inversion layer devices and conventional thickness mode transducers (by setting the inversed layer thickness to zero). Also, this model is useful to gain insight into how a back face IL transducer works and compares it with the front face inversion layer case developed in [29].
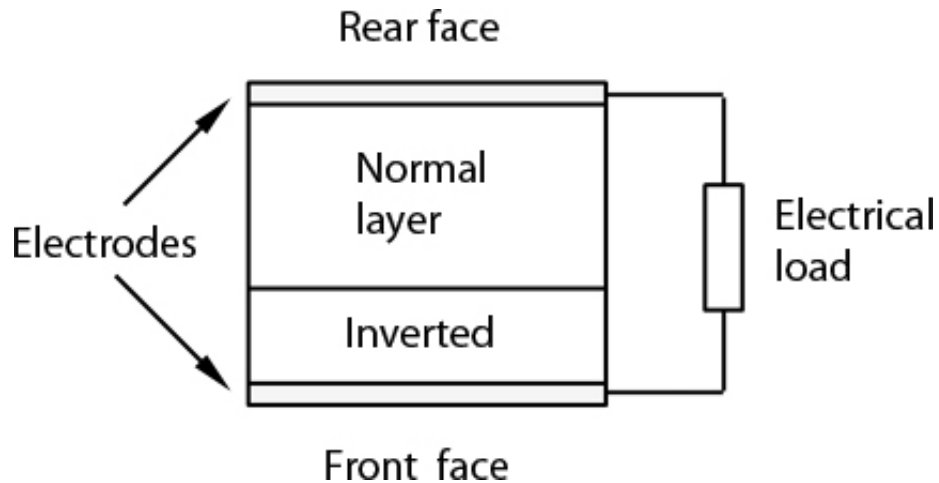

Figure 3.7: A front face inversion layer (FFIL) device structure
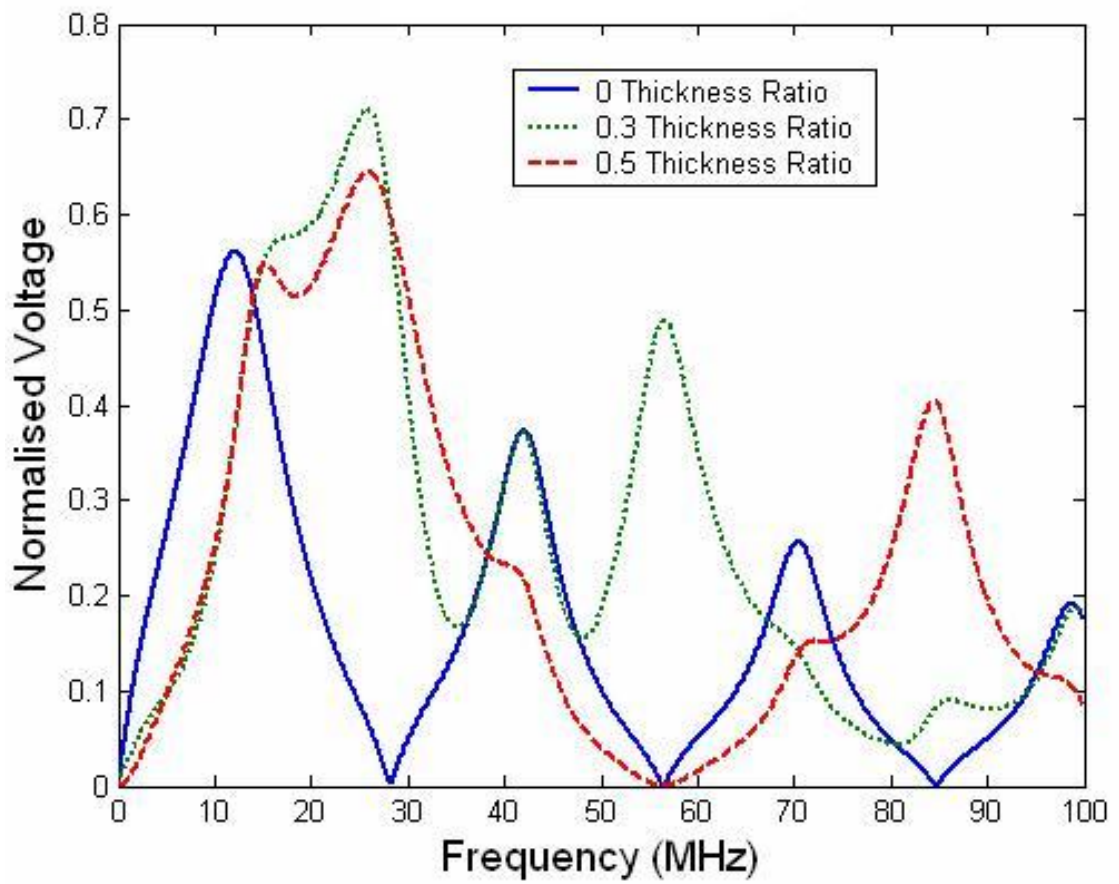
Figure 3.8: Comparison between conventional and ILT device receive frequency response plots, for varied front layer thickness values
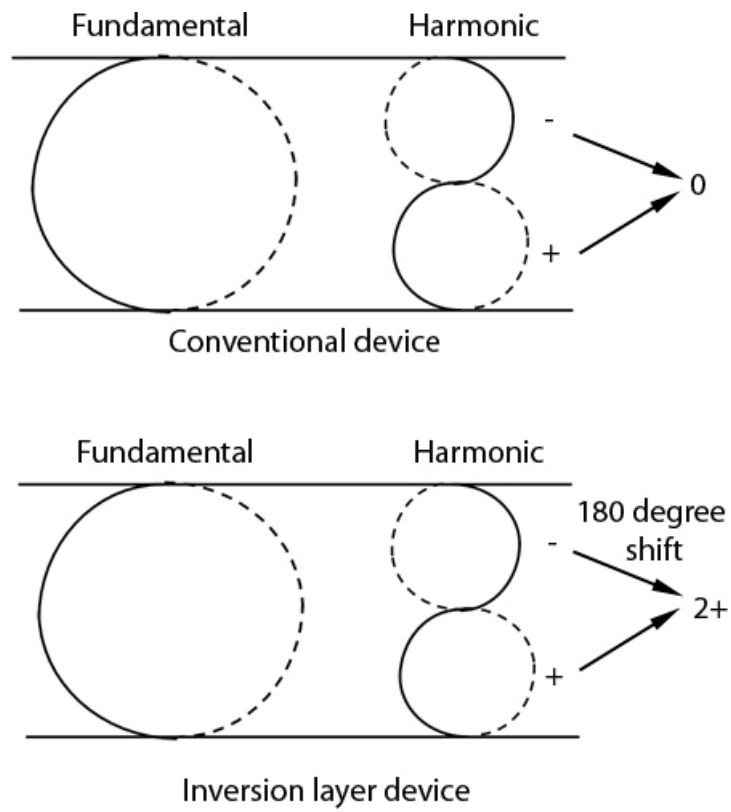
Figure 3.9: Illustration of harmonic generation in the presence of an additional layer along the thickness direction of a conventional thickness mode transducer

3.1.2.1 Systems Model for Back Face Inversion Layer Transducer

Starting with the 1D assumption of the basic equations describing the behavior of a piezoelectric system, as originally proposed by Mason [7]

$$\Gamma = \hat{Y}\frac{\partial \xi}{\partial x} - hD \ldots \ldots \ldots \ldots \text{Indirect} \tag{3.3}$$

$$E = -h\frac{\partial \xi}{\partial x} + D/\epsilon \ldots \ldots \ldots \ldots \text{Direct} \tag{3.4}$$

where Γ is the tensile or compressive stress, $[\text{newtons/m}^2]$

$\hat{Y}$ is the elastic constant measured under constant electrical displacement (open circuit), $[\text{Newtons/m}^2]$

h is the piezoelectric constant relating the stress and charge [Newtons/Coulomb] or the electrical field and mechanical strain $[1/\text{Coulombs per m}^2]$, measured under constant electrical displacement

D is the electrical displacement, $[\text{Coulombs/m}^2]$

E is the electrical field strength, [volts/m]

ξ is the mechanical displacement in any point x within the transducer [m]

ϵ is the relative permittivity (measured under conditions of constant, or zero, strain) (F/m)

The fundamental relationship describing the force and voltage present in this system is established as described by Hayward [14], and is presented next. Assume there is no net charge within the transducer(i.e. $\frac{\partial D}{\partial x} = 0$), we get

$$\frac{\partial \Gamma}{\partial x} = \frac{\hat{Y}\partial^2 \xi}{\partial x^2} \tag{3.5}$$

Also considering a very small area within the transducer and applying Newton's law relating acceleration to force,

$$\frac{\partial \Gamma}{\partial x} = \rho\frac{\partial^2 \xi}{\partial t^2} \tag{3.6}$$

43

where ρ is the material density

From (3.5) and (3.6), we get

$$\frac{\partial^2 \xi}{\partial t^2} = v^2 \frac{\partial^2 \xi}{\partial x^2} \qquad (3.7)$$

where v is the longitudinal wave velocity measured in [m/s], $v^2 = \hat{Y}/\rho$

The solution to Equation (3.7) is of the form

$$\xi(s) = Ae^{-s(x/v)} + Be^{s(x/v)} \qquad (3.8)$$

where

s is the complex Laplace domain variable

A and B are constants related to the boundary conditions at x=0 and x=L

Equation (3.8) represents two waves travelling inside the transducer in the positive and negative x directions. When there is no net free charge within the transducer, all the charge resides on the transducer surface; hence the electrical displacement D can be defined as

$$D = \frac{Q}{A_R} \ C/m^2 \qquad (3.9)$$

Where

A_R is the area of the transducer surface

Q is the net charge residing on either of the surfaces

Now the Equation 3.3 for the indirect piezoelectric effect can be re written as

$$\frac{F}{A_R} + \frac{hQ}{A_R} = \hat{Y}\frac{\partial \xi}{\partial x} \Rightarrow F + hQ = A_R \hat{Y}\frac{\partial \xi}{\partial x} \qquad (3.10)$$

where F is the force in the x direction.

Substituting Equation (3.8) in the above equation, we get

$$F(s) + hQ(s) = sZ_c\{-Ae^{-s(x/v)} + Be^{s(x/v)}\} \tag{3.11}$$

Where

$Z_c = \rho v_c A_R$ is the acoustic impedance of the transducer.

v_c is the longitudinal acoustic velocity of the transducer material.

Similarly, the force in any non-piezoelectric medium can be described as follows:

$$F(s) = sZ_m\{-Ae^{-s(x/v_m)} + Be^{s(x/v_m)}\} \tag{3.12}$$

Where

v_m is the longitudinal acoustic velocity of the medium.

Z_m is the acoustic impedance of the medium.

From the direct piezoelectric effect, the voltage developed across the transducer can be obtained by integrating the electric field, as shown below.

$$V = \int_0^\rho E dx = \int_0^\rho \left[\frac{-h\partial\xi}{\partial x} + \frac{Q}{A_R\epsilon} \right] dx$$

$$= -h\{\xi_{(x=L)} - \xi_{(x=0)}\} + \frac{QL}{A_R\epsilon} \tag{3.13}$$

where

$C_0 = (A_R\epsilon)/L$ is the bulk or static capacitance of the transducer

$\xi_{(x=L)} - \xi_{(x=0)}$ indicates the net strain on the device.

The remainder of the section presents the derivation of the linear systems model for the transducer with a back face inversion layer, as shown in Figure 3.10. In this case, the overall voltage across the transducer is the sum of the voltages across the inverted and the normal layer.

$$V = V_{\text{Normal}} + V_{\text{Inverted}}$$

$$= -h\{\xi_{c(x=l)} - \xi_{c(x=0)}\} + \frac{Ql}{A_R\epsilon} + h\{\xi_{c'(x=L)} - \xi_{c'(x=l)}\} + \frac{Ql'}{A_R\epsilon}$$

$$= -h\{\xi_{c(x=l)} - \xi_{c(x=0)} - \xi_{c'(x=L)} + \xi_{c'(x=l)}\} + \frac{Q}{C_0}$$

$$= -h\{2\xi_{c(x=l)} - 2\xi_{c(x=0)} - \xi_{c'(x=L)}\} + \frac{Q}{C_0} \qquad (3.14)$$
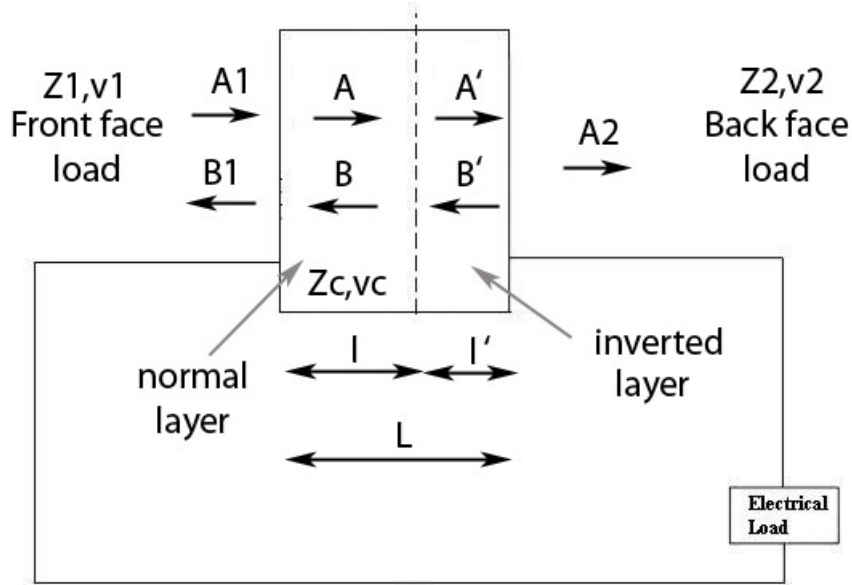
Figure 3.10: A back face inversion layer transducer configured as a receiver

The force incident on the transducer surface produces charge because of the direct piezoelectric effect, which causes a current I(t) to flow through the arbitrary electrical impedance connected across the transducer. This produces a voltage V(t) across the transducer. The relation between current I(t) and the charge Q is given by

$$I(t) = dQ/dt$$

Taking the Laplace transformation and assuming zero initial conditions:

$$I(s) = -sQ(s) \tag{3.15}$$

Hence,

$$V(s) = -sQ(s)Z_E(s)$$

$$Q(s) = -V(s)/sZ_E(s) \tag{3.16}$$

Substituting this in Equation (3.14) yields

$$V(s) = -h\{2\xi_{c(x=l)} - \xi_{c(x=0)} - \xi_{c'(x=L)}\}(s) - \frac{V(s)}{sC_0 Z_E(s)}$$

$$= -h\{2\xi_{c(x=l)} - \xi_{c(x=0)} - \xi_{c'(x=L)}\}(s)u(s) \tag{3.17}$$

where $u(s) = (s\tau(s))/(1 + s\tau(s))$ and $\tau(s) = C_0 Z_E(s)$

Consider that the IL transducer shown earlier in Figure 3.10 is positioned between two semi-infinite media and assuming that all media are lossless, so they can be represented purely by their real acoustic impedances, then from Equation (3.8), we can write

$$\xi 1(s) = A1e^{-s(x/v1)} + B1e^{s(x/v1)}$$

$$\xi 2(s) = A2e^{-s(x/v2)}$$

$$\xi c(s) = Ae^{-s(x/vc)} + Be^{s(x/vc)}$$

$$\xi c'(s) = A'e^{-s(x/vc)} + B'e^{s(x/vc)} \tag{3.18}$$

47

The constants A1, B1, A, B, A', B' and A2 represent the constants A, and B mentioned in Equation 3.8 for the boundary conditions at x = 0, l' and L for the load medium (at the front face of the transducer), the normal layer, the inversion layer, and the backing medium (at the rear face of the transducer), respectively. A is an amplitude factor related to the incident wave, and B is an amplitude factor related to reflected wave in each medium at the boundary. Similarly, the constants Zc,vc,Z1,v1 and Z2,v2 are used to denote the acoustic impedance and the longitudinal wave velocity for the transducer, the load medium and the backing medium respectively. Note that the acoustic impedance (product of the material density and its longitudinal velocity per unit area) and the longitudinal velocity is the same for normal or inverted layer.

From (3.11) and (3.12), we get

$$F1(s) = sZ1\{-A1e^{-s(x/v1)} + B1e^{s(x/v1)}\}$$

$$F2(s) = sZ2\{-A2e^{-s(x/v2)}\}$$

$$Fc(s) + hQ(s) = sZc\{-Ae^{-s(x/vc)} + Be^{s(x/vc)}\}$$

$$Fc'(s) - hQ(s) = sZc\{-A'e^{-s(x/vc)} + B'e^{s(x/vc)}\} \tag{3.19}$$

At the interfaces between two adjacent layers, there is continuity of particle displacement and force. Applying these boundary conditions, shown in Table 3.3, we get the following set of equations

$$A1 + B1 = A + B \tag{3.20}$$

$$Ae^{-s(l/vc)} + Be^{s(l/vc)} = A'e^{-s(l/vc)} + B'e^{s(l/vc)} \tag{3.21}$$

$$A'e^{-s(L/vc)} + B'e^{s(L/vc)} = A2e^{-s(L/v2)} \tag{3.22}$$

$$sZ1[-A1 + B1] = -hQ(s) + sZc[-A + B] \tag{3.23}$$

$$-hQ(s) + sZc[-Ae^{-s(L/vc)} + Be^{s(L/vc)}] = hQ(s) + sZc[-A'e^{-s(l/vc)}$$
$$+B'e^{s(l/vc)}] \tag{3.24}$$

$$hQ(s) + sZc[-A'e^{-s(L/vc)} + B'e^{s(L/vc)}] = sZ2[-A2e^{-s(L/v2)}] \tag{3.25}$$

Continuity of displacement	Continuity of the normal stress
$\xi1(x = 0) = \xi c(x = 0)$	$F1(x = 0) = Fc(x = 0)$
$\xi c(x = l) = \xi c'(x = l)$	$Fc(x = l) = Fc'(x = l)$
$\xi c'(x = L) = \xi2(x = L)$	$Fc'(x = L) = F2(x = L)$

Table 3.3: Boundary conditions

From Equation (3.20) and (3.23), gives

$$sZ1[-2A1 + A + B] = -hQ(s) + sZc[-A + B] \tag{3.26}$$

From Equation (3.22) and (3.25), we get

$$sZc[-A'e^{-sT} + B'e^{sT}] + hQ(s) = -sZ2[A'e^{-sT} + B'e^{sT}] \tag{3.27}$$

where T=L/vc is the time taken by the acoustic wave to travel across the transducer thickness. Similarly, symbols t and t′ will be used in the remainder of this section to denote the transit time for acoustic wave to across the normal (front side) layer and the inversed (back side) face in the transducer.

From (3.21), the following relation can be obtained,

$$A' - A = (B - B')e^{2s(l/vc)}$$

$$B - B' = (A' - A)e^{-2s(l/vc)} \tag{3.28}$$

From (3.24), we get

$$\frac{2hQ(s)}{sZc} = (A' - A)e^{-s(l/vc)} + (B - B')e^{s(l/vc)} \tag{3.29}$$

Substituting the value of $(A' - A)$ and $(B - B')$ in the above Equation 3.29, we get

$$\frac{2hQ(s)}{sZc} = (A' - A)e^{-s(l/vc)} + (A' - A)e^{-s(l/vc)}$$

$$\frac{2hQ(s)}{sZc} = (B - B')e^{s(l/vc)} + (B - B')e^{s(l/vc)} \tag{3.30}$$

From Equation 3.30, we get

$$A' = \frac{hQ(s)}{sZc}e^{s(l/vc)} + A$$

$$B' = \frac{-hQ(s)}{sZc}e^{-s(l/vc)} + B \tag{3.31}$$

From Equation (3.27), we get

$$-A'se^{-sT}[Zc - Z2] + B'se^{sT}[Zc + Z2] + hQ(s) = 0$$

$$-A'se^{-sT}R_B + B'se^{sT} + \frac{hQ(s)}{Zc + Z2} = 0 \tag{3.32}$$

where

$$R_B = (Zc - Z2)/(Zc + Z2) \tag{3.33}$$

Substituting A′ and B′ from Equation (3.31) and manipulating the resulting expression, we get

$$Ae^{-2sT}R_B - B = \frac{-hQ(s)}{s(Zc + Z2)}e^{-sT}\{X\} \tag{3.34}$$

where $X = (Z2/Zc)e^{st'} - (Z2/Zc)e^{-st'} - 1 + e^{st'} + e^{-st'}$

From Equation (3.26), we obtain

$$A(sZ1 + sZc) + Bs(Z1 - Zc) = 2A1sZ1 - hQ(s)$$

$$A - BR_F = (1 - R_F)A1 - \frac{hQ(s)}{s(Zc + Z1)} \tag{3.35}$$

Where

$$R_F = (Zc - Z1)/(Zc + Z1) \tag{3.36}$$

Equations (3.34) and (3.35) can be put into a matrix form as follows,

$$\begin{bmatrix} 1 & -R_F \\ R_Be^{-2sT} & -1 \end{bmatrix} \begin{bmatrix} A \\ B \end{bmatrix} = \begin{bmatrix} A1(1 - R_F) - \frac{hQ(s)}{s(Zc+Z1)} \\ -\frac{hQ(s)}{s(Zc+Z2)}e^{-sT}\{X\} \end{bmatrix} \tag{3.37}$$

Solution for A and B can be obtained by applying Cramer's Rule

$$A = \begin{vmatrix} A1(1 - R_F) - \frac{hQ(s)}{s(Zc+Z1)} & -R_F \\ \frac{-hQ(s)}{s(Zc+Z2)}e^{-sT}\{X\} & -1 \end{vmatrix} \Bigg/ \begin{vmatrix} 1 & -R_F \\ R_Be^{-2sT} & -1 \end{vmatrix}$$

$$A = \frac{A1(1 - R_F)}{\Delta} - \frac{hQ(s)}{\Delta s(Zc + Z1)} + \frac{hQ(s)}{\Delta s(Zc + Z2)}e^{-sT}XR_F \tag{3.38}$$

Similarly, we get

$$B = \frac{A1(1 - R_F)R_Be^{-2sT}}{\Delta} - \frac{hQ(s)R_Be^{-sT}}{\Delta s(Zc + Z1)} + \frac{hQ(s)}{\Delta s(Zc + Z2)}e^{-sT}X \tag{3.39}$$

51

where

$$\Delta = 1 - R_F R_B e^{-2sT}$$

From Equation (3.17), we have

$$V(s) = -h\{2(Ae^{-st} + Be^{st}) - (A + B) - (A'e^{-sT} + B'e^{sT})\}(s)u(s) \qquad (3.40)$$

Representing A' and B' in terms of of A and B in the above Equation, we get

$$V(s) = -h\{A(2e^{-st} - 1 - e^{-sT}) + B(2e^{st} - 1 - e^{sT})$$
$$+ \frac{hQ(s)}{sZc}(-e^{-st'} + e^{st'})\}(s)u(s) \qquad (3.41)$$

Substituting A and B in terms of A1 the incident wave, we obtain

$$V(s) = -hu(s)\{A1(1 - R_F)K_{FI}(s) - \frac{hQ(s)}{s(Zc + Z1)}K_{FI}(s)$$
$$- \frac{hQ(s)}{s(Zc + Z2)}XK_{BI}(s) + \frac{hQ(s)}{sZc}(e^{st'} - e^{-st'})\} \qquad (3.42)$$

where

$$K_{FI}(s) = \frac{-e^{-sT} + 2e^{-st} - 1 - R_B e^{-sT} + 2R_B e^{-2sT}e^{st} - R_B e^{-2sT}}{\Delta}$$

$$K_{BI}(s) = \frac{e^{-sT} - 2e^{-sT}e^{st} + 1 + R_F e^{-sT} - 2R_F e^{-sT}e^{-st} + R_F e^{-2sT}}{\Delta}$$

The initial force incident on the transducer is given by the equation

$$F1(s) = sZ1(-A1e^{-s(x/v1)} + B1e^{s(x/v1)})$$

52

Considering only the incident wave at x=0, we have

$$A1 = -\frac{F1(s)}{sZ1} \tag{3.43}$$

Also

$$R_F = \frac{Zc - Z1}{Zc + Z1} \Rightarrow 1 - R_F = \frac{2Z1}{Zc + Z1} \tag{3.44}$$

Let

$$T_F = \frac{2Zc}{Zc + Z1} \Rightarrow T_B = \frac{2Zc}{Zc + Z2} \tag{3.45}$$

Substituting these and $Q(s) = -\frac{V(s)}{sZ_E(s)}$ in Equation (3.42), we obtain V(s) in terms of F1(s)

$$\frac{V(s)}{F1(s)} = \frac{\frac{-hu(s)T_F K_{FI}(s)}{sZc}}{1 - \frac{h^2 u(s)}{s^2 ZcZ_E(s)} \left[K_{FI}(s)\frac{T_F}{2} + K_{BI}(s)\frac{T_B}{2}X - (e^{st'} - e^{-st'}) \right]} \tag{3.46}$$

Equation (3.46) gives the receive transfer function of the BFIL. Figure 3.11 represents the receive transfer function in Equation (3.46) using a block diagram. The physical nature of this back face inversion layer transduction process can be explained easily from the block diagram in the same procedure followed by Hayward [14] and Estanbouli [30].

Firstly, consider the direct piezoelectric effect (black colour in the Figure 3.11), which is the voltage created across the electrodes as a direct function of the incident force input at the transducer front face. When a force hits the transducer front face, a portion of it is is transmitted into the device, which will reverberate forward and backward within the transducer, creating particle displacement in both the device and the surrounding media. The term $1/sZ_c$ converts the pressure function inside the transducer to a function of particle displacement [66]. This particle displacement

will propagate into the transducer and reverberate within the transducer structure. The particle displacement is converted to a function of strain by KFI(s), referred to as the reverberation factor within the transducer. When no inversion layer exists this term will be equal to the difference in displacement between the front and the back face of the transducer as explained by Hayward [45]. The piezoelectric constant (h) relates the particle displacement to voltage, which is modified by the external electrical load (U(s)), producing a voltage across the electrodes.
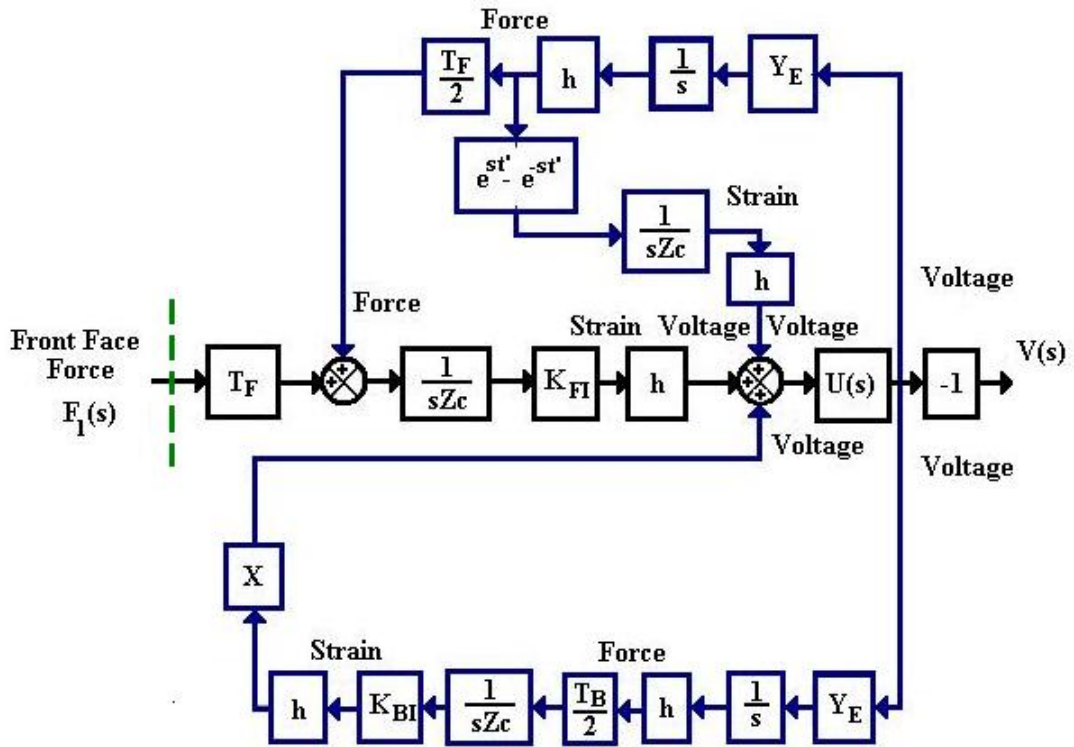
Figure 3.11: Receive feedback model for back face inversion layer transducer

However, the voltage generated on the electrodes produces a secondary piezoelectric effect at the transducer boundaries (i.e. the front face, back face and the boundary between the two active layers), as shown by the feedback loops (blue colour in Figure 3.11). Contrary to the conventional single layer device (where the two feedback loops are symmetric), the presence of the inversion layer has created an additional term (indicated by X) in the feedback loop to the back face of the transducer. It is worth noting at this point that the reverberation factors (both K_{FI} and K_{BI})

in the case of back face inversion layer (BFIL) device, is of similar form to the front face inversion layer (FFIL) device [30], except that they are now functions of the non-inverted front piezoelectric layer thickness. This is a very important finding, because the amount of feedback in an inversion layer device (in both BFIL and FFIL configuration) is directly proportional to the front layer thickness, and highlights the importance in optmially designing the front layer to acheive desired transducer characteristics. Another main difference between this model and a front face IL model developed earlier, is the block X, which now appears in the feedback loop to the back face. The additional third component in case of an inversion layer transducer (ILT) configuration, generated at the boundary between the two piezoelectric layers, remains the same for the FFIL and BFIL configuration. To verify the present model, if we assume there is no inversion layer present (i.e l'=0), as we would expect the system transfer function reduces to that of Hayward [14], which describes the conventional, single layer device.

SOME SPECIFIC ELECTRICAL AND MECHANICAL LOADING CONDITIONS:

Consider an open circuit across the transducer ($Z_E = \infty$), Equation (3.46) now reduces to

$$\frac{V(s)}{F1(s)} = \frac{-hT_F K_{FI}(s)}{sZc} \tag{3.47}$$

Here K_{FI} is the only term related to t, the thickness of front face layer l. Also considering the transducer to have a matched backing ($R_B = 0$), we get

$$K_{FI}(s) = -e^{-sT} + 2e^{-st} - 1 \tag{3.48}$$

For no inversion layer case (t'=0), K_{FI} becomes

$$K_{FI}(s) = e^{-sT} - 1 \tag{3.49}$$

Similarly for the non-inversion layer case ($t' = T$), K_{FI} becomes

$$K_{FI}(s) = -e^{-sT} + 1 \tag{3.50}$$
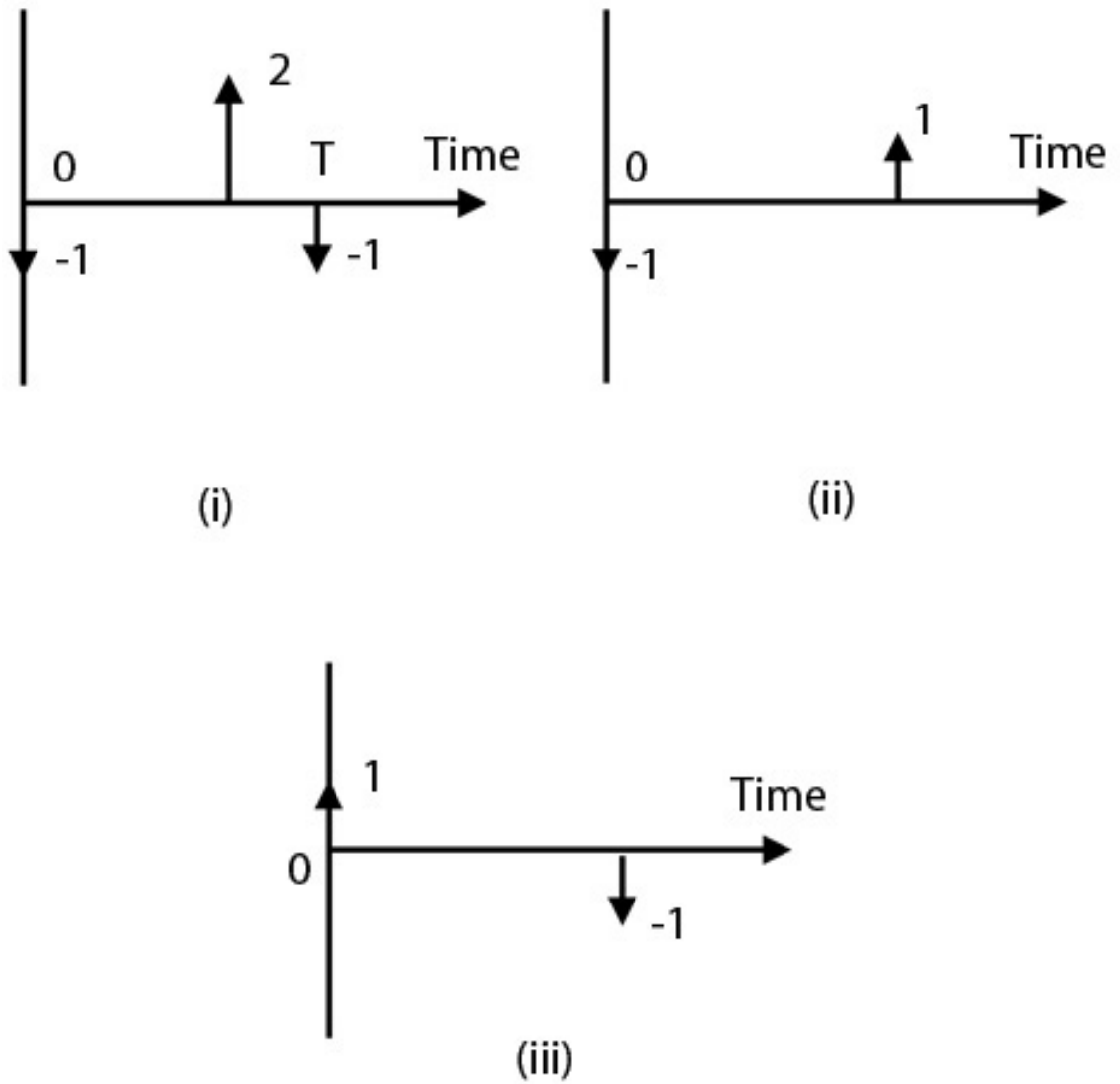
Figure 3.12: Time domain representation of the fundamental reverberation factor (K_{FI}), for a (i) back face inversion layer transducer, (ii) conventional device and (iii) transducer with only the inverse layer.
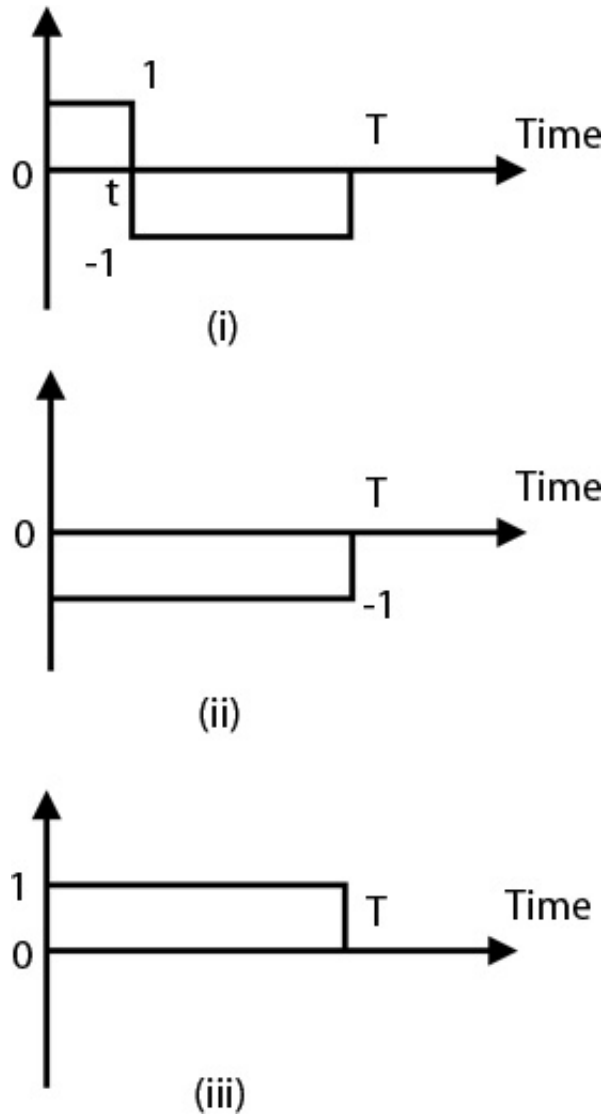
Figure 3.13: Voltage across a (i) back face inversion layer transducer, (ii) conventional device and (iii) transducer with only the inverse layer.
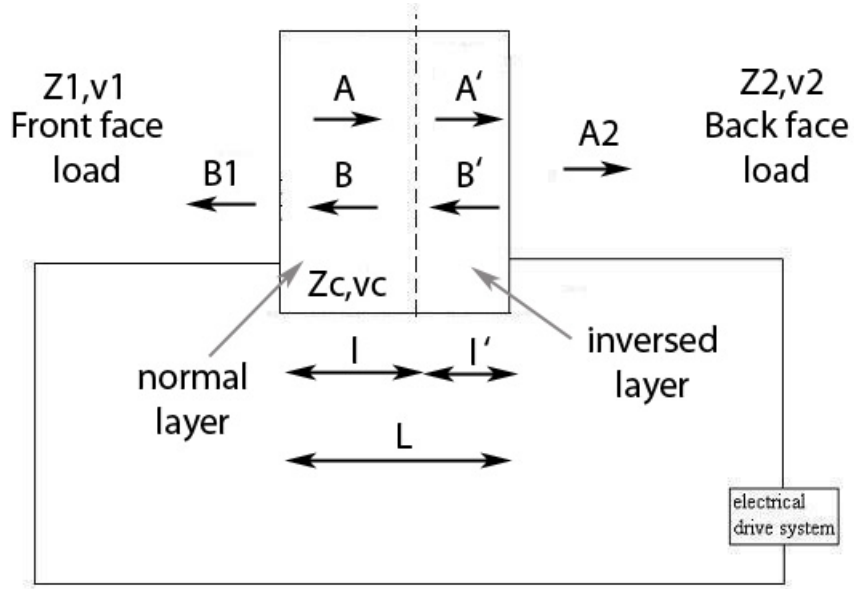
Figure 3.14: A BFIL transducer configured as a transmitter

Equations (3.49) and (3.50), having opposite sign, confirm opposite electrical polarity. Figure 3.12 represents Equations (3.48-3.50) in the time domain. From Equation (3.47), for an impulse input (F1(s) = 1), the voltage across the transducer is proportional to the integration of the time function $K_{FI}(s)$. Figure 3.13 shows the voltage across the transducer for the three cases discussed so far. Similar to the analysis carried by Hayward [14] and Estanbouli [30], it can be showed here that the presence of the inversion layer results in increased frequency content.

Figure 3.14 shows the transducer configured to act as a transmitter. This situation is similar to the receive case, except that there is no incident wave (A1=0). The amplitude factors A and B inside the transducer can now be represented as follows

$$A = \frac{-hQ(s)T_F}{2\Delta sZc} + \frac{hQ(s)T_B}{2\Delta sZc}e^{-sT}XR_F$$

$$B = \frac{hQ(s)T_Be^{-sT}X}{2\Delta sZc} - \frac{hQ(s)T_FR_Be^{-2sT}}{2\Delta sZc}$$

Where $T_F = 1 + R_F$ and $T_B = 1 + R_B$

The force at any point within the transducer is given by

$$F_x(s) + hQ(s) = sZc\{-Ae^{-s(x/vc)} + Be^{s(x/vc)}\} \tag{3.51}$$

$$F'_x(s) - hQ(s) = sZc\{-A'e^{-s(x/vc)} + B'e^{s(x/vc)}\} \tag{3.52}$$

From Equation (3.51), we obtain the stress wave generated at the front face,

$$F_F(s) = hQ(s)\frac{Z1}{Zc + Z1}K_{FI}(s) \tag{3.53}$$

Similarly from Equation (3.52), by substituting A' and B' in terms of A and B, the stress wave at the back face is,

$$F_B(s) = hQ(s)\frac{Z2}{Zc + Z2}K_{BI}(s) \tag{3.54}$$

Equations (3.53) and (3.54) represent the Laplace transform of the wave of force radiating into the surrounding medium, when the transducer is excited by a function of charge whose Laplace transformation is denoted by Q(s). It is essential at this stage to replace Q(s) with the input voltage V(s) in Equations (3.53) and (3.54) in order to get a transfer function relating applied voltage and force output. From Equation (3.14) , we can write

$$V(s) = -h\{2\xi_{c(x=l)} - \xi_{c(x=0)} - \xi_{c'(x=L)}\}(s) + \frac{Q(s)}{C_O} \tag{3.55}$$

Expanding Equation (3.55) and substituting for A, B, A'and B', we get the relation between voltage across the transmitting transducer and charge developed on the electrodes, as follows:

$$V(s) = \frac{Q(s)}{C_O}\left\{1 + \frac{h^2 C_O}{sZc}\left[K_{FI}(s)\frac{T_F}{2} + XK_{BI}(s)\frac{T_B}{2} + e^{-st'} - e^{st'}\right]\right\} \tag{3.56}$$

59

Considering that $Z_T(s) = V(s)/I(s) = V(s)/(sQ(s))$, the electrical impedance of the transducer is defined by the following equation

$$Z_T(s) = \frac{1}{sC_0} \left\{ 1 - \frac{h^2 C_O}{sZc} \left[K_{FI}(s)X\frac{T_F}{2} + K_{BI}(s)\frac{T_B}{2} + e^{st'} - e^{-st'} \right] \right\} \qquad (3.57)$$

Similar to the receive transfer function, the transducer's operational admittance can be implemented as a block diagram, as shown in Figure 3.15. For a fixed voltage input, the current through the transducer can be considered as a sum of the primary current arising directly as a result of the input voltage and a feedback current generated by the secondary piezoelectric action. Figure 3.15 clearly highlights the various relationships between force, particle displacement and current. A comparison of simulated device operational impedance of a IL device with a conventional device is shown in Figure 3.16, and the following observations, are noteworthy:

1. When there is no inverted layer present, that is for a conventional thickness mode transducer configuration, there is null at the even harmonic frequency.

2. By introducing an inversion layer with the same thickness as the non-inverted layer, the two resonance mode (i.e. fundamental and the first even harmonic) combine to form a new resonance frequency, much closer to the even harmonic.

3. However, by keeping the inverted layer much smaller (30% of overall device thickess in this case) compared to that of the non-inversed layer, both the fundamental and even harmonic frequencies are present. This is extremely valuable, as this allows operating this device in both these frequencies. Also, by carefull design of multiple front face matching profiles, it is possible to produce ultra-wideband transducers from such configuration.

To develop a transfer function for the transmit case including electrical loading, consider the electrical circuit configuration outlined in Figure 3.17; where the transducer is connected to a non-ideal voltage source e, having an output impedance Z_0,

60
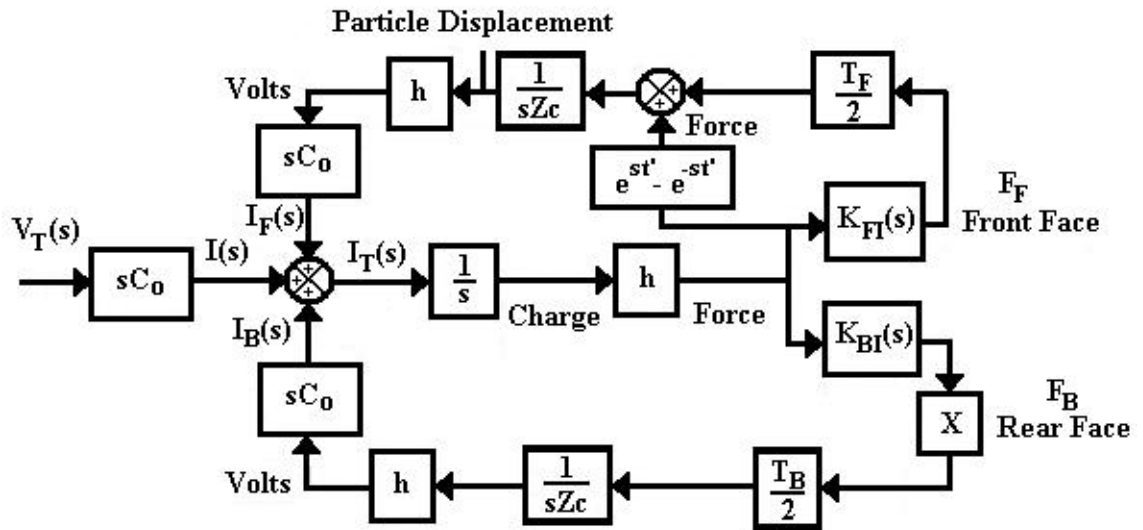
Figure 3.15: Admittance block diagram for an ILT
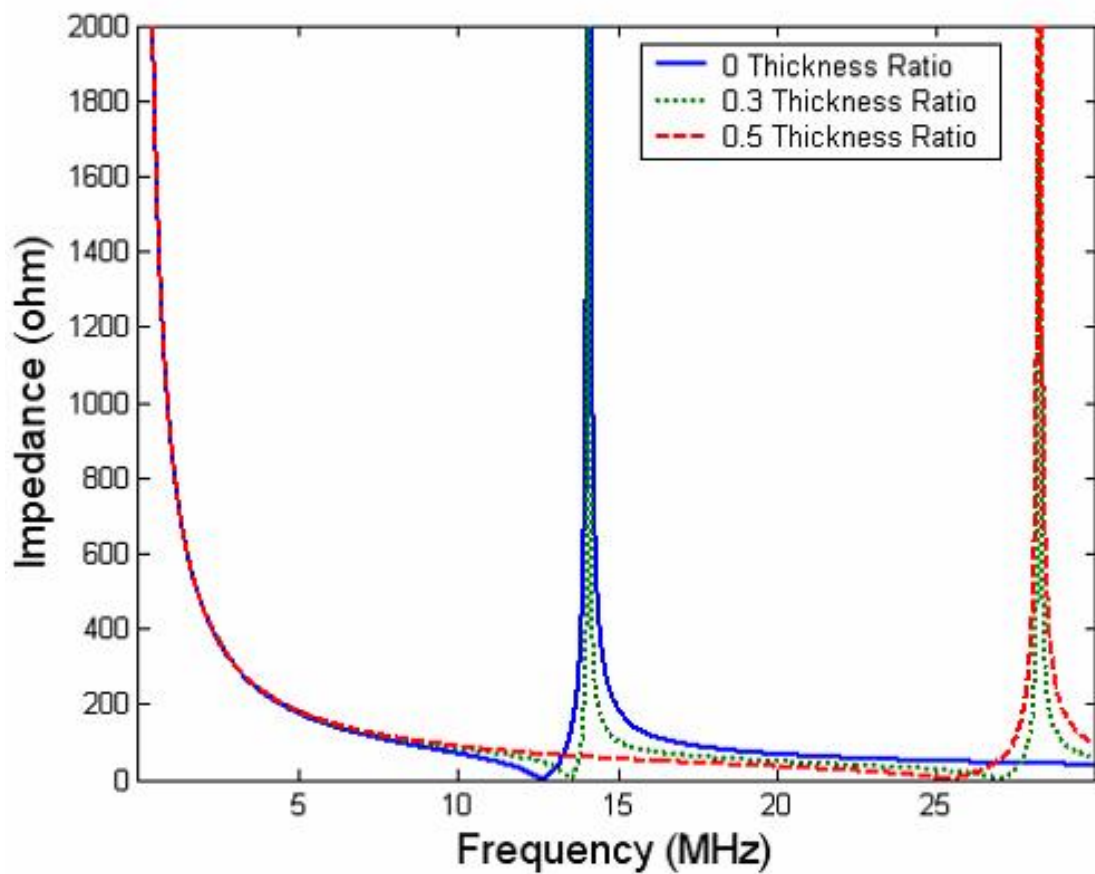
Figure 3.16: Operational impedance simulation of an ILT device

61
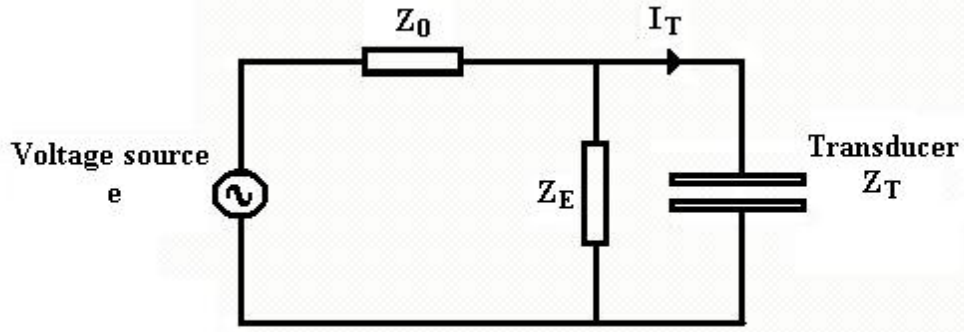
Figure 3.17: Transmitter electrical configuration

and an arbitrary electrical load impedance denoted by Z_E. For this electrical config-
uration, the voltage-current relationship of the voltage source $e(s)$ and the current
through the transducer $I_T(s)$ is given in the Laplace domain by,

$$\frac{I_T(s)}{e(s)} = \frac{Z_E(s)}{Z_T(s)(Z_0(s) + Z_E(s)) + Z_0(s)Z_E(s)}$$

Where all the impedances Z_E, Z_0 and Z_T are functions of s. Substituting for $Z_T(s)$,

$$\frac{I_T(s)}{e(s)} = \frac{Z_E(s)/(Z_0(s) + Z_E(s))}{Z_T(s) + (Z_0(s)Z_E(s))/(Z_0(s) + Z_E(s))} = \frac{a(s)}{Z_T(s) + b(s)} \Rightarrow I_T(s) = \frac{a(s)e(s)}{Z_T(s) + b(s)}$$

Hence,

$$Q(s) = \frac{a(s)e(s)}{s\{Z_T(s) + b(s)\}} \tag{3.58}$$

But, $F_F(s) = hQ(s)(A_F/2)K_{FI}(s), \text{where}(A_F/2) = Z1/(Zc + Z1)$

Substituting $Q(s)$ from Equation (3.58), we obtain

$$\frac{F_F(s)}{e(s)} = \frac{-ha(s)(A_F/2)}{s\{Z_T(s) + b(s)\}}K_{FI}(s)$$

62

Substituting $Z_T(s)$ from Equation (3.57), we get

$$\frac{F_F(s)}{e(s)} = \frac{ha(s)(A_F/2)Y(s)K_{FI}(s)}{1 + \frac{h^2}{sZc}Y(s)\{K_{FI}(s)X(T_F/2) + K_{BI}(s)\frac{T_B}{2} + e^{st'} - e^{-st'}\}} \quad (3.59)$$

Where $Y(s) = C_0/(1 + sb(s)C_0)$

Equation (3.59) gives the transmit transfer function for a transducer with a back face inversion layer, relating the stress wave generated into the load medium to the input voltage. Equation (3.59) can be implemented as a block diagram shown in Figure 3.18. In a similar fashion to the receive case, the transmit block diagram can offer physical insight into the working of such IL devices. Consider the general lossless model of an BFIL receiver as shown in Figure 3.18. The direct piezoelectric effect (i.e. force generated on both the faces directly as a consequence of the voltage applied across the electrodes) are indicated by the forward loop (black colour in Figure 3.18) in the block diagram. The secondary piezoelectric effect, formed as a result of stresses created at the device boundaries, are represented as the feedback loops (blue colour in Figure 3.18). It is clear as in the case of a conventional transducer, that the amount of feedback is proportional to the electromechanical coupling coefficient (as h/Z_c is a function of k_t^2), the mechanical load at the front and back face, and any external electrical load (due to the presence of $Y(s)$, which is the operational admittance of the equivalent electrical circuit at the transducer input). In addition to these there is an additional contribution from the interface between the two active layers. Note that the feedback loop from the front and back face is not symetric anymore due to the presence of the additional term X (a function of the inverted layer thickness).
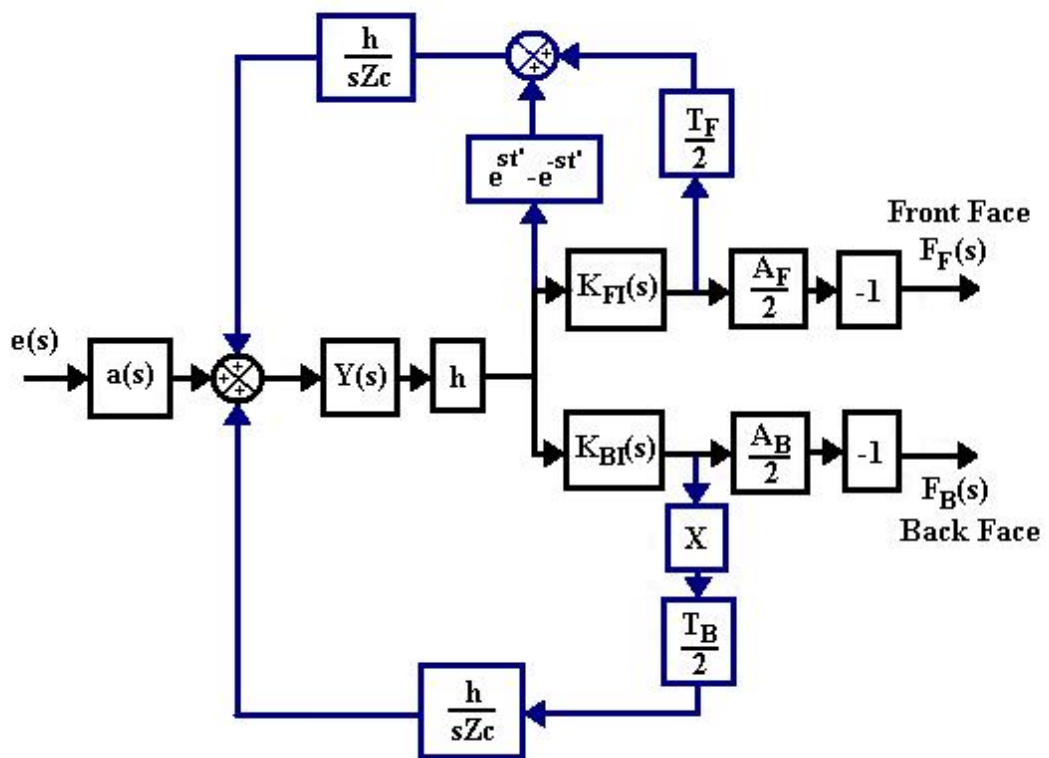
Figure 3.18: Transmit feedback model for back face inversion layer transducer
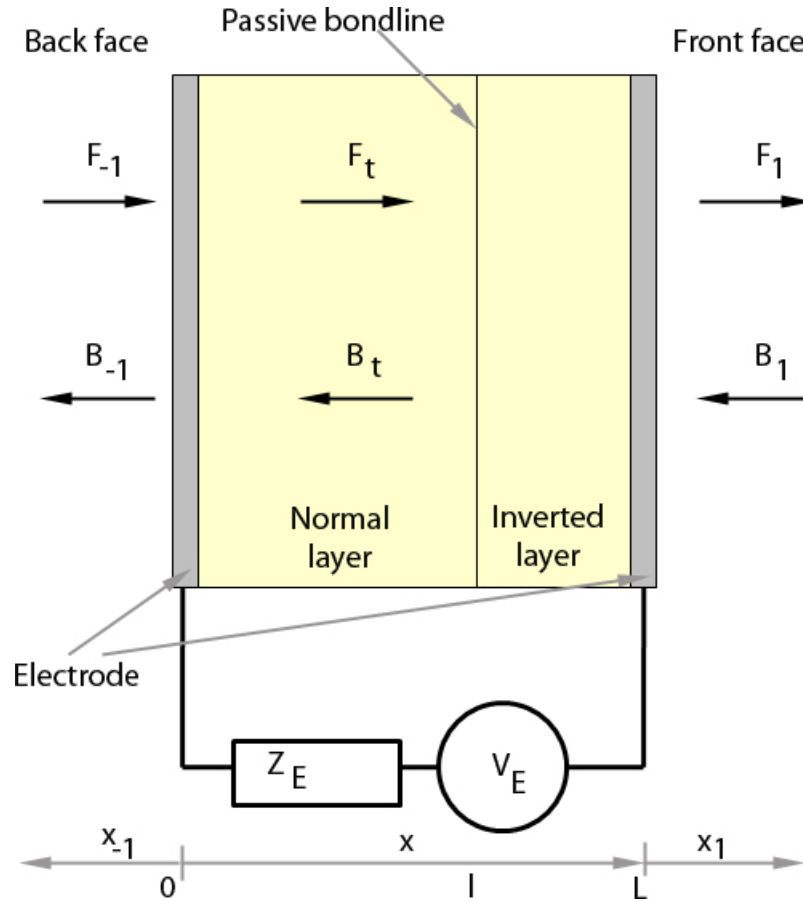
Figure 3.19: An inversion layer (IL) transducer configured as a transmitter

3.1.2.2 Lattice Model for Inversion Layer(IL) Transducers

The new systems methods developed in the previous section to simulate inversion layer devices have some limitations, and are not easily extendable to model transducers with multiple matching and backing layers. For this reason, an alternative lattice model for IL devices is proposed. This method is developed in similar fashion to the three-port systems model developed by Jackson [63, 62] for conventional single layer devices.

Consider the layered system shown in Figure 3.19, which depicts a two-layered system with the inversion layer at the front face. The transducer is connected to an arbitrary electrical load (Z_E) in series with a Thevenin equivalent voltage source (V_E). The piezoelectric structure is positioned between two semi-infinite media. All

media are assumed to be lossless and hence can be represented by their real specific acoustic impedances (Zj, where j represents the layer number). Similarly, the force componenets within each layer is denoted by a forward (denoted by Fj) and a backward travelling wave (denoted by Bj). Please note that for convenience the Laplace variable s is dropped from the remainder of this derivation, i.e. $Q_t(s)$ will now be denoted simply as Q_t.

For plane wave propagation in the thickness direction, the expressions for particle displacement and force within a piezoelectric medium [11] are given as follows:

$$\xi t = A_{ft}e^{-s(xt/vt)} + B_{bt}e^{s(xt/vt)} \tag{3.60}$$

$$\Gamma = sZ_t \left\{ -A_{ft}e^{-s(xt/vt)} + B_{bt}e^{s(xt/vt)} \right\} - hQ_t \tag{3.61}$$

Where f,b represent forward and backward travelling wave components, respectively.

At the interfaces between two adjacent layers, there is continuity of particle displacement and force. Applying these boundary conditions, we get the following relationships.

$$(-F_{-10} + B_{-10})/Z_{-1} = (-F_{t0} + B_{t0})/Z_t$$

$$(-F_{tl} + B_{tl}) = (-F_{t'0} + B_{t'0})$$

$$(-F_{t'l'} + B_{t'l'})/Z_t = (-F_{10} + B_{10})/Z_1$$

$$F_{-10} + B_{-10} = F_{t0} + B_{t0} - hQ_t$$

$$F_{tl} + B_{tl} - hQ_t = F_{t'0} + B_{t'0} + hQ_t$$

$$F_{t'l'} + B_{t'l'} + hQ_t = F_{10} + B_{10} \tag{3.62}$$

Where

F and B are the forward and backward force components in each layer

l, l′, and L are the normal, inversed and the whole device thicness, respectively

Equations 3.62 can be rearranged in a matrix form, as shown below

$$\begin{bmatrix} B_{-10} \\ F_{t0} \end{bmatrix} = \begin{bmatrix} R_{-1} & 1-R_{-1} \\ 1+R_{-1} & -R_{-1} \end{bmatrix} \begin{bmatrix} F_{-10} \\ B_{t0} \end{bmatrix} + \frac{hQ(t)}{2} \begin{bmatrix} 1-R_{-1} \\ -(1+R_{-1}) \end{bmatrix}$$

$$\begin{bmatrix} F_{10} \\ B_{t'l'} \end{bmatrix} = \begin{bmatrix} R_1 & 1-R_1 \\ 1+R_1 & -R_1 \end{bmatrix} \begin{bmatrix} B_{10} \\ F_{t'l'} \end{bmatrix} + \frac{hQ(t)}{2} \begin{bmatrix} (1-R_1) \\ -(1+R_1) \end{bmatrix}$$

$$B_{tl} = B_{t'0} + hQ_t$$

$$F_{t'0} = F_{tl} - hQ_t \tag{3.63}$$

Where $R_1 = (Z_t - Z_1)/(Z_t + Z_1)$ and $R_{-1} = (Z_t - Z_{-1})/(Z_t + Z_{-1})$ are the reflection coefficients for the waves of force reflected into the two piezoelectric media, at the front and rear faces respectively.

Also, the forward and backward travelling waves in any layer are given by the following Equation,

$$\begin{bmatrix} F_{il_i} \\ B_{il_i} \end{bmatrix} = \begin{bmatrix} e^{-sT_i} & 0 \\ 0 & e^{sT_i} \end{bmatrix} \begin{bmatrix} F_{i0} \\ B_{i0} \end{bmatrix} \tag{3.64}$$

Where the subscript i represents the layer number.

Equations 3.63 and 3.64 describe the system lattice for a front face ILT. It is now required to obtain the relation between source voltage and charge and incorporate this into the model. The overall voltage across the piezoelectric transducer [30] is given by

$$V = V_{\text{Normal}} + V_{\text{Inverted}}$$

$$= -h\{2\xi_{(x=l)} - \xi_{(x=0)} - \xi'_{(x=L)}\} + \frac{Q_t}{C_t} \tag{3.65}$$

From Figure 3.17, $I_t = -sQ_t$ and $V_t = V_E - I_t Z_E$. Substituting these in the Equation 3.65, Q_t can be expressed in terms of the drive voltage as

$$Q_t = \frac{C_t}{1 + sZ_E C_t}(V_E + h\{2\xi_{(x=l)} - \xi_{(x=0)} - \xi'_{(x=L)}\}) \tag{3.66}$$

Substituting Equation 3.62 in the previous Equation gives,

$$\begin{aligned} Q_t = &\frac{C_t}{1 + sZ_E C_t}(V_E + \frac{h}{sZ_t}\{(e^{-st'} - 1) \\ &(F_{t'l} + B_{t'L}) + (1 - e^{-st})(F_{t0} + B_{tl})\}) \end{aligned} \tag{3.67}$$

However, it is easier to measure voltage across the transducer than the charge on the electrodes. That is,

$$\begin{aligned} V_t = &\frac{V_E}{1 + sZ_E C_t} - \frac{hZ_E C_t}{Z_t(1 + sZ_E C_t)}\{(e^{-st'} - 1) \\ &(F_{t'l} + B_{t'L}) + (1 - e^{-st})(F_{t0} + B_{tl})\} \end{aligned} \tag{3.68}$$

Equation 3.68, along with Equations 3.63 and 3.64 can be represented in block diagram format as shown in Figure 3.20, which is a three-port system model with F_{-10}, B_{10} and V_E as the input ports and F_{10}, B_{-10} and V_t forming the output ports. The main advantage of this model is the lattice formulation, which facilitates the understanding of the fundamental physics behind a transduction process of an ILT device and which can incorporate multiple mechanical layers. Physical interpretation
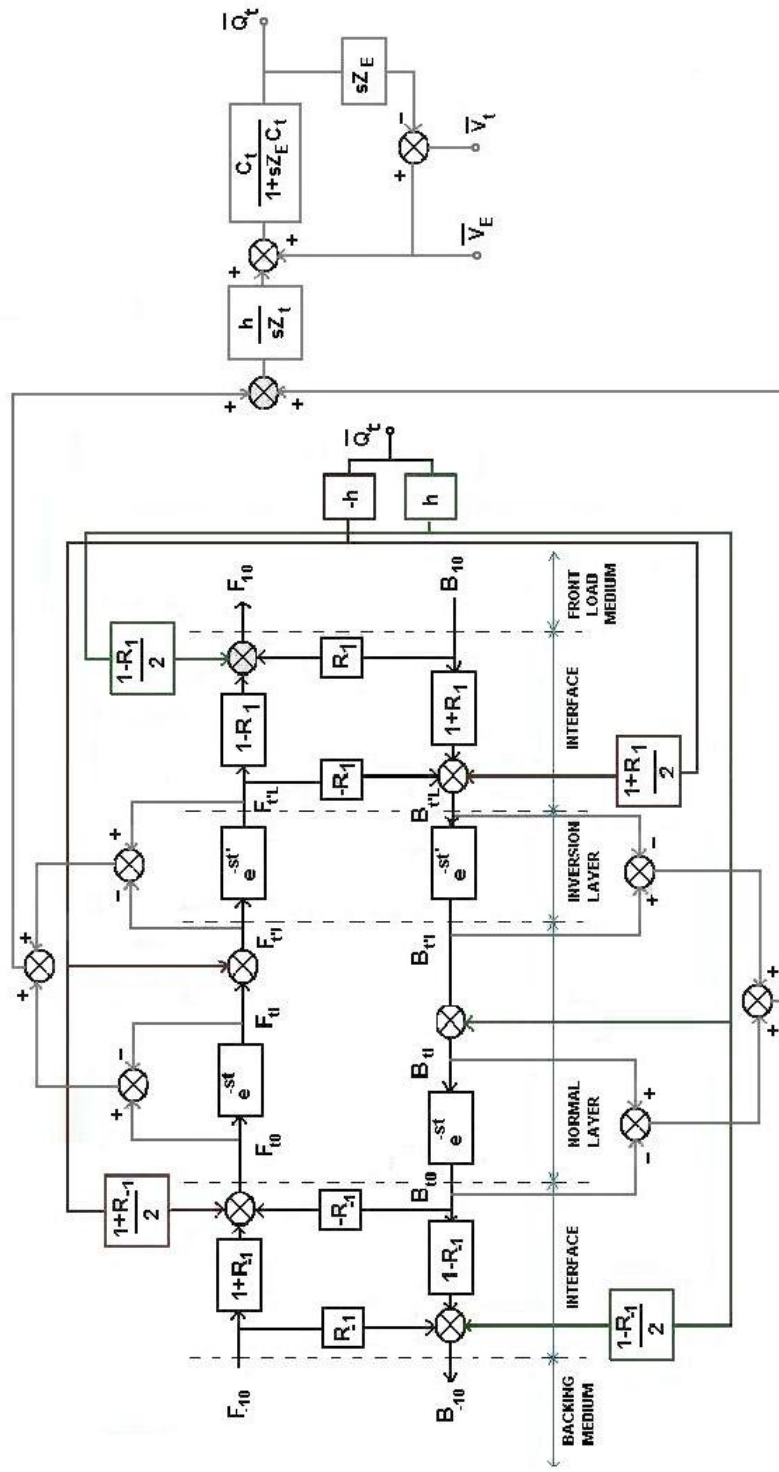
Figure 3.20: Lattice model for a FFIL device including electrical section of the system

69

of an ILT lattice can be carried out in similar fashion to [63] and the contribution of the inverted layer can be readily identified.

The model presented in Figure 3.20 is a general three port (two mechanical and one electrical) model that may be used for both transmit and receive cases. For illustration purpose, consider a transducer operating in reception mode. A portion of the incident force on the front face of the transducer (B_{10}) is transmitted into the transducer. Due to the direct piezoelectric effect, the mechanical stress waves within the transducer generate charge Q_t at the electrical port, which is modified by the external electrical load to produce a voltage V_t across the transducer. The secondary piezoelectric effect then produces feedback stresses at the device boundaries (i.e. the front face, back face and the boundary between the two active layers). It is important to note that the stress component travelling into the transducer structure (as a result of the secondary effect) from the outer two boundaries are infact produced by the inversion layer effect. This provides additional insight into working of an IL device and explains why the front face layer thickness plays a vital role in the device operational characterisitics (as shown by the systems model in the earlier section).

Also, alternative lattice formulations can be obtained easily from the system equations, which could further enhance the understanding of these devices. For example, the system equations shown in 3.67 and 3.68 can be rearranged into a form shown in Equations 3.69 and 3.70, for an alternative lattice formation.

$$Q_t = \frac{\frac{V_E C_t}{1+sZ_E C_t} + \frac{hC_t}{sZ_t(1+sZ_E C_t)}\{(1+R_1)(F_{t'L} - B_{10}) + (1+R_{-1})(F_{-10} - B_{t0}) + 2B_{t'l} - 2F_{tl})\}}{[1 - \frac{h^2}{2sZ_t}(\frac{C_t}{1+sZ_E C_t})(4 + R_1 + R_{-1})]} \tag{3.69}$$

$$V_t = \frac{V_E\{1 - (\frac{C_t}{sZ_t(1+sZ_E C_t)})(sZ_E + \frac{h^2}{2sZ_t}(4 + R_1 + R_{-1}))\} \frac{-hZ_E}{Z_t}(\frac{C_t}{1+sZ_E C_t})[(1+R_1)(F_{t'L} - B_{10}) + (1+R_{-1}) (F_{-10} - B_{t0}) + 2B_{t'l} - 2F_{tl})]}{1 - \frac{h^2}{2sZ_t}(\frac{C_t}{1+sZ_E C_t})(4 + R1 + R_{-1})} \tag{3.70}$$

This is a general lattice model which can be extended to a general multilayer case, with m matching and n backing layers, as shown in Figure 3.21, using approaches described in existing literature [63]. Where the W matrix describe the general 3-port lattice model described in 3.20, and matrices U^F and U^B model the acoustic wave propogation in the front and back face passive layers.
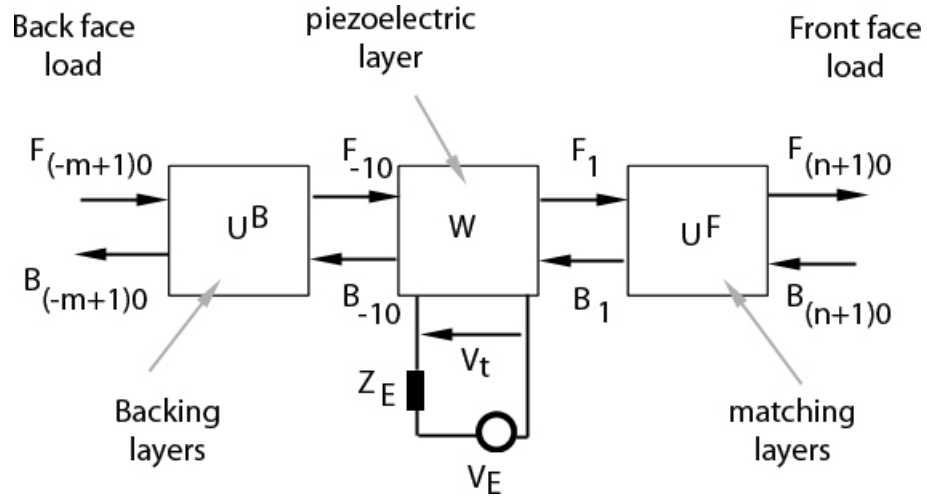
Figure 3.21: An illustration of a three port lattice model formulation for thickness mode transducer

3.1.3 Other multi-layer transducer configurations

One dimensional thickness mode multi layered piezoelectric transducers, are complex devices which can provide to improvement in both transducer bandwidth and sensitivity [33]–[34]. Some of the possible structures for such mechanically stacked thickness mode devices include all the piezoelectrically active layers connected electrically either in series (continuous current), parallel (common voltage across each piezoelectric layer), or independently (separate signals across each individual layer) as shown in Figure 3.22. Key modelling strategies to simulate such complex multi-layered thickness mode device configurations will be discussed in the following section.

3.1.3.1 Lewis Matrix inversion method

One of the most convenient approaches to simulate multiple active layer thickness mode devices is the Lewis Matrix inversion method [11]. This uses the fundamental piezoelectric equations shown:

$$\xi t = A_{ft} e^{-s(xt/vt)} + B_{bt} e^{s(xt/vt)} \tag{3.71}$$

$$\Gamma = sZ_t \left\{ -A_{ft} e^{-s(xt/vt)} + B_{bt} e^{s(xt/vt)} \right\} - hQ_t \tag{3.72}$$

Where f,b represent forward and backward traveling wave components respectively.

These fundamental wave equations are solved by applying relevant boundary conditions to obtain a set of simultaneous equations, which can be expressed in the matrix format A.X = B, where X contains the unknown variables to solve and can be obtained using matrix manipulation.
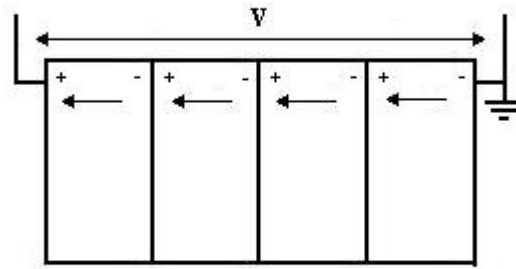
(a) Series excitation
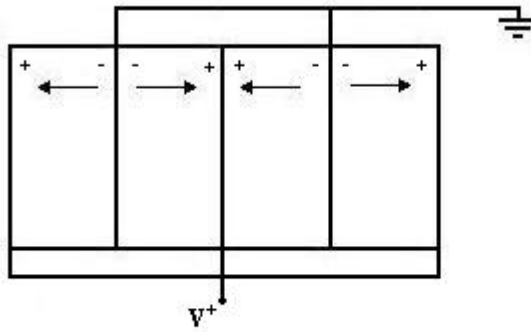
(b) Parallel excitation
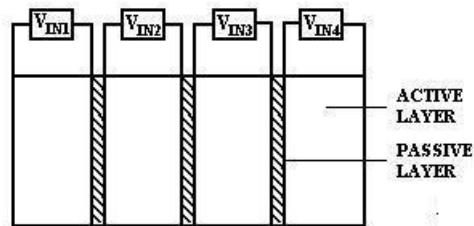
(c) Independent excitation

Figure 3.22: Different electrical excitation scenarios for a 1D stacked thickness mode piezoelectric transducer

However, straight forward application of this technique cannot be used for complex transducer configurations involving multiple active and passive layers. This requires solving a large set of simultaneous equations by matrix inversion, which often give inaccurate results, due to the fact that the matrices involved are badly conditioned. Figure 3.23 shows the transmit transfer function plot of a FFIL transducer with two passive matching and one backing layer configuration. It is clear from Figure 3.23, that the predicted impulse response is not very accurate, as it starts from a non zero value at the origin. To overcome this, the variables involved in the simultaneous equations need to be scaled, so we get a matrix which does not become singular upon inversion. To achieve this is, a dimensional analysis approach to scale variables, prior to matrix inversion is proposed. For example, the variables involved in a typical transducer system and their dimensional units are listed as follows,
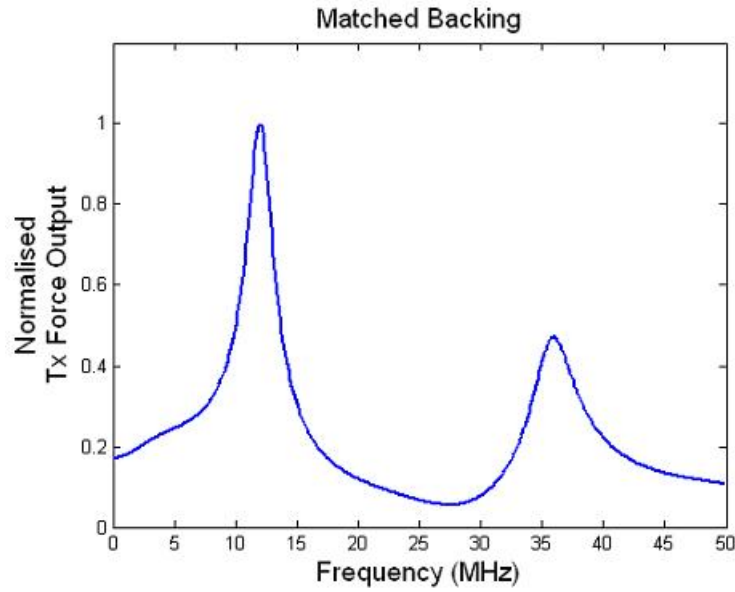
Figure 3.23: Transmit frequency response simulation of an IL device (incorporating 2 front face matching layers) performed using Lewis matrix inversion technique, prior to applying dimensional scaling technique

$$Z - \text{Specific Acoustic Impedance} - MT^{-1} \tag{3.73}$$

$$Z_E - \text{Electrical Impedance} - ML^2T^{-1}C^{-2} \tag{3.74}$$

74

$$h - \text{Piezoelectric Constant} - \text{MLT}^{-2}\text{C}^{-1} \tag{3.75}$$

$$C_0 - \text{Capacitance} - \text{M}^{-1}\text{L}^{-2}\text{T}^2\text{C}^2 \tag{3.76}$$

$$L - \text{Length} - \text{L} \tag{3.77}$$

$$v - \text{Velocity of Sound} - \text{LT}^{-1} \tag{3.78}$$

Where M= Mass (kg), L= Length (m), T=Time (s), and C=Charge (C).

Assume $\widehat{M} = \alpha M$, $\widehat{L} = \beta L$, $\widehat{T} = \gamma T$ and $\widehat{C} = \theta C$. Where α, β, γ and θ are the scaling factors, which for the IL case are obtained by solving the nonlinear simultaneous equations below,

$$Z : \widehat{M}\widehat{T}^{-1} = 1 \Rightarrow \alpha\gamma^{-1} = 10^{-3} \Rightarrow \alpha = 10^4 \tag{3.79}$$

$$Z_{\text{E}} : \alpha\beta^2\gamma^{-1}\theta^{-2} = 10^{-1} \Rightarrow \theta = 10^3 \tag{3.80}$$

$$C_0 : \alpha^{-1}\beta^{-2}\gamma^2\theta^2 = 10^{10} \Rightarrow \theta = 10^4 \tag{3.81}$$

$$h : \alpha\beta\gamma^{-2}\theta^{-1} = 10^{-10} \Rightarrow \theta = 10^4 \tag{3.82}$$

$$L : \beta = 10^4 \tag{3.83}$$

$$v : \beta\gamma^{-1} = 10^{-3} \Rightarrow \gamma = 10^7 \tag{3.84}$$

In the Equations (3.79-3.84), we have four unknowns. There is more than one solution to the above equations, considering one such solution, we get $\alpha = 10^4$,

$\beta = 10^4$, $\gamma = 10^7$, and $\theta = 10^4$. The scaling factors derived using this solution are listed as,

$$Z - \text{Specific Acoustic Impedance} - 10^4 10^{-7} = 10^{-3} \tag{3.85}$$

$$Z_E - \text{Electrical Impedance} - 10^4 10^8 10^{-7} 10^{-8} = 10^{-3} \tag{3.86}$$

$$h - \text{PiezoelectricConstant} - 10^4 10^8 10^{-7} 10^{-8} = 10^{-3} \tag{3.87}$$

$$C_0 - \text{Capacitance} - 10^{-4} 10^{-8} 10^{14} 10^8 = 10^{-10} \tag{3.88}$$

$$L - \text{Length} - [10^4] \tag{3.89}$$

$$v - \text{Velocity of sound} 10^4 10^{-7} = 10^{-3} \tag{3.90}$$

Figure 3.24 shows the transmit transfer function plot of the same IL device used for the initial simulation in Figure 3.23, after applying the dimensional scaling technique. The simulation indicates clearly that the results, have improved considerably. This is largely due to the fact the matrix inbalance during inversion operation is greatly reduced by scaling operation. However, the presence of a non zero value at the origin, indicates that the result is still not entirely accurate. This is not a surprise given the fact that the simultaneous equations in (3.79-3.84) do not have an unique solution. Trying to get the best scaling parameters in order to reduce inaccuracies in simulation is both time consuming and complex, and has to be performed for each different design case.
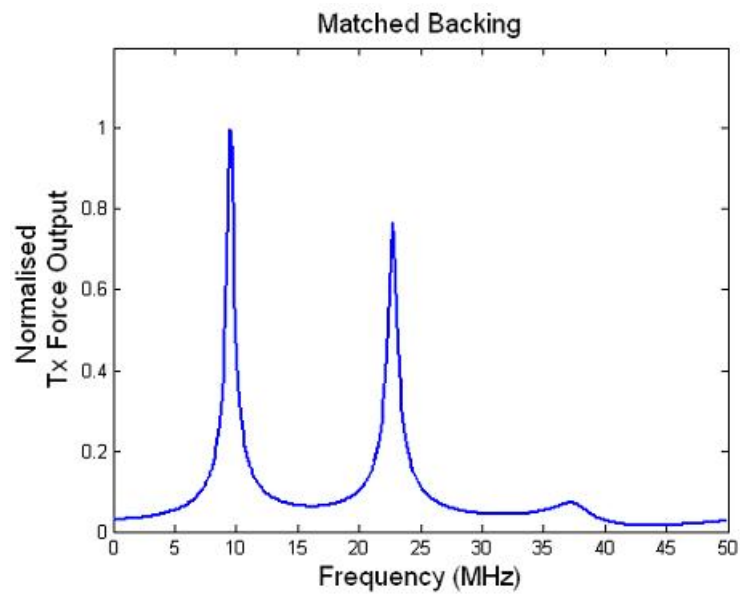
Figure 3.24: Improved frequency response simulation after performing matrix scaling prior to inversion operation ($\alpha = 10^4, \beta = 10^4, \gamma = 10^7, \text{and} \theta = 10^4$)

3.1.3.2   Simplified analytical model using rank reduction

One of the simplest analytical models for simulation of multilayer transducers is the rank reduction method proposed by Huang et al [43]. For example, consider an ILT system as shown in Figure 3.25, consisting of two active layers a and b, forming the front and back face of the transducer respectively. a1,a2...aM denote the passive layers attached to the a layer and similarly b1,b2....bN denote the layers attached to the back face active layer b. Note that the layers a and b are made up of the same material, but with opposing piezoelectric polarisation. Consequently, there are two configurations possible, i.e. the inverted layer positioned at the front face (FFIL) or at the back face (BFIL) of the transducer. Only the BFIL configuration is presented in remainder of this section to define the mathematical model.

The wave equation representing a multi layer ultrasonic system (in Figure 3.25) is shown below:

$$M_{bN}G_{bN}^{-}x_{bN} = M_{b(N-1)}G_{b(N-1)}^{+}x_{b(N-1)}$$

$$M_{b(N-1)}G_{b(N-1)}^{-}x_{b(N-1)} = M_{b(N-2)}G_{b(N-2)}^{+}x_{b(N-2)}$$

$$M_{b2}G_{b2}^{-}x_{b2} = M_{b1}G_{b1}^{+}x_{b1}$$

$$M_{b1}G_{b1}^{-}x_{b1} = M_{b}G_{b}^{+}x_{b} - s$$

$$M_{b}G_{b}^{-}x_{b} - s = M_{a}G_{a}^{+}x_{a} + s$$

$$M_{a}G_{a}^{-}x_{a} + s = M_{a1}G_{a1}^{+}x_{a1}$$

$$M_{a1}G_{a1}^{-}x_{a1} = M_{a2}G_{a2}^{+}x_{a2}$$

$$M_{a(M-2)}G^-_{a(M-2)}x_{a(M-2)} = M_{a(M-1)}G^+_{a(M-1)}x_{a(M-1)}$$

$$M_{a(M-1)}G^-_{a(M-1)}x_{a(M-1)} = M_{aM}G^+_{aM}x_{aM} \tag{3.91}$$

Where the diagonal matrix M contains all the matching layer properties (acoustic impedance), G contains layer geometry (i.e. thickness) information, and x is the unknown variable vector to be solved.
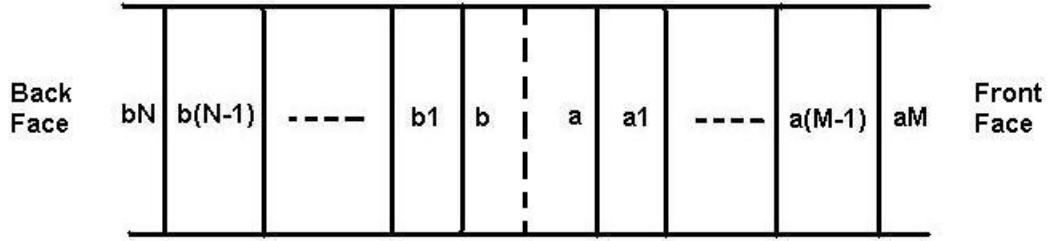
Figure 3.25: An inversion layer transducer with multiple matching and backing layers, where ai and bi denote the passive layers at the front and back face, respectively

Using rank reduction, the total number of equations can be reduced as shown below

$$T^-_b M_{bN} G^-_{bN} x_{bN} = M_b G^+_b x_b - s$$

$$M_b G^-_b x_b - s = M_a G^+_a x_a + s$$

$$M_a G^+_a x_a + s = T^+_a M_{aM} G^+_{aM} x_{aM} \tag{3.92}$$

Where T^+_a and T^-_b represent the lumped transmission matrix for the front and back matching layers.

These equations in reduced form can be expressed in the form Ax = b, or written

explicitly as shown below,

$$
\begin{pmatrix}
a_{11} & 0 & -c_a^- & -is_a^- & 0 & 0 \\
a_{21} & 0 & -is_a^- & -c_a^- + k_T^2\mu_a & 0 & k_T^2\mu_b \\
0 & a_{32} & 0 & 0 & c_b^+ & is_b^+ \\
0 & a_{42} & 0 & +k_T^2\mu_a & is_b^+ & c_b^+ - k_T^2\mu_b \\
0 & 0 & -c_a^+ & -is_a^+ & c_b^- & is_b^- \\
0 & 0 & -is_a^+ & -c_a^+ + 2k_T^2\mu_a & is_b^- & c_b^- - 2k_T^2\mu_a
\end{pmatrix}
\begin{pmatrix}
A'_{aM} \\
B'_{bN} \\
H_a \\
F_a \\
H_b \\
F_b
\end{pmatrix}
=
\begin{pmatrix}
0 \\
1 \\
0 \\
1 \\
0 \\
2
\end{pmatrix}
\quad (3.93)
$$

Where variables as described in [43] are $c_j^\pm = \cos(\pm\alpha_j/2)$, $s_j^\pm = \sin(\pm\alpha_j/2)$, j indicates layer number, α is the phase angle for the entire piezoelectric layer, $\mu_a = (2\sin(\alpha_a/2))/\alpha$, $\mu_b = (2\sin(\alpha_b/2))/\alpha$, and variables $\{a_{11}, a_{21}, a_{32}, a_{42}\}$ are functions of lumped transmission matrix T.

Using Cramer's rule Equation 3.93 can be solved for unknown variables. For example, to calculate the force output at the front face.

$$
F_a = \frac{C_4}{C + k_T^2\mu_a C_4 - k_T^2\mu_b C_6} \quad (3.94)
$$

$$
C = (c_1 \ c_2 \ c_3 \ c_4 \ c_5 \ c_6) \quad (3.95)
$$

$$
=
\begin{pmatrix}
a_{11} & 0 & -c_a^- & -is_a^- & 0 & 0 \\
a_{21} & 0 & -is_a^- & -c_a^- & 0 & 0 \\
0 & a_{32} & 0 & 0 & c_b^+ & is_b^+ \\
0 & a_{42} & 0 & 0 & is_b^+ & c_b^+ \\
0 & 0 & -c_a^+ & -is_a^+ & c_b^- & is_b^- \\
0 & 0 & -is_a^+ & -c_a^+ & is_b^- & c_b^-
\end{pmatrix}
$$

Also, using the simplified rank reduced system model, it is relatively straight forward to calculate the electrical impedance and efficiency of the transducer

$$
Z = \frac{V}{I} = \frac{1}{iwC_0} \cdot \frac{1}{1 + k_T^2\mu_b F_b - k_T^2\mu_a F_a} \quad (3.96)
$$

Where K_T^2 is the electromechanical coupling coefficient, and C_0 is the clamped capacitance of the entire piezoelectric layer.

To illustrate the concept, the model was coded and implemented in MATLAB environment. Results for a 50% 1-3 piezoelectric disc transducer, containing a front face inversion layer is presented. Simulations of operational impedance, device thermal noise and transmit impulse response are shown in Figure 3.26. One of the main advantages of this model is that the device operational impedance can be expressed as a sum two terms; a classical motional impedance (X1) and a coupled motional impedance (X2) due to the presence of an inversion layer.

$$Z(\omega, \chi_b) = 1/(i\omega C_0) + X1(\omega) + X2(\omega, \chi_b)$$

where χ_b is the thickness ratio of the inverted layer. This approach is useful in analysing the influence of the inverted layer on the overall system behaviour. The transducer thermal noise is proportional to the real part of the device operational impedance in Figure 3.26(b), as shown by [77]. A detail introduction into modelling noise within a transducer system is presented in Chapter 5.

3.1.4   Implementing loss in linear systems models

One of the key assumptions in all the transducer models included in the proposed software is that the transducer and all the surrounding media are lossess. Although this can be justified experimentally for a limited set of transducer types (i.e. PZT device operating under water load conditions), implementing loss is extememly important to simulate the device behaviour more accurately, for a more wider application. The three main type of loss in such transducers are:

1. Mechanical losses

2. Dielectric losses
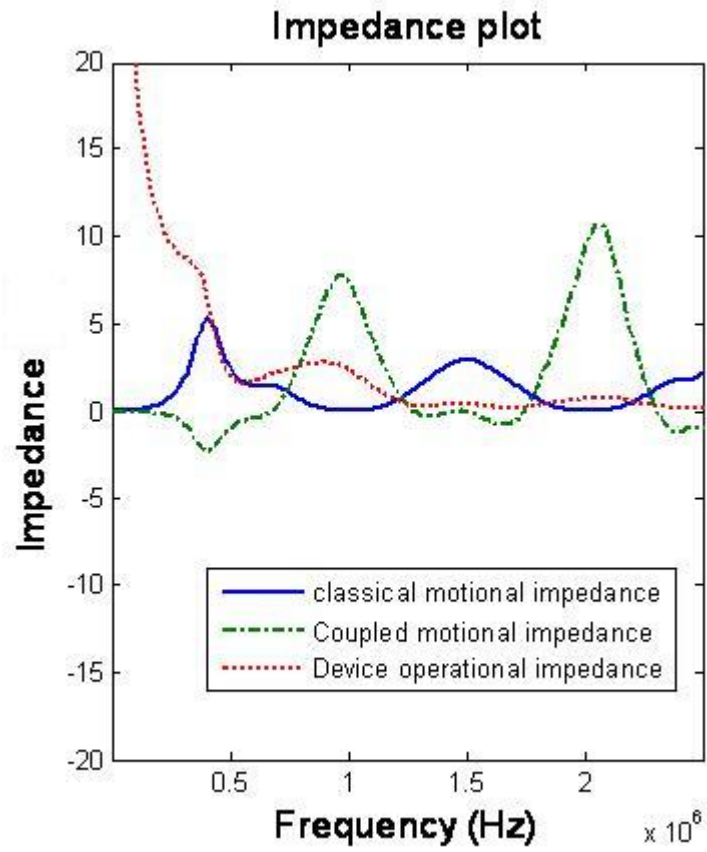
(a) Operational impedance plot
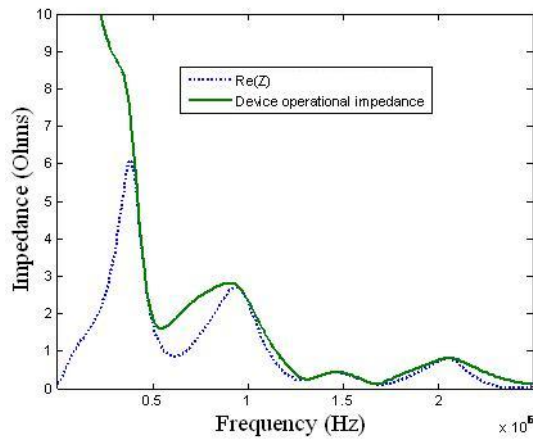
(b) Real part of device operational impedance which is proportional to the transducer's thermal noise

Figure 3.26: 1MHz FFIL transducer simulation

82

3. Piezoelectric losses

In order to account for loss in the linear systems models included in the proposed software, the overall attenuation with distance could be modelled in the active layer by a loss factor α, as shown in [66]. In other words, all e^{-sT} terms in the transducer system equations are replaced with the term $e^{-sT}e^{-\alpha L}$, where L is the length of the layer, s the complex frequency, and T the transit time in that layer. Also, the dielectric losses present in the active piezoelectric layer(s) are modelled through the use of complex clamped capcitance, as shown in the equation below:

$$C_0 = (\epsilon_r \epsilon_0 A (1 - j \tan(\delta)))/d \qquad (3.97)$$

Where ϵ_r is the relative clamped permittivity

ϵ_0 is the permittivity of freespace

t is the active layer thickness and

$\tan(\delta)$ represent the loss tangent

Only mechanical loss is present in all the passive (i.e. matching and backing) layers for a given frequency and can be calculated by stiffened wave velocity, as shown below:

$$Z_{mech} = Ar\rho v_{Re}(1 - j/(2Q_m)) \qquad (3.98)$$

Where Z_{mech} is the complex impedance term

Ar is the transducer surface area

v_{Re} is the real part of the stiffened wave velocity

$Q_m = 4.343(2\pi f)/(c\alpha)$ is the loss quality factor

f is the frequency

c is the longitudinal wave speed in the layer

α is the measured attenuation (dB/unit length)

This approach, although by no means comprehensive, offers encouraging results. Figure 3.27 shows an improvement in simulation performance by including loss in a conventional transducer Linear System Model (LSM). A loss factor $\alpha = 5$ dB/m and $\tan(\delta) = $ 20e-3 is used in the above simulation. Implementing loss mechanisms within these models will make them more comparable with experiments, and help to minimise exaggerated peaks appearing in such LSM models. However, further investigation is required to validate, refine and develop more accurate modelling of loss and extend this to all the approximate analytical models included in the proposed software.
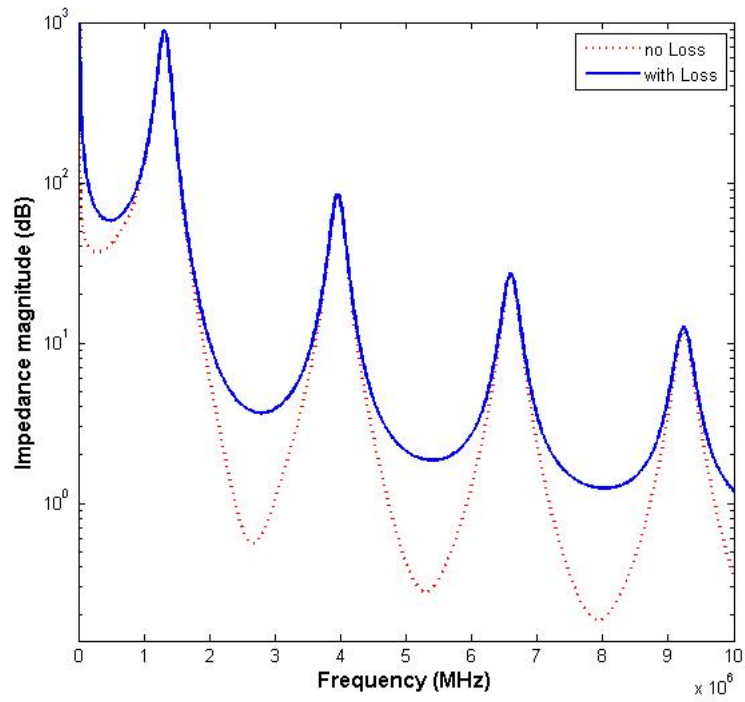
(a) Operational impedance comparison of a lossy and lossless simulation result
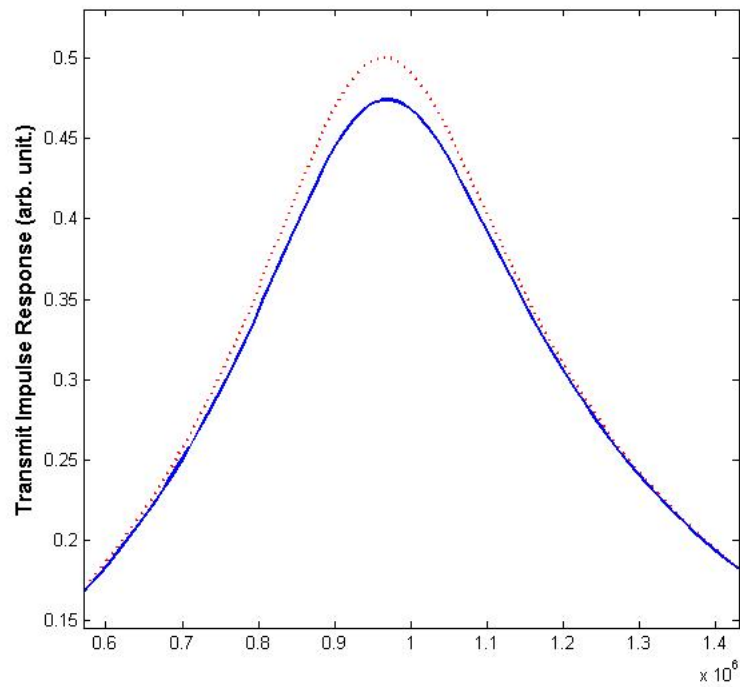
(b) Transmit frequency response prediction using a lossless (dotted) and a lossy (solid line) linear systems model

Figure 3.27: A comparison analysis of a lossy and lossless LSM model for a 1MHz conventional transducer design

3.1.5 Modelling ultrasonic arrays

An array transducer [38] is simply an instrument made-up of number of individual piezoelectric elements (typically from 16 to 256) in a single housing. In other words, array transducers are a cluster of miniature piezoelectric elements and each element is wired and addressed individually via an array controller, to produce the desired ultrasound beam. Such array devices come in a wide range of sizes and shapes, such as a 1 dimensional (1D) linear array, a 2 dimensional (2D) matrix array, a circular array, or a more complex form. Figure 3.28 illustrates some of the common element patterns used in array transducer construction.
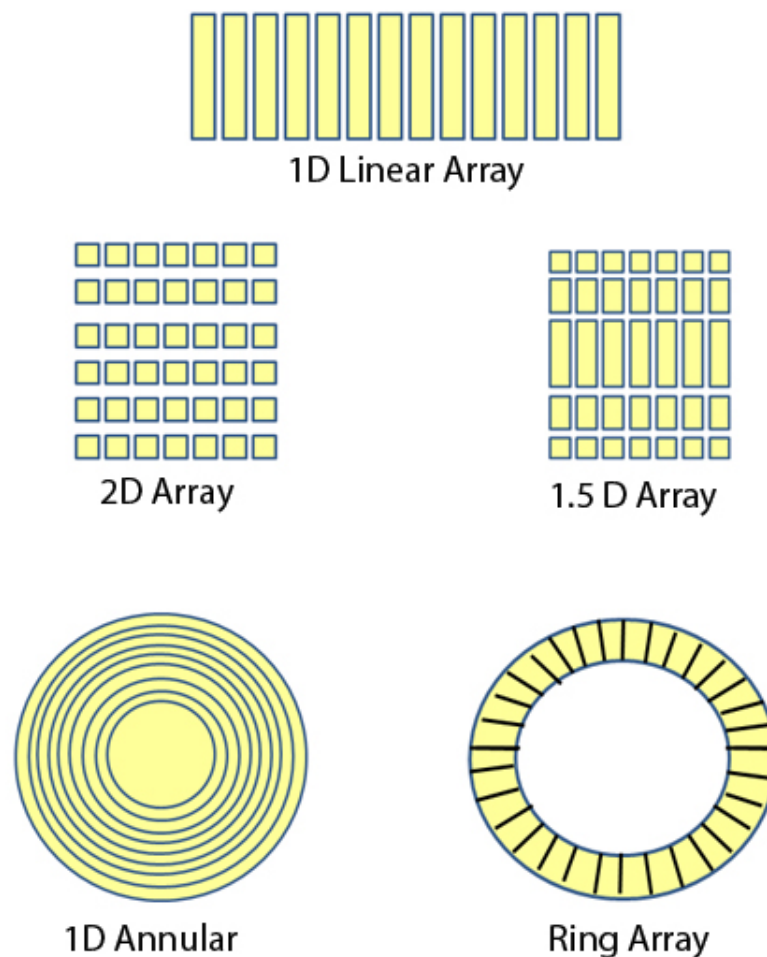
Figure 3.28: Common element configurations (or footprints) used in array transducers

Array transducers offer significant technical advantages over conventional single-probe ultrasonics; mainly:

1. Electronic scanning (permits beam manipulation)

2. Dynamic focusing (one device can focus at several depths through a sample, leading to faster inspection of the volume of thick samples, and improve signal-to-noise ratio (which in turn, permits operating at lower pulser voltages))

3. Electronic beam steering (also referred to as S-scans) - one device can inspect a sample at different angles - faster inspection of complex geometries

However, all these technical advantages mentioned come at the price of manufacturing complexity and cost. Even while considering a simple 1D linear array configuration, the array elements should be spaced no further than half wavelength distance to avoid any grating lobes, a form of aliasing caused by the periodic spacing of the array elements. At the same time, a wide spatial extension is required to achieve high resolution. Satisfying these two key requirements is costly and often prohibitive in array configurations.

Also, the lateral resolution of an one dimensional array is directly dependent on the array aperture size. Figure 3.29 shows a simulation illustrating the effect of array beamwidth as a function of array aperture size. Nevertheless, not all problems are worth the investment in time and instrumentation to use array instrumentation. Consequently, it is desirable to minimise number of elements in an array, as more elements mean more array controller channels, increasing expense of the device. Increasing the element spacing in an array would minimise the element count. However, it introduces undesirable grating lobes, when the element pitch is greater than $\lambda/2$, as mentioned earlier. Figure 3.30 shows the effect of a grating lobe introduced in the array field profile as a result of having larger element spacing instead to $\lambda/2$ spacing.

One of the most promising approaches to reducing the number of array elements is to make the array structure non periodic [41]—-[42], wherein a fully sampled array is thinned by removing a fraction of the original set of elements, thus obtaining a sparse array element layout. Because of the non periodic nature of the array layout, aliasing effects are not present in such sparse array configurations. The main drawback however, is an often unacceptable high level of the side lobes present in the beam pattern. This highlights the need for the proposed transducer design tool to include an accurate simulation model for such sparse array configurations, in order to optimise their design to match specific application requirement.
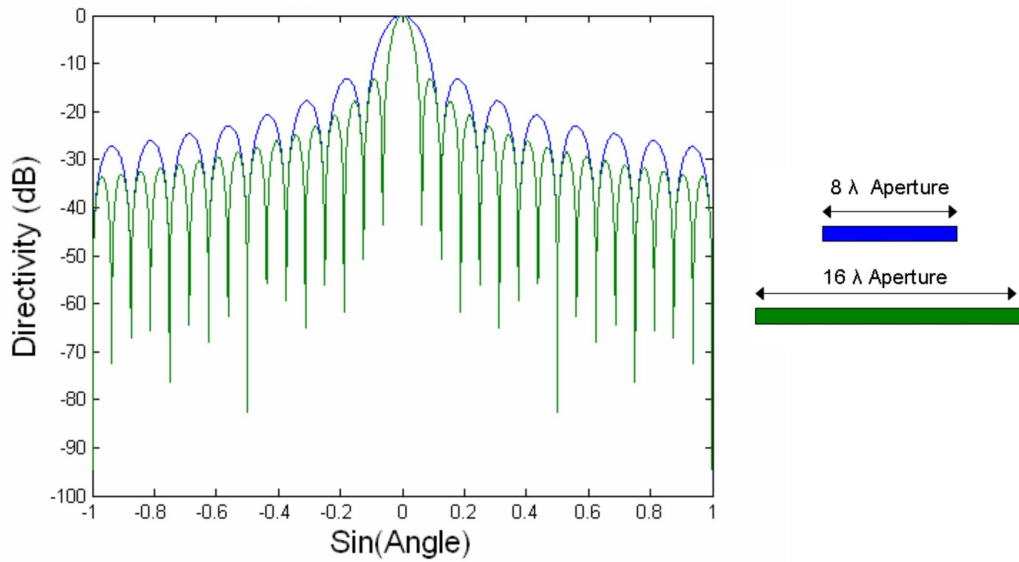
Figure 3.29: Effect of array aperture on bandwidth

In the proposed design tool the representation of the transducer structure is allied to a wave propagation model in order to analyse both monolithic and array configurations operating into a variety of media. For example, in order to model one-dimensional arrays, the directivity of each array was calculated using the discrete Rayleigh integral, which is a mathematical representation of Huygens principle [39]. The field was calculated at a fixed radius in the far field, with the angle to the normal varied from -90 to 90 degrees to provide a relative measure of directivity. Continuous wave (cw) operation at the center frequency was modelled, as this gives
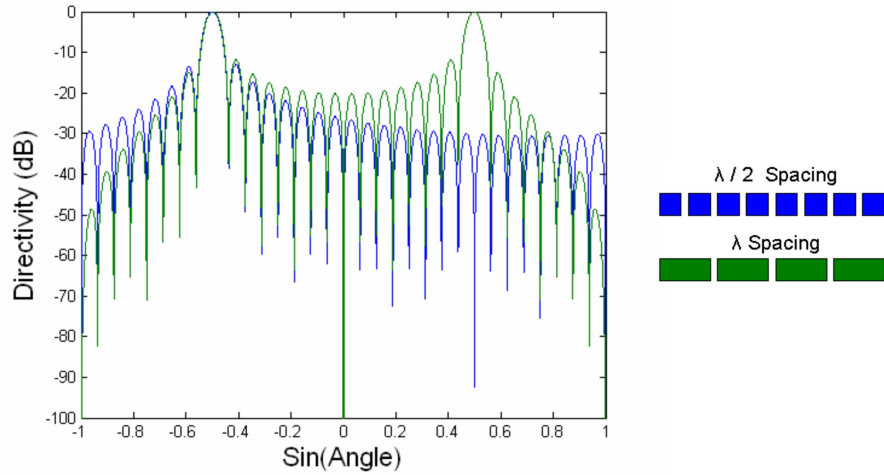
Figure 3.30: An example to illustrate grating lobes in array directivity profile

a good approximation of pulsed beam performance, but requires considerably less computation. The relative pressure field under cw operation can be expressed as in Equation 3.99:

$$P_r(f) = \sum_t \frac{e^{jKR(t,f)}}{R(t,f)} \qquad (3.99)$$

Where, P_r is the relative pressure at the field point f

K is the wavenumber

R is the distance from the transducer point t to f

MATLAB scrips were developed to take array element positions as inputs and predict the spatial response (i.e. beam pattern) of the device and calculate its beamwidth and sidelobe levels. Figure 3.31 shows the predicted field response for a 32 element 1D sparse array configuration, using the model described in this section. The array layout is optimised in this case to reduce the sidelobe levels and to satisfy a design criterion that the array be able to steer between ±20degrees. As indicated in Figure

3.31, for the optimum layout design, the sidelobe levels are reduced to about 18 dB, while satisfying the design requirement.
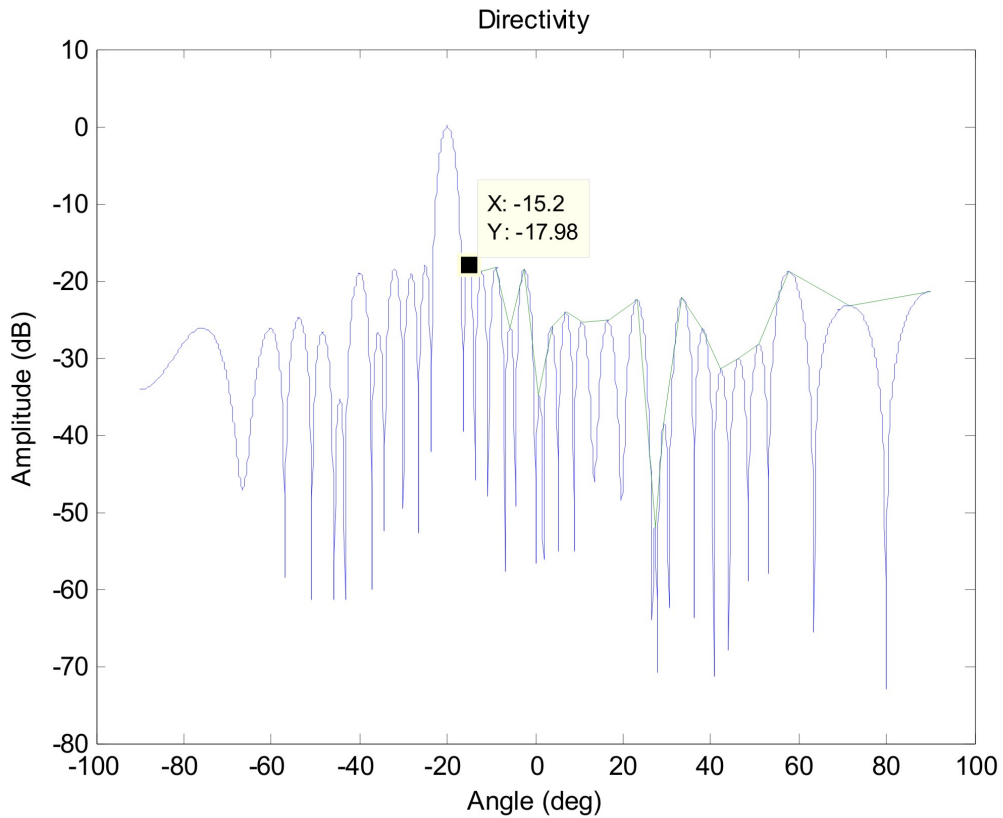
Figure 3.31: Predicted beam profile plot for a 32 element array, optimised to reduce sidelobe level

3.2   Summary

A brief discussion on different ways to model thickness mode transducers has been presented. This was followed by a detailed description of new models developed during the course of this research. Some issues faced while modelling more complex transducer models and the suggestions for overcoming these artifacts were discussed. At the present stage of development for illustration purposes, only a limited set of transducer models are included in the proposed software, this include conventional devices, ILTs, series excited stacked devices and 1D arrays.

Also, all the linear systems models programmed into the proposed transducer design software include the assumption that the transducer and all surrounding media are lossless. Although a loss free model is justifiable to model a limited set of transducer configurations, such an approach is not applicable to model transducer construction incorporating piezocomposites and lossy passive materials (such as crown glass). Consequently, it is vital to implement loss in these analystical models for more wider application. Extending the 1D linear systems model to loss is presented in Chapter 8.

The details of an analogue filter design technique applied to design matching layer schemes and ways to experimentally validate it during manufacture is presented in the following chapter.

Chapter 4

Matching layer design using analogue filter design techniques

A typical thickness mode transducer will have an acoustic impedance around 16 to 30 MRayl, and using such devices in low impedance loads such as water and human tissue (approximately 1.5 MRayl) will make the device usable only in a very narrow band of frequencies due to the mechanical mismatch. Designing and optimising matching layers will greatly increase the operational bandwidth and efficiency of a transducer and has to be considered carefully at any design stage. This chapter presents an analogue filter technique approach to design and optimise multiple matching layer for thickness mode transducers. Finally, an experimental procedure to validate matching layer structure and its bond quality, during the transducer manufacture is discussed.

4.1 Using analogue filter design techniques to design matching layer impedance profiles

Several authors have proposed different methods for calculating optimum values for intermediate acoustic matching layers and hence overcome the impedance mismatch problem. Notably, Lewis [11] and Desilets [12] used multiple matching layers with each layer impedance being a fixed percentage lower or higher than the preceding one. That is, for an n layer system to match two impedances Z_C and Z_L, the intermediate layer impedances are given by $Z_{i+1} = a\, Z_i$, where $a = \sqrt[n+1]{Z_L/Z_C}$. Also, multiple quarter wave length transformers and analog filter techniques such as Chebyshev type I and II, Binomial transforms, have been studied in depth for many years for electrical impedance matching problems [12], [19]. The suitability of applying similar methods of designing filters to the problem of acoustic matching will be studied.

This section details the application of such analogue filter techniques to design matching layer acoustic impedance profiles effectively for a transducer system. To facilitate the design process, a graphical user interface is built into the proposed software to design matching layer impedance profiles. The mathematical basis [19] of analogue filter design techniques and how they can be used to efficiently design matching layers will now be presented, together with design examples and simulations.

Any load impedance Z_L can be transformed into an input impedance Z_1, via a transmission line with characteristic impedance Z_2, phase constant β, and length l, as shown below,

$$Z_1 = Z_2 \frac{Z_L + jZ_2 \, \tan\beta l}{Z_2 + jZ_L \, \tan\beta l} \tag{4.1}$$

Alternatively, the reflection coefficient at given length l is given by

$$\Gamma_l = \frac{Z_{1l} - Z_2}{Z_{1l} + Z_2} \qquad (4.2)$$

Using Equation 4.2, the normalised input and load impedance in terms of the reflection coefficient can be written as shown,

$$\hat{Z}_1 = \frac{Z_1}{Z_2} = \frac{1 + \Gamma_l}{1 - \Gamma_l} = \frac{1 + \Gamma_L \ e^{-2j\beta l}}{1 - \Gamma_L \ e^{-2j\beta l}}$$

$$\hat{Z}_L = \frac{Z_L}{Z_2} = \frac{1 + \Gamma_L}{1 - \Gamma_L}$$

Where Γ_L is the reflection coefficient of the load.

Quarter wave transformers (QWT) are used primarily to match two waveguiding systems having different characteristic impedances. If the transmission line is considered to be a QWT and the load to be purely resistive, Equation 4.1 then becomes,

$$Z_1 = Z_2 \frac{Z_L + j \ Z_2 \ \tan\beta \ \frac{\lambda}{4}}{Z_2 + j \ Z_L \ \tan\beta \ \frac{\lambda}{4}} = \frac{Z_2^2}{Z_L} \qquad (4.3)$$

By considering the matching impedance to be the geometric mean of the transducer and load impedances, (i.e) $Z_2 = \sqrt{Z_1 \ Z_L}$, then the load is matched perfectly to the main line. However, this condition is only obtained at the frequency for which the transformer is $\frac{\lambda}{4}$ or $(n\frac{\lambda}{2} + \frac{\lambda}{4}, n = 0, 1, 2, ...etc)$ long. Consequently, the reflection coefficient can be obtained by

$$\Gamma = \frac{Z_L - Z_2}{Z_L + Z_1 + j(\tan\beta l)2\sqrt{Z_1 Z_L}} \qquad (4.4)$$

From this equation the magnitude of Γ can be evaluated easily and is given by [19],

$$|\Gamma| = R = \frac{|Z_L - Z_1|}{2\sqrt{Z_1 Z_L}} |\cos\theta| \qquad (4.5)$$

94

Where $\theta = \beta l$ is the electrical length of the transformer for a given frequency f.

From Equation 4.5, the value of θ at the 3/6dB cutoff point is given by,

$$\theta_{\mathrm{m}} = \mathrm{Cos}^{-1} \left| \frac{2R_{\mathrm{m}}\sqrt{Z_1 Z_{\mathrm{L}}}}{(Z_{\mathrm{L}} Z_1)\sqrt{1 - R_{\mathrm{m}}^2}} \right| \tag{4.6}$$

Where R_{m} is the maximum value of reflection coefficient that can be tolerated.

The plot as shown in Figure 4.1 between the reflection coefficient R against θ (in other words frequency), illustrates the bandwidth characteristics of a single QWT matching layer. It can be noted that the variation of R with frequency is periodic, and also the useful bandwidth is small (as R increases rapidly on either side of the centre frequency f_0, where $\theta = \pi/2$). The bandwidth (Δf) and fractional bandwidth (fb) can be evaluated using the following equations, respectively

$$\Delta f = 2\,(f_0 - f_{\mathrm{m}}) = 2\,(f_0 - \frac{2f_0}{\pi}\theta_{\mathrm{m}}) \tag{4.7}$$

$$fb = \frac{\Delta f}{f_0} = 2 - \frac{4}{\pi}\mathrm{Cos}^{-1} \left| \frac{2R_{\mathrm{m}}\sqrt{Z_1 Z_{\mathrm{L}}}}{(Z_{\mathrm{L}} Z_1)\sqrt{1 - R_{\mathrm{m}}^2}} \right| \tag{4.8}$$
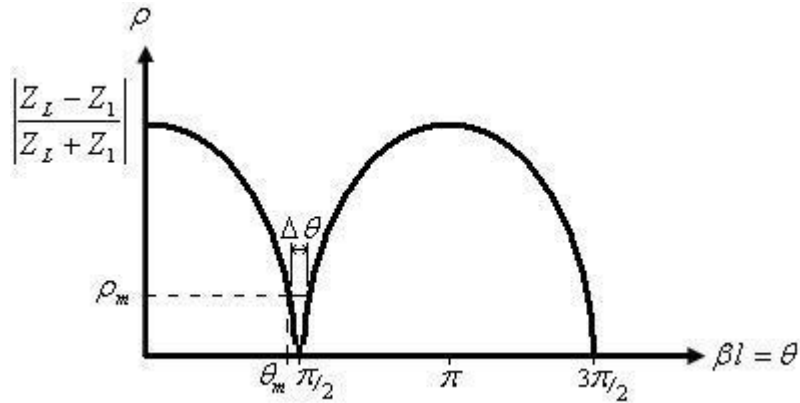
Figure 4.1: Bandwidth characteristics of a single section QWT transformer

Often matching a narrowband frequency is not sufficient for most practical applications and as a result, two, three, or more intermediate matching layers have to be

95

used to achieve acoustic matching over wide frequency range. Consider an N section QWT as shown in Figure. 4.2, the reflection coefficient at each section is given by

$$\Gamma_i = \frac{Z_{i+1} - Z_i}{Z_{i+1} + Z_i} \qquad (4.9)$$

Where i is the section number
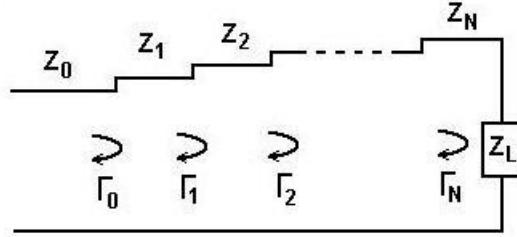
Figure 4.2: N section QWT transformer

The total reflection coefficient in a N section QWT is given by,

$$\Gamma = R_0 + R_1 e^{-2j\theta} + R_2 e^{-4j\theta} + \ldots + R_N e^{-2jN\theta} \qquad (4.10)$$

Note in the Equation 4.10 $Z_L < Z_0$, and if we assume that the transformer is symmetric, that is, $R_0 = R_N, R_1 = R_{N-1}, R_2 = R_{N-2}, \ldots$, then the Equation 4.10 becomes

$$\Gamma = e^{-jN\theta}[R_0(e^{jN\theta} + e^{-jN\theta}) + R_1(e^{j(N-2)\theta} + e^{-j(N-2)\theta}) + \ldots$$

$$\ldots + R_{\frac{N-1}{2}}(e^{j\theta} + e^{j\theta}) \text{ or } R_{\frac{N}{2}} \qquad (4.11)$$

$$\Gamma = 2e^{-jN\theta}[R_0 \cos(N\theta) + R_1 \cos((N-2)\theta) + \ldots$$

$$\ldots + R_n \cos((N-2n)\theta) + \ldots + R_{\frac{N-1}{2}} \cos(\theta) \text{ or } \frac{1}{2}R_{\frac{N}{2}} \qquad (4.12)$$

96

By varying R_n, a variety of pass band characteristics can be obtained. For example, to get a maximally flat response, a Binomial or Butterworth transformation can be used and for a equal ripple feature, the Chebyshev filter design technique can be used.

4.2   Binomial transformer

Maximally flat passband characteristics [19] are obtained, if $R = |r|$ and the first $(N - 1)$ derivatives with respect to frequency varies at $\theta = \frac{\pi}{2}$ (the matching frequency). Such characteristic can be obtained when

$$\Gamma = A(1 + e^{-2j\theta})^N \Rightarrow R = |\Gamma| = \left| A2^N (\cos\theta)^N \right| \tag{4.13}$$

Where $A = 2^{-N}(Z_L - Z_0)/(Z_L + Z_0)$

Expanding Equation 4.13 by binomial expansion, gives

$$\Gamma = 2^{-N}\left(\frac{Z_L - Z_0}{Z_L + Z_0}\right)(1 + e^{-2j\theta})^N = 2^{-N}\frac{Z_L - Z_0}{Z_L + Z_0}\sum_{n=0}^{N} C_n^N e^{-j2n\theta} \tag{4.14}$$

Where $C_n^N = N!/((N - n)!n!)$

The characteristic impedance Z_n can be obtained from a simple approximate solution to the above equation,

$$\ln\frac{Z_{n+1}}{Z_n} = 2R_n = 2^{-N}C_n^N \ln\frac{Z_L}{Z_0} \tag{4.15}$$

For example, consider a two section transformer example. From Equation 4.15,

$$\ln\frac{Z_1}{Z_0} = \frac{1}{4}\ln\frac{Z_L}{Z_0} \Rightarrow Z_1 = Z_L^{\frac{1}{4}}Z_0^{\frac{3}{4}} \tag{4.16}$$

97

$$\ln \frac{Z_2}{Z_1} = \frac{1}{2} \ln \frac{Z_L}{Z_0} \Rightarrow Z_2 = Z_L^{\frac{3}{4}} Z_0^{\frac{1}{4}} \qquad (4.17)$$

θ_m and fractional bandwidth can be calculated using the following relationship,

$$\theta_m = \cos^{-1} \left| \frac{2R_m}{\ln \frac{Z_L}{Z_0}} \right|^{\frac{1}{N}} \qquad (4.18)$$

$$\frac{\Delta f}{f_0} = \frac{2(f_0 - f_m)}{f_0} = 2 - \frac{4}{\pi} \cos^{-1} \left| \frac{2R_m}{\ln \frac{Z_L}{Z_0}} \right|^{\frac{1}{N}} \qquad (4.19)$$

Where R_m is the maximum value of R that can be tolerated (typically $R_m = 0.1$).

As may be seen from the pass band characteristics of a two section binomial transformer shown in Figure 4.3, the band width is more than a single QWT matching layer shown in Figure 4.1. The operational bandwidth can still be improved by allowing additional ripple in the pass band. This can be achieved by using a Chebyshev polynomial instead of a binomial transformation, and will be described in the following section.
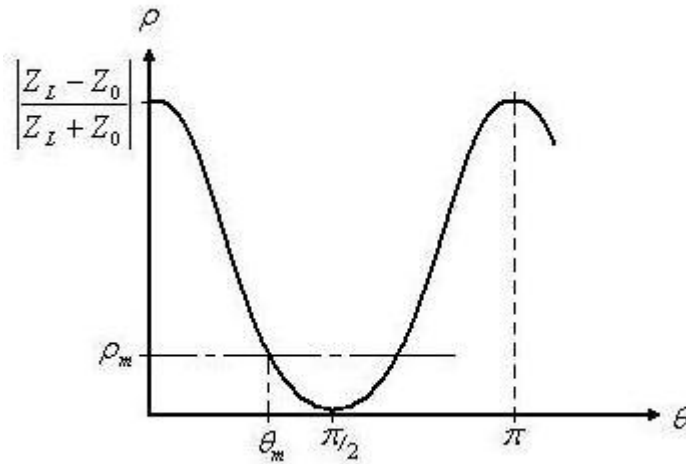
Figure 4.3: Bandwidth characteristics of a binomial transformer

4.3 Chebyshev transformation

The equal ripple characteristics can be obtained if R varies in accordance with the Chebyshev polynomial. The first four polynomials and the recurrence relation of an nth order Chebyshev polynomial are given as follows,

$$T1(x) = x$$

$$T2(x) = 2x^2 - 1$$

$$T3(x) = 4x^3 - 3x$$

$$T4(x) = 8x^4 - 8x^2 + 1$$

$$Tn(x) = 2xT_{n-1} - T_{n-2} \tag{4.20}$$

The Chebysev polynomials of the first kind are defined by the identity $T_n(\cos\theta) = \cos(n\theta)$. However, a polynomial of variable $\cos\theta$ cannot be used directly, as the desired ripple characteristics are needed only in the pass band. This can be achieved by considering

$$T_n(\sec(\theta)\,\cos(\theta)) = \cos\, n(\cos^{-1}\frac{\cos\theta}{\cos\theta m}) \tag{4.21}$$

Equation 4.21 is similar to Equation 4.12 and can be expressed as a cosine series as shown,

$$\Gamma = 2e^{-jN\theta}[R_0\cos(N\theta) + R_1\cos((N-2)\theta) + \ldots$$

$$\ldots + R_n\cos((N-2n)\theta) + \ldots + R_{\frac{N-1}{2}}\cos(\theta)\,\text{or}\,\frac{1}{2}R_{\frac{N}{2}}$$

$$= A\,e^{-jN\theta}\,T_N\,(\sec\theta\,\cos\theta) \tag{4.22}$$

99

Where A $=$ $(Z_L - Z_0)/((Z_L - Z_0)T_N(\sec\theta_m))$, obtained by substituting $\theta = 0$ in the above equation.

In this transformation the maximum value in the pass band for $T_n(\sec(\theta)\,\cos(\theta))$ is unity, hence an expression relating R_m and $T_N(\sec(\theta_m))$ can be expressed as follows,

$$R_m = \frac{Z_L - Z_0}{(Z_L + Z_0)T_N(\sec(\theta_m))} \quad [\text{or}] \quad T_N(\sec(\theta_m)) = \frac{(Z_L - Z_0)R_m^{-1}}{(Z_L + Z_0)} \qquad (4.23)$$

Figure 4.4 shows the bandwidth characteristics of a Chebyshev transformer. For example, to design a four matching layer system, that is, N=4, Equation 4.22 gives

$$\Gamma = 2e^{-j4\theta}[R_0 \cos 4\theta + R_1 \cos 2\theta + \frac{1}{2}R_2] = R_m e^{-j4\theta} T_4 \frac{\cos\theta}{\cos\theta_m}$$
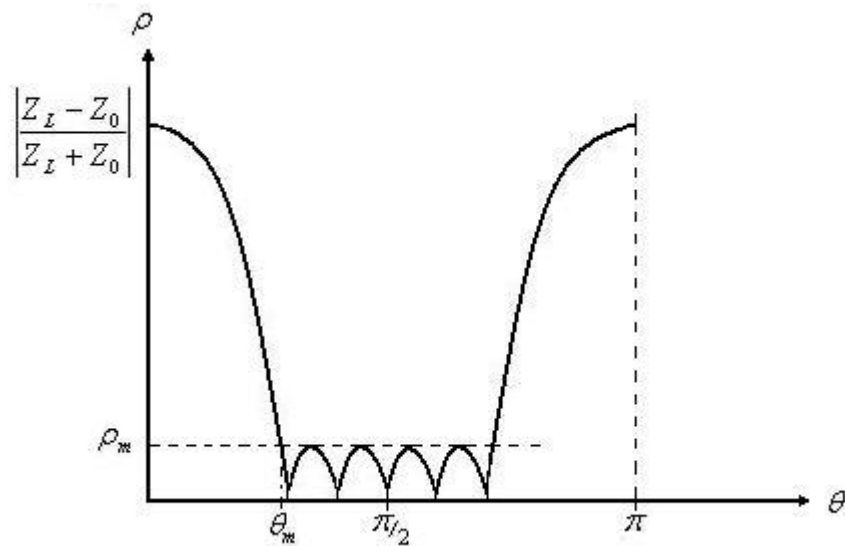
Figure 4.4: Bandwidth characteristics of a Chebyshev transformer

Equating coefficients in this equation, we get

$$R_0 = \frac{R_m}{2}(\sec^4\theta_m) = R_4$$

$$R_1 = 2R_m(\sec^4\theta_m - \sec^2\theta_m) = R_3$$

$$R_2 = R_m(3 \sec^4 \theta_m - 4 \sec^2 \theta_m + 1) \tag{4.24}$$

By way of illustration, consider a system with $R_m = -0.1$, input impedance $Z_0 = 15$MRayl and load impedance $Z_L = 1.5$MRayl (water). From Equation 4.21, we get,

$$\sec \theta_m = \cos(\frac{1}{4} \cos^{-1}(\frac{\ln(1.5/15)}{2 \times 0.1})) = 0.71 \Rightarrow \theta_m = 1.32$$

The fractional bandwidth is

$$\frac{\Delta \theta}{\frac{\pi}{2}} = \frac{2(\frac{\pi}{2} - 0.71)}{\frac{\pi}{2}} = 1.1 \tag{4.25}$$

Using θ_m, we can calculate R_i from Equation 4.24, which in turn can be used to calculate the impedance values using the relation $Z_{i+1} = Z_i \, e^{2R_i}$.

It is clear from Table 4.1 that the Z values calculated using both Binomial and Chebyshev are comparable in this case, and performance depends to a greater extent on the availability of suitable materials to achieve this impedance profile. Note also that, the matching layer impedances calculated by the Chebyshev technique also depend on the tolerance (θ_m) value used. The effect of tolerance on the 6dB fractional bandwidth (calculated using Equation 4.25) for the present case is shown in Table 4.2.

Once the matching layer impedance profile is calculated, individual thicknesses may be refined using a general purpose optmisation routine. The details of optimiser structure and implementation are discussed in Chapter 6. Figure 4.5 shows the receive impulse response of a conventional 500 kHz air backed thickness mode transducer with four matching layers operating in a water load, designed using the filter design technique.

A graphical interface shown in Figure 4.6 was built to design matching impedance profile using the filter design techniques presented previously. This filter design GUI

101

allows the user to enter the impedance values of the device and propagation medium, and allows creation of a stepped impedance profile using the filter design techniques mentioned in preceding sections. Once the matching layer impedance values are designed, the materials database can be queried to obtain practical material properties for further simulation purposes.

			Chebyshev Method (MRayl)	Binomial Method (MRayl)
$R_0 = R_4$	-0.15	Z_1	11	13
$R_1 = R_3$	-0.26	Z_2	6.4	7.3
R_2	-0.32	Z_3	3.3	3.1
		Z_4	1.9	1.7

Table 4.1: Calculated acoustic impedance value for a four layer matching scheme using the analogue filter design technique

Tolerance (R_m)	% -6dB Fractional Bandwidth
-0.1	109
-0.05	94
-0.01	65

Table 4.2: Effect of tolerance on device fractional bandwidth (calculated using Equation 4.25)
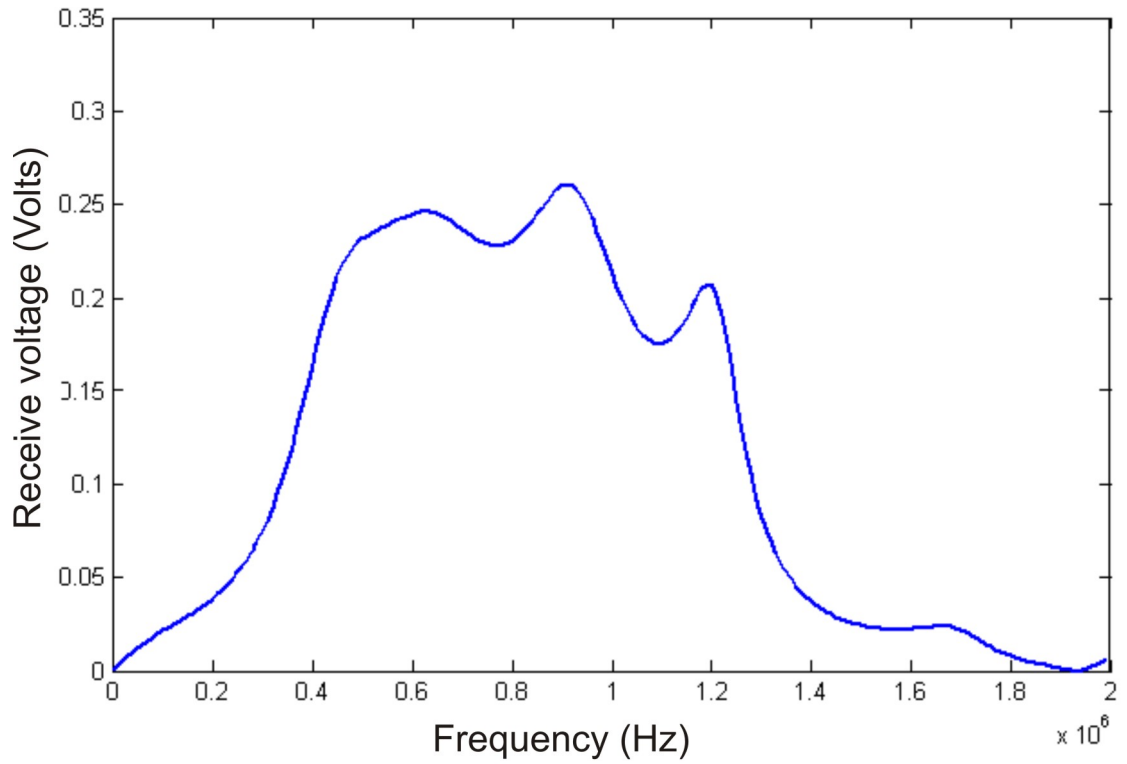
Figure 4.5: Sample transducer output simulation with four matching layers
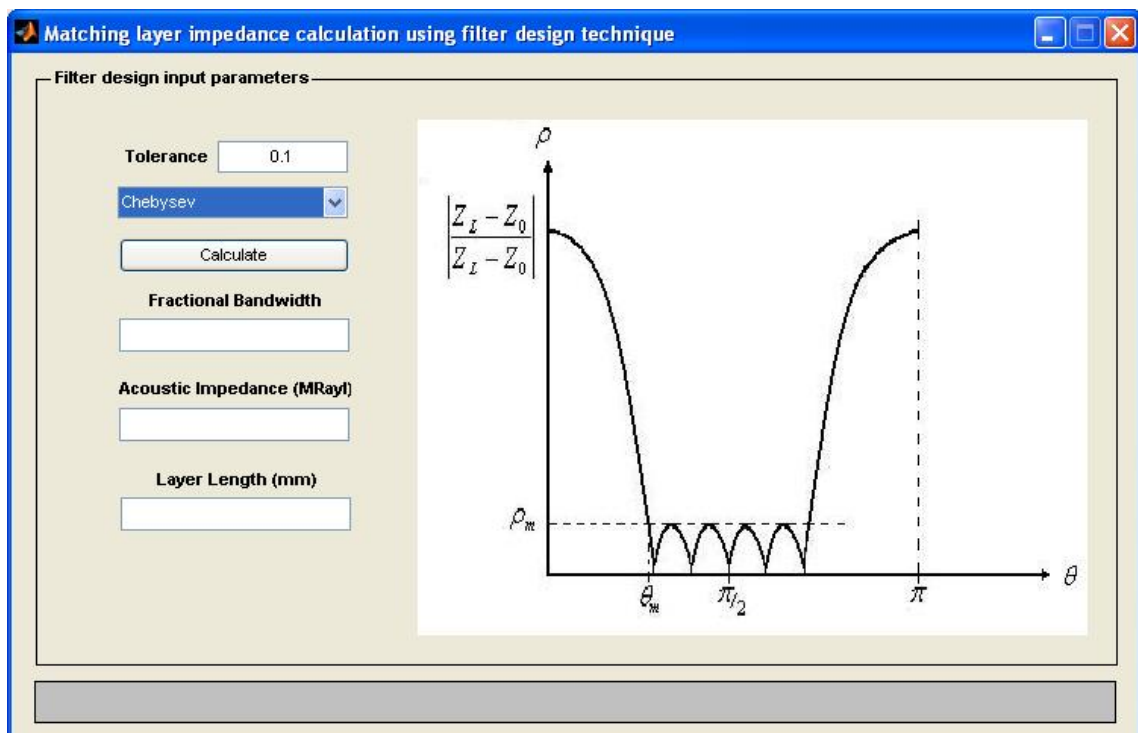
Figure 4.6: Filter design GUI in the proposed transducer design tool

103

4.4 Manufacture and analysis of passive layers used in a transducer assembly

In order to effectively manufacture passive layers with a broad range of acoustic properties that are suitable for application in piezoelectric probe assemblies, a methodology based on photo-polymerisation developed by Troge [20]–[22] is employed. Firstly, photo cured polymers are prepared by mixing a specific quantitly of polymer such as Glycidyl ether of bisphenol A (BisA) or 1,4-cyclohexanedimethanol diglycidyl ether (CHDG), with photoacid generator (PAG) solution, such as triarylsulfonium hexafluorophosphate salt in 50% solution of propylene carbonate [22]. This mixture is then cured under an ultraviolet lamp (LIDAM Scientific UV lamp, at wavelength of 368nm and 5mW/cm2 intensity). Thicker layers were created by multiple progressive thin layer deposition. Significant variations in the acoustic impedance of the finished layer were achieved by variation of the composition of both the polymer blends. This range could be further extended, by the addition of a suitable particle filler to form a 0-3 connectivity composite material [24],[25] to produce loaded systems, with impedance magnitudes much greater than that can be achieved from a complete polymer system (which typically has acoustic impedance around 2 to 3MRayl). Higher impedance materials used in this thesis were produced using barium sulphate (BaSO4) salt (density of 4100 kg/m3 and the particle size in the range 8-12 μm) loaded polyer blends.

In order to reliably manufacture the multiple matching layer technology it is important to consider some of the processing variables. Curing of thermosetting polymers can give rise to variations in mechanical properties due to the cure cycle, in addition to entrapped air in the mixture and/or settlement of any included particulates, such as tungsten. The processing of the polymer materials utilised in the manufacture of the multilayer matching scheme was very closely controlled. Measures such as

employing controlled temperature environments, vacuum chambers to remove entrapped air and rapid polymer curing to minimise particle settlement [20]–[21] were incorporated into the manufacturing methodology. The remainder of this section presents the experimental method developed to characterise matching layers and their bonding quality.

4.4.1 Experimental procedure to characterise matching/backing layers in a transducer

The optimum matching layer properties are difficult to predict correctly during the design phase, especially as their acoustic properties could depend significantly on the manufacturing process itself. It is thus very important to make the optimisation adaptable, to suit the fabrication process. If the component parameters are precise, the design optimisation process can be controlled more closely and is preferable to trial-and-error which is based mostly on experience. The key point in achieving an adaptive optimisation process is the characterization of each component in the fabrication process. Consequently methods to test the integrity of multiple passive layers before they are attached to the active piezoelectric element are critical for reliable production of piezoelectric devices. This section describes a robust procedure to test the matching layer integrity during manufacture, by processing the through test data obtained from the experimental apparatus shown in Figure. 4.7. The procedure is based on a through transmission system, in which the impulse response is well quantified, prior to insertion of the layered sample under examination. The layered structure is then inserted and the measured through transmission signal is compared directly with the predicted data from a mathematical model. In this way, the integrity of the structure can be evaluated, prior to bonding onto the transducer front face. Since single and multiple layers can be tested, the process provides a straightforward and reliable indication of manufacturing quality.

105

The experimental system consist of a water tank with two transducers operating in pitch catch mode. The matching layer structure under consideration, is placed half way between the transmit and receive transducers. The distance between the test material (also referred to as 'target' in this thesis) and the transmit transducer needs to be sufficiently large to allow for the incident sound wave to be planar in nature. Also, by placing the target in the transducer's far field region, the effects of pressure variations in the near field (which affects measurement) can be avoided.

Consider that both the transmit (Tx) and receive (Rx) transducers are driven by a 10Vpp, 1 cycle (or less) sine wave at their fundamental frequency. Now, the overall system model (neglecting diffraction effects) for the experimental set up shown in Figure 4.7 can be written in the frequency domain as,
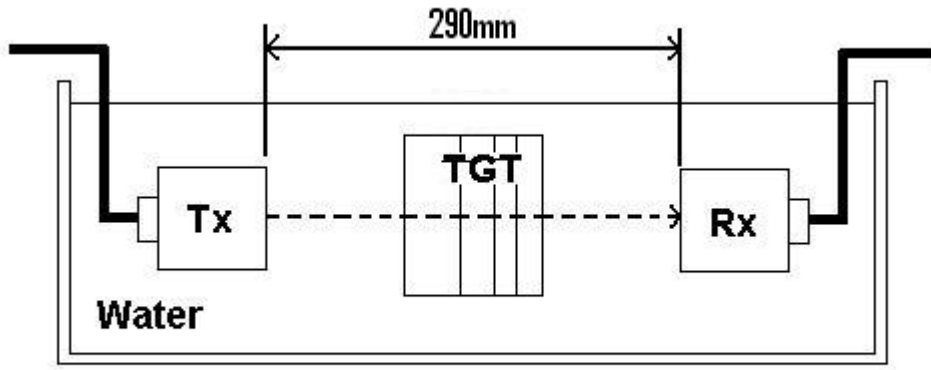
Figure 4.7: Experimental setup to test matching layer bond quality

$$R_{Overall} = E \times IR_{Tx} \times IRTGT \times IR_{Rx} = R_{tt} \times IRTGT \qquad (4.26)$$

Where IR stands for impulse response in frequency domain, R_{tt} is the through transmission response data without the target and IRTGT is the impulse response of the target.

$R_{Overall}$ and R_{tt} in Equation 4.26 can be measured experimentally. For example, the

experimental data obtained for a single layer glass target (1.28mm thick) and the reference through test (tt) data in water without the glass sample and both their frequency spectrum (obtained by Fourier transforming the captured time domain signal) is presented in Figure. 4.8. If the impulse response of the target (IRTGT) can be predicted analytically, it would then be possible to compare with the experimental data and evaluate its degree of goodness. In order to predict the impulse response of the target, a user friendly SIMULINK [37] model was developed. The fundamental element in this model is a layer system block (as shown in Figure 4.9), which describes a single target layer using its fundamental characteristics such as the acoustic impedance, density, thickness, longitudinal wave velocity, reflection coefficients at the boundaries and thickness. The layer block model accepts a force function (in time domain) as an input at either of its faces, and the output will be the force function radiating from these two faces as a result of the input. Such a block model can be connected in series to achieve the desired multiple matching layer configuration. For example, a cascaded four layer matching SIMULINK system model is included in Appendix B for illustration purpose. A comparison of overall system response (in the frequency domain), obtained using an experimental and analytical four layer matching system target is shown in Figure 4.10. The theoretical response is obtained by simulating IRTGT (using a cascaded simulink model) and multiplying it with the through test data obtained experimentally (R_{tt}). Please note that the effect due to the bonding layer is ignored while simulating the target impulse response. The result in Figure 4.10 is promising and provides confidence that using the above approach, it is possible to come up with a procedure to check matching layers, provided sufficiently wideband transducers are available to perform the through test experiments without the need to model them. Some possible further work suggestions to improve the proposed methodology, includes:

1. Applying more sophisticated signal processing techniques that could extract

107

features from the experimental and the part simulated data to relate to bond line thickness in the target.

2. Using the extracted feature quantify or score the difference between the two data sets.
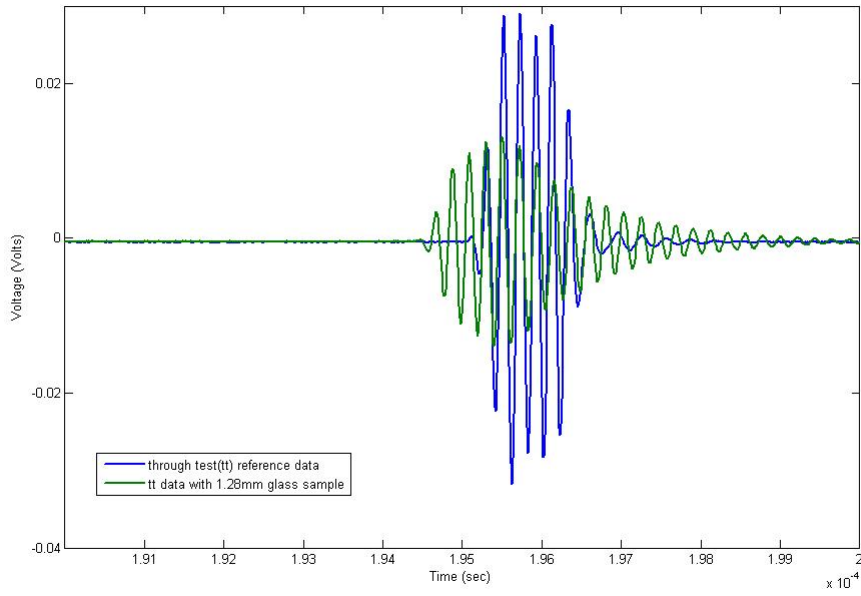
(a) Time domain signal transmitted through a glass target (green) and the through test carried without the target (blue)
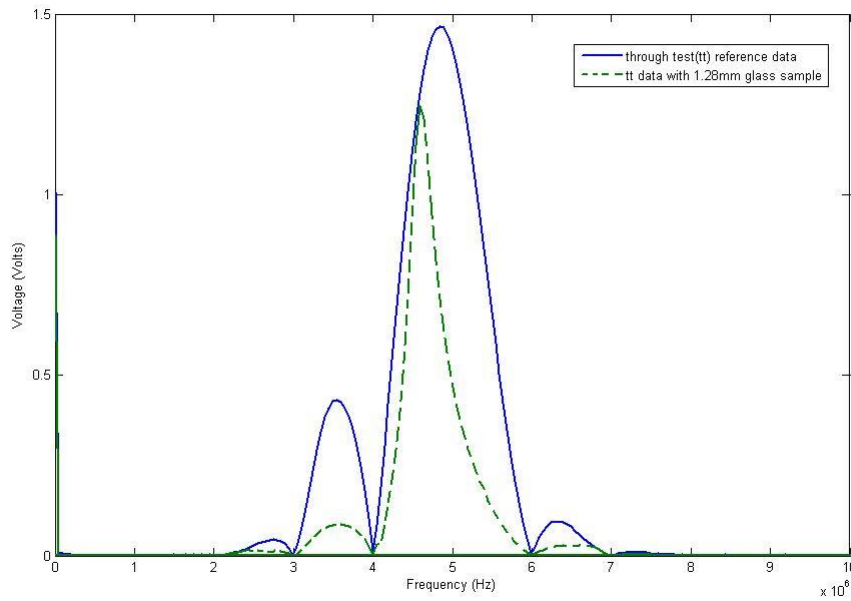
(b) Frequency domain representation of the signal transmitted through glass target (green) and the through test data without the target (blue)

Figure 4.8: Comparison of experimental data obtained from an experimental water tank with and without a 1.28mm glass target

109
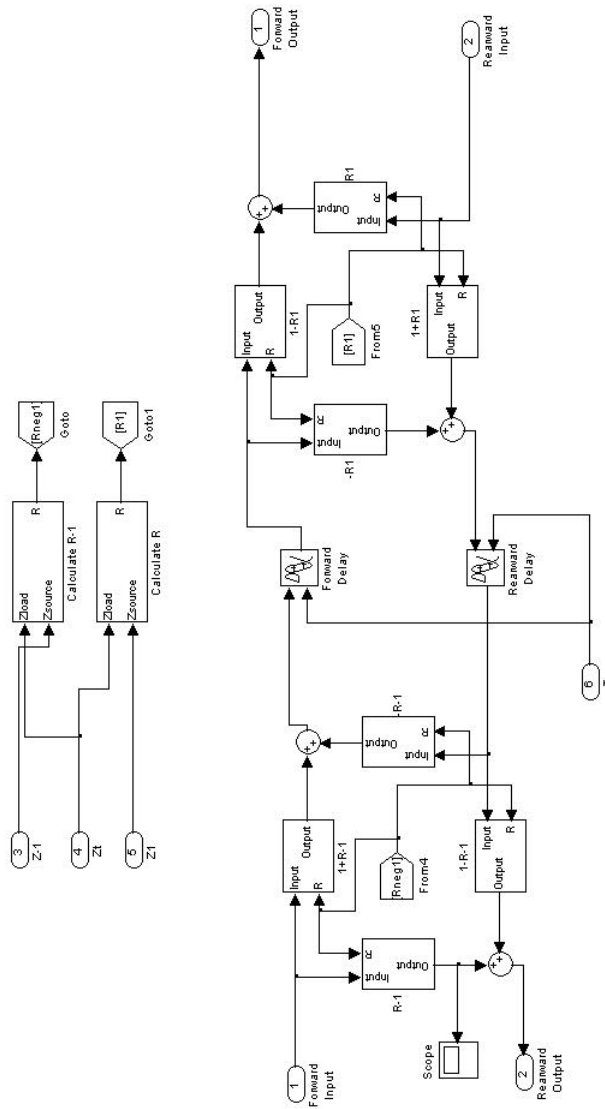
Figure 4.9: SIMULINK sub circuit model of a single passive layer

110
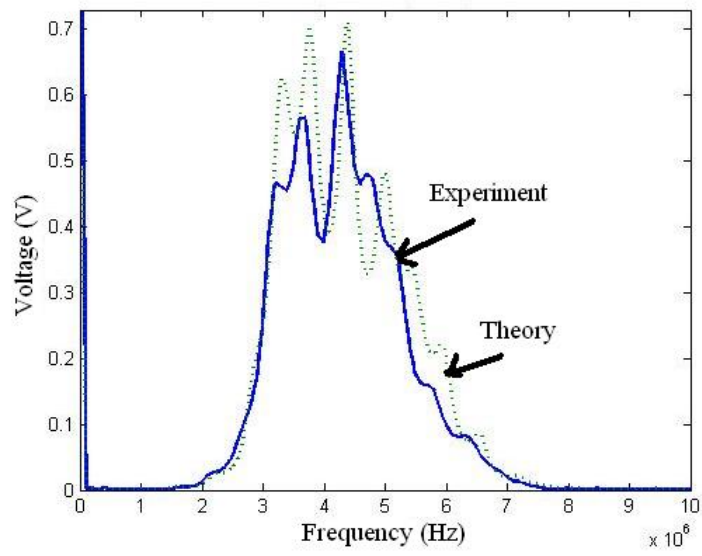
Figure 4.10: Comparison of experimental and simulated overall system response (frequency domain) to evaluate matching layer integrity

4.4.2   Analysis of bonding method

Another key processing variable in a multi variable system is the method by which the individual layers are combined. Here again, type and thickness of the bonding layer, surface roughness of the component and the pressure applied during fixation could affect the layer characterisitics. Using the non contact through transmission test described earlier, an analysis of bonding layer quality was carried out. A 5MHz immersion probe (details given in Appendix C) is used for the purpose of this initial investigation. A number of trials employing aluminium test pieces, nominal dimensions of 30mm square and 2mm thick, were performed and variation of bond line thickness and bonding pressure were analysed. The wet film thickness of the bond was controlled using a K-Bar applicator [26], the components were then placed under pressure between the platens of a hydraulic press and the bonding agent allowed to cure. Table 4.3 summaries the trials carried out. In each case the components were carefully degreased using appropriate solvents. Using the experimental procedure detailed in the preceding Section, the time domain waveforms transmitted through the water channel alone and in the presence of the samples under test were recorded. The modelled response without a physical representation of the bond line was considered for the comparison with experimental data and as such can be considered to be an intimately bonded structure comprising only the bonded components, aluminium in this case. The theoretical impulse response of the aluminium target is predicted using the model developed in the earlier section, and the experimental impulse response obtained by dividing the overall experimental system response by its through transmission result without the target (i.e. $R_{\text{Overall}}/R_{\text{tt}}$ in Equation 4.26). From Figure 4.11 it is clear that, from the trials carried out, that a bond line wet film thickness of $48\mu m$ subjected to 600psi, Trial 6 in Table 4.3 and Figure 4.11(f), offers the most appropriate method of bonding. Please note that the optimal thickness identified is the applied thickness of the adhesive, in other words, the true bondline

thickness is very small.

Trial	Bondline wetfilm thickness (μm)	Bonding pressure (psi)
1	18	200
2	18	400
3	18	600
4	48	200
5	48	400
6	48	600

Table 4.3: Description of bonding trials
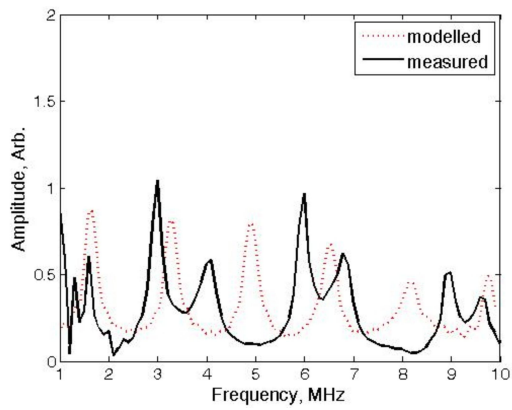
(a) Trial 1
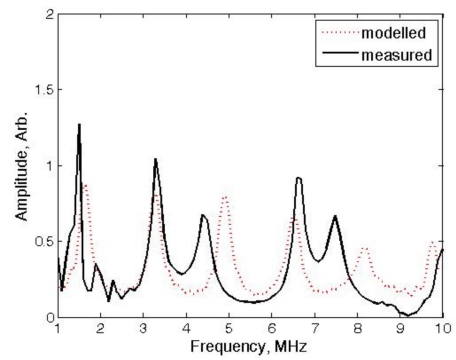
(b) Trial 2
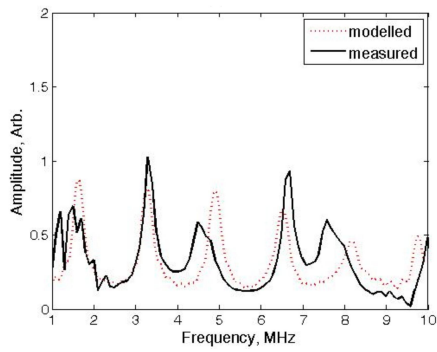
(c) Trial 3
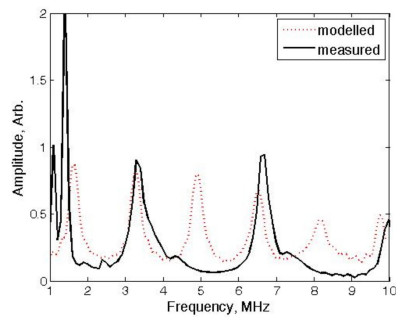
(d) Trial 4
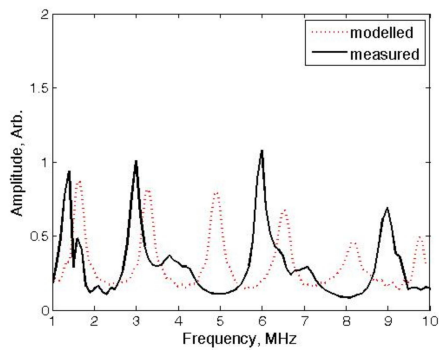
(e) Trial 5
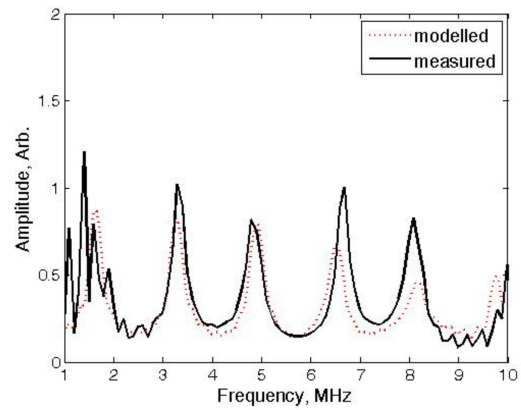
(f) Trial 6

Figure 4.11: Comparison of modelled and measured frequency domain impulse response for evaluation of bonding methodology

4.4.3 A four layer bonding example

Employing the methods described in the previous Section, an example four matching layer was constructed. As before, the through transmission impulse response method using a 5MHz immersion probe was employed to verify the quality of the bond, Figure 4.12 details the comparison of the modelled and measured frequency domain through transmission data. The data shown in Figure 4.12 illustrates the sequential bonding of the matching layer system, with the layers being analysed after each bonding operation. As was seen previously the peaks in the frequency domain data represent a transit within the multilayer system, in each of the plots detailed in Figure 4.12. The modelled and measured responses compare favourably, indicating that the layers are intimately bonded, and this approach will be used to manufacture the multi layered matching layer later in Section 7.

4.5   Summary

The use of analogue filter techniques to design matching layers, has been presented and the theory behind binomial and Chebyshev filter design techniques presented in detail. However, it should be noted there are some limitations in using these techniques due to the underlying assumptions involved. For example, the binomial filter design technique can be used to design only a limited number of layers, the range of Z_L is restricted to about $0.5Z_0 < Z_L < 2Z_0$, to provide accurate results. The proposed software includes filter design models that would support design of up to four matching layers, which is sufficient for most practical purposes. Other filter design techniques such as Butterworth transformation, and techniques based on tapered transmission line theory [13], should be included at later stage, to provide the user with extended design choices.

(a) Layer 1 and Layer 2

(b) Layer 1, Layer 2 and Layer 3

(c) All 4 Layers
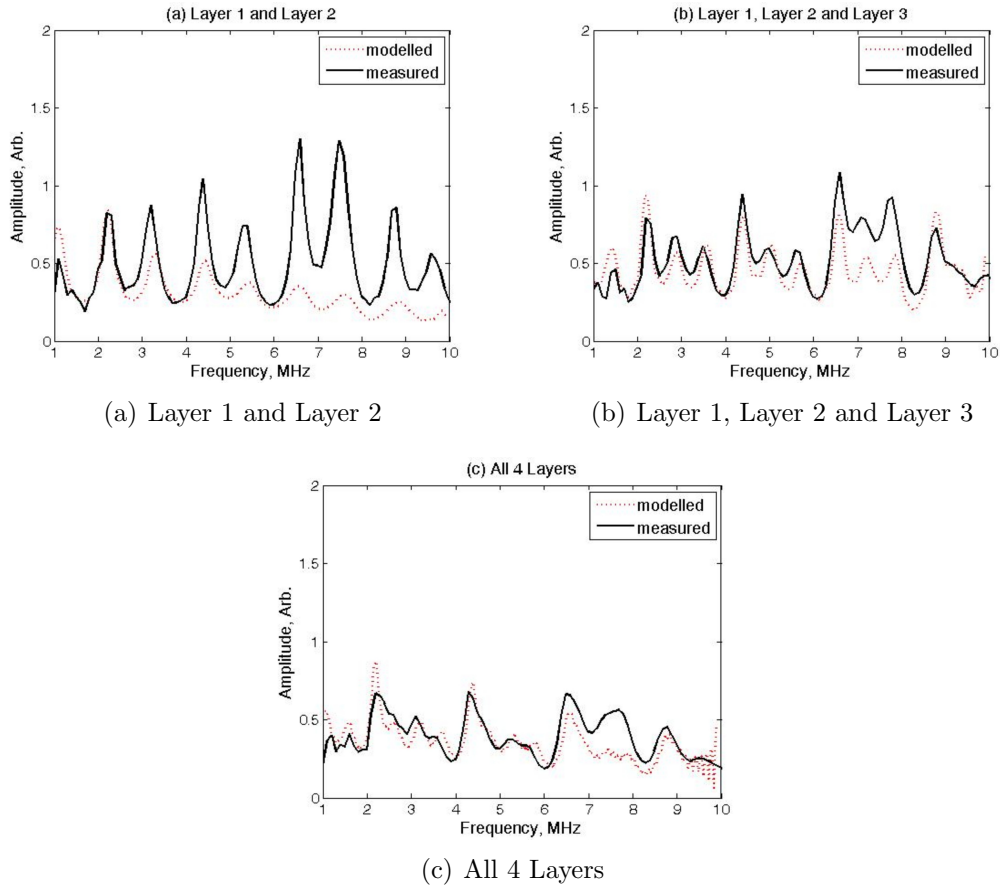
Figure 4.12: Comparison of modelled and measured frequency domain impulse response for the sequential bonding of the 4 layer matching scheme

Also, a method to test the integrity of matching layers was presented. The experiment procedure proposed and the initial work performed in checking matching layer integrity was reported. Including robust data for virtual prototyping of transducer systems and their ancillary components, is vital during a design iteration to deliver consistent results. However, further investigation is required, specially to improve signal processing to quantify the quality of bonding, and should be carried out as further development.

The next Chapter describes how commercial circuit simulation packages can be incorporated into the proposed design software and explain how it may be expanded to accommodate alternative, more sophisticated modelling strategies.

Chapter 5

Integration with commercial circuit simulation software packages

While designing an ultrasonic system, electrical load is an important parameter to be included. Consequently, it is desirable for the systems model to include comprehensive electrical circuit models, making the entire system design and optimisation process more straight-forward and robust. This chapter introduces the suitable strategies for the integration of a commercial SPICE circuit simulation package with the proposed transducer design tool. Firstly, a detailed description of intrinsic noise mechanisms that occur within transducer system and introduction to some of the common terminology used in noise analysis is presented. This is followed by an investigation of different strategies to interface a commercial SPICE circuit simulation environment, such as PSPICE and LTSPICE, with the proposed transducer design tool. A selection of simulation results are presented to highlight the feasibility of such an integrated approach.

5.1 Evaluation of noise sources within a transducer system

Many ultrasonic applications, including biomedical imaging and SONAR, are becoming increasingly restricted by intrinsic noise levels, and therefore it is necessary to develop a comprehensive understanding of noise (both within the active element and its associated electronics) in order to design optimal ultrasonic devices. For example, in a receiving transducer, the minimum detectable pressure signal is determined by the intrinsic noise levels within the system. Consequently, receiver design for maximum signal to noise ratio (SNR) requires the ability to simulate all relevant noise sources, arising from within the transducer and any associated electronics. This Section presents brief description of some of the noise sources present within an ultrasonic transducer system.

Figure 5.1 shows a typical transducer system configured for pulse echo operation. All sensors have a basic noise level, and one of the key challenges for a design engineer is to produce electronics circuitry that adds a minimum noise contribution to the overall system. In the broadest sense, noise can be defined as *any unwanted disturbance that can obscure or interferes with a desired signal* [70]. Such noise arises from either within the system (intrinsic noise such as the transducer noise, and circuitry noise) or from the outside (extrinsic noise such as environmental noise).
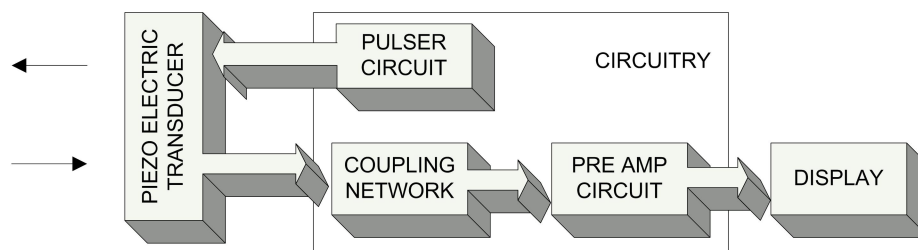
Figure 5.1: A typical transducer pulse echo configuration

Some of the other noise contributors within the system are thermal noise, shot noise

and 1/f noise. *Thermal noise*, also known as Johnson or Nyquist noise, is the most common intrinsic noise source and is caused by the random movement of thermally excited charge carriers in a conductor [69]–[70]. The mean square voltage of the thermal noise voltage is given by,

$$\hat{E}_t = \sqrt{4kTR\Delta f} \qquad\qquad (5.1)$$

where

k = Boltzmann's constant = 1.38×10^{-23} J/K

T = temperature of the conductor in degrees Kelvin (K)

R = resistance or real part of the conductor's impedance

Δf = noise bandwidth of the measuring system in hertz

A thermal noise generating element or device in the circuit is equivalent to an ideal noiseless resistance in series with a white noise voltage generator, valid over a flat frequency spectrum, corresponding to the noise bandwidth. It can also be represented as an ideal noiseless resistance in parallel with a noise current generator. An earlier study by Banks [77] indicated that transducer noise power spectral density (PSD) is equivalent to the thermal noise produced by the resistive portion of the transducer operational impedance. Using the mathematical model described in the earlier section (Chapter 3.1.2), a front face inversion layer (FFIL) transducer, with a nominal fundamental thickness mode of 1MHz, comprising 40% volume fraction PZT5A (Ferroperm, Kvistgard, Denmark) and CY1301/HY1300 epoxy (Vantico Ltd, Duxford, UK) was analysed. The total and real part of the operational impedance of the FFIL transducer, along with the device thermal noise plot at different temperatures is presented in Figure 5.2. It is evident from the simulations that the thermal noise is a frequency dependent term, which at higher frequencies, tracks the spectrum of the device operational impedance. In addition to the frequency of operation, the transdcuer thermal noise is also directly proportional to the absolute temperature of

119

the resistor (Figure 5.2(b)). Some of the practical ways to minimise broadband thermal noise are to maintain low sensor resistance (avoid additional series resistance elements), low operational temperature, and by limiting the operational bandwidth.

The thermal noise is the single significant noise source within the sensing element. Consequently, thermal noise within the transducer element, and a combination of thermal and shot noise to model the associated electronics is sufficient to perform noise analysis in most transducer preamplifier arrangements, as they contribute most to the overall noise within such transducer system [77]. The *shot noise* [69]–[70] results from the current flow in devices such as transistors and diodes. Since the random movement of charge carriers across a potential barrier results in shot noise, they are absent in simple conductors, which have no such barriers. Other noise sources, such as the 1/f noise (or excess noise), and flicker noise are not considered in this analysis. Also, environmental noises (interferences that are external to the transducer system) are ignored, as they do not change the overall noise profile of the transducer system, instead will only raise the noise floor. However, if necessary these noise models could be added readily to the proposed simulation package while performing noise analysis, which is described in detail in the following section.

5.2   Need for integration with SPICE

SPICE (simulated program for integrated circuit emphasis) is a powerful general purpose analog and mixed-mode circuit simulator that is used to verify circuit designs and to predict circuit behavior. SPICE [73]–[74] was originally developed at The University of California, Berkeley in 1975, and has continue to be the industry standard. PSPICE from Orcad, Meta software HTSPICE, and LTSPICE from Linear technologies are a few popular commercial circuit simulation packages based on the SPICE engine.
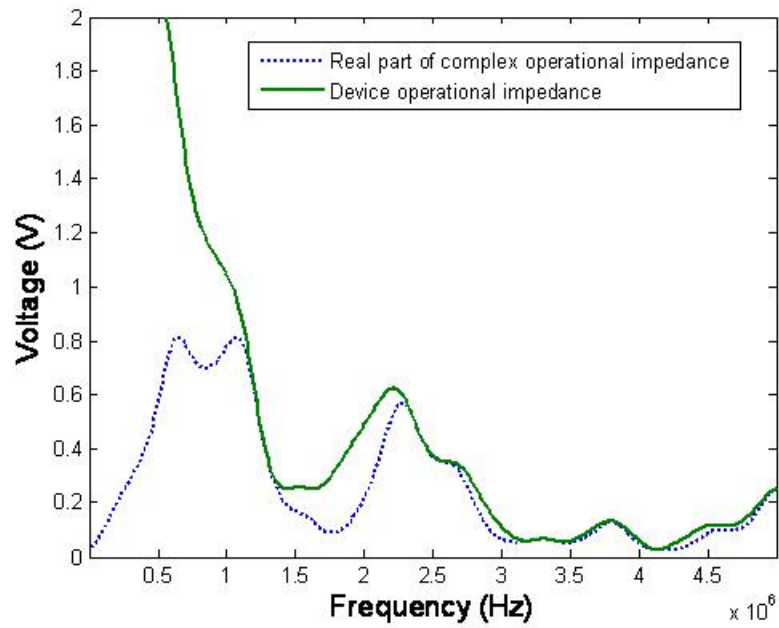
(a) Complex and real device operational impedance plot
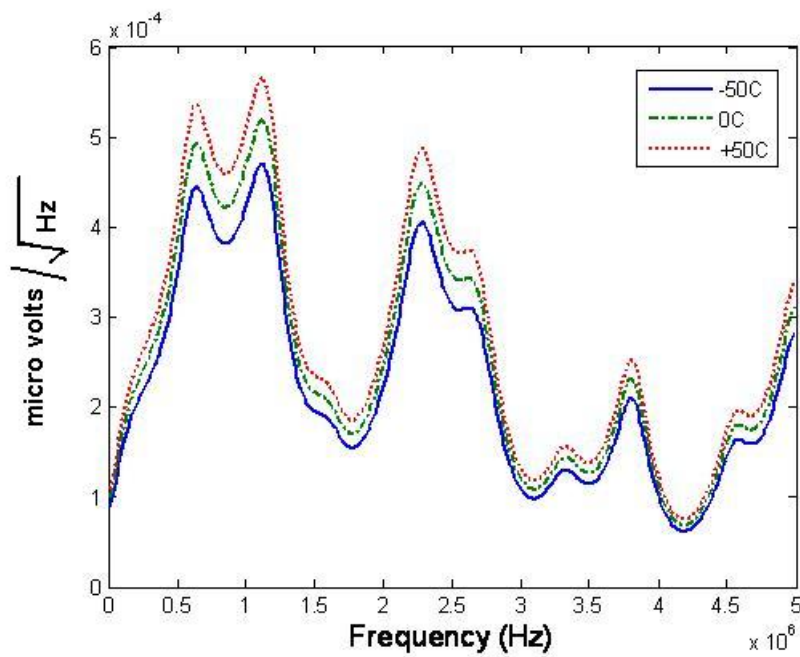
(b) Device thermal noise model at different operating temperatures, normalised to unity noise bandwidth

Figure 5.2: Simulated thermal noise in a front face inversion layer (FFIL) transducer

121

SPICE facilitates many forms of time domain analysis, including ac, dc, and noise analysis. Also, commercial SPICE circuit simulation software benefits from the extensive library of electrical components readily available as SPICE models for simulation. However, one of the main disadvantages with the SPICE time domain circuit simulators, is that they cannot perform any system level designing. Even though commercial SPICE packages such as PSPICE are supplied with a post processor package called PROBE (which can be used to plot simulation results and enable simple frequency domain analysis such as applying the Fourier Transform), PROBE'S functional capability is limited when compared to system design packages such as the MATLAB/SIMULINK environment [37]. Conversely, MATLAB in spite of having numerous functions for numerical computation, data analysis, optimisation and result plotting, does not comprise any facility for electrical circuit modelling. Consequently, if the system model in MATLAB can incorporate electrical circuit analysis functionality, this will result in a powerful package for transducer system design and optimisation. For example, using system simulation, a transducer system can be designed and combined with the electrical matching circuitry designed using SPICE. Also, design optimisation could incorporate both the noise model for the electrical and the acoustical part of the transducer system.

In this Chapter only a limited version of PSPICE [78] that is freely available from Orcad and LTSPICE [79], another freely distributed complete circuit simulation software will be considered for integration with the proposed transducer design software. The availability of analogue behaviour modelling (ABM), which allows modelling of analogue circuits using mathematical equations, look up tables, and transfer functions, extends the features of PSPICE and LTSPICE beyond other commercial circuit simulation packages.

5.3 Strategy to integrate SPICE into the proposed transducer design optimisation software

As mentioned in the earlier section, system design and circuit design usually are separate processes that employ separate simulators. Since the simulators are not linked, there is no straightforward way for the design engineer to close the loop, using the actual circuit data in the system design. As a result, designers will not know the influence of the actual circuit module on the system and vice versa. The following section investigates various strategies to integrate a circuit simulation package with the proposed transducer design software.

5.3.1 SLPS interface for PSPICE

One of the straight forward solutions to interface circuit simulation and system simulation software is to use the SLPS [80] interface supplied by Orcad. The SLPS interface connects MATLAB/SIMULINK and PSPICE to achieve the best of both, by including any PSPICE circuit in a SIMULINK model and calling the SPICE engine to co-simulate. Fig 5.3 shows how the SLPS interface could be used to simulate transducer design, both in the transmission and reception configurations. In the transmission configuration as shown in Figure 5.3(a), the waveform generated using MATLAB is used to excite the electrical circuitry specified in the SIMULINK block. At this point the PSPICE engine is called by the SLPS block to co-simulate with SIMULINK. The output signals obtained from SIMULINK are used to design the transmitter transducer systems model and finally the results can be displayed in MATLAB in any desired format. Alternatively, while operating in the receiver configuration, as shown in Figure 5.3(b), the force or pressure at the receiver transducer system model could be simulated in MATLAB/SIMULINK. The signal ob-

tained from this model is then used in the electrical circuitry model using the SLPS block and the results plotted in MATLAB using an appropriate display function. The SLPS block in SIMULINK can be associated with any electrical circuit file (alternatively know as a netlist) that can be simulated in Orcad PSPICE software.
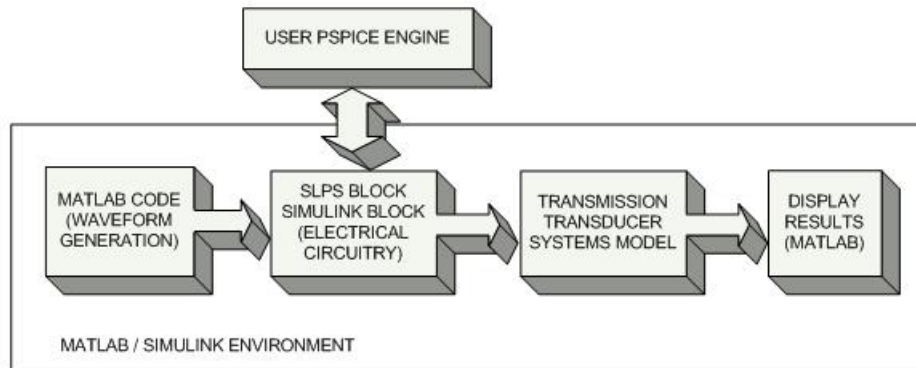
(a) Transmitter configuration
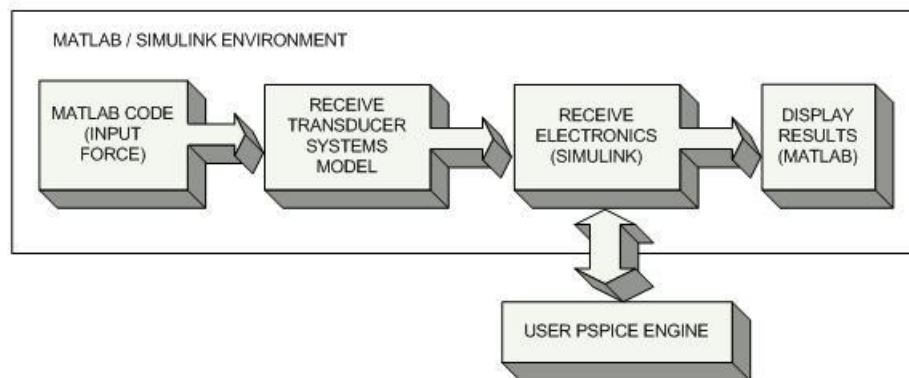
(b) Receiver configuration

Figure 5.3: SLPS integrated approach to circuit and system modelling

The SLPS interface allows the designer to perform system-level simulations that include realistic electrical PSpice models of actual components, and enables designers of electro-mechanical systems, such as; sensors, control systems and power converters, to perform integrated system and circuit simulation. However, the SLPS interface is a third party software and requires a separate license and a full version of Cadence OrCAD products (R10.5 or higher) to function. The PSPICE SLPS interface described earlier could be unavailable for variety of reasons, including the

version conflicts between MATLAB and PSPICE software in use, and cost. Some of the more general strategies to achieve the integration of the freely available PSPICE student version software and LTSPICE software are presented in the following sub sections.

5.3.2 Performing noise analysis at system level

The simplest approach to reduce additional noise added by a preamplifier stage would be to use the amplifier with lowest noise contributions specified by a manufacturer. If an operational amplifier is used, the corresponding data sheet will indicate the voltage and current noise spectral densities, $\hat{E}_n$ and $\hat{I}_n$, respectively. Minimizing these two values will be sufficient to reduce noise introduced by the preamplifier. However, this approach is not a panacea and what is good for one type of ultrasonic transducer arrangement might be of little or no use for others.

Alternatively, the preamplifier output noise can be minimised, taking into account the influence of all possible noise sources. Consider a relatively straight forward front face inversion layer (FFIL) transducer configuration as shown in Figure 5.4(a). Based on existing literature [77], a Thevenin equivalent noise model of an ILT including the pre-amplifier stage is shown in Figure 5.4(b). The noise source $\hat{E}_T$ represents the thermal noise within the transducer, and $\hat{E}_n$ and $\hat{I}_n$ represent the equivalent input noise voltage and current contributions (a combination of thermal, shot and $1/f$ noise) arising from the pre-amplifier circuitry, respectively. Each noise generator contributes to the overall noise output of the system and it is normal to refer all noise contributions back to the source. Let the equivalent mean square input noise voltage of the system be $\hat{E}_{ni}^2$, which can calculated by summing the mean square value of individual noise contributions.

$$\hat{E}_{ni}^2 = \hat{E}_n^2 + \hat{E}_T^2 + \hat{I}_n^2 |Z_{th}|^2 \tag{5.2}$$

where $\hat{E}_T$ is the rms thermal noise of the source as described earlier in Equation 5.1.

Once the total noise voltage is calculated, the overall system signal to noise ratio

(SNR) can be calculated as:

$$\text{SNR} \;=\; \frac{V_{o-c}^2}{\hat{E}_{ni}^2} \tag{5.3}$$

where

V_{o-c} is the open circuit Thevenin voltage response of the FFIL device

Considering a low noise pre-amplifier arrangement with following specification, $\hat{E}n = 800\text{pV}/\sqrt{\text{Hz}}$, and $\hat{I}n = 1\text{pA}/\sqrt{\text{Hz}}$, are the noise spectral densities. The contribution to the overall noise mechanisms within a FFIL receiver are shown in Figure 5.5(a). Figure 5.5(b) shows the SNR for the FFIL receiver calculated using Equation 5.3 and the region of maximum SNR are readily identified. In this case, the major noise contributions occurs in the vicinity of the resonant peaks that relate to the fundamental and second harmonic frequencies. Similar system level noise analysis can be applied also to the transmit transducer configuration. Note that while designing a transduction system for any practical applications, emphasis should be to maximise SNR at the input at the amplifier stage. Consequently any design optimisation task should be able to use amplifier input impedance as a cost function. Some strategies to simulate this scenario is presented in the following sections.
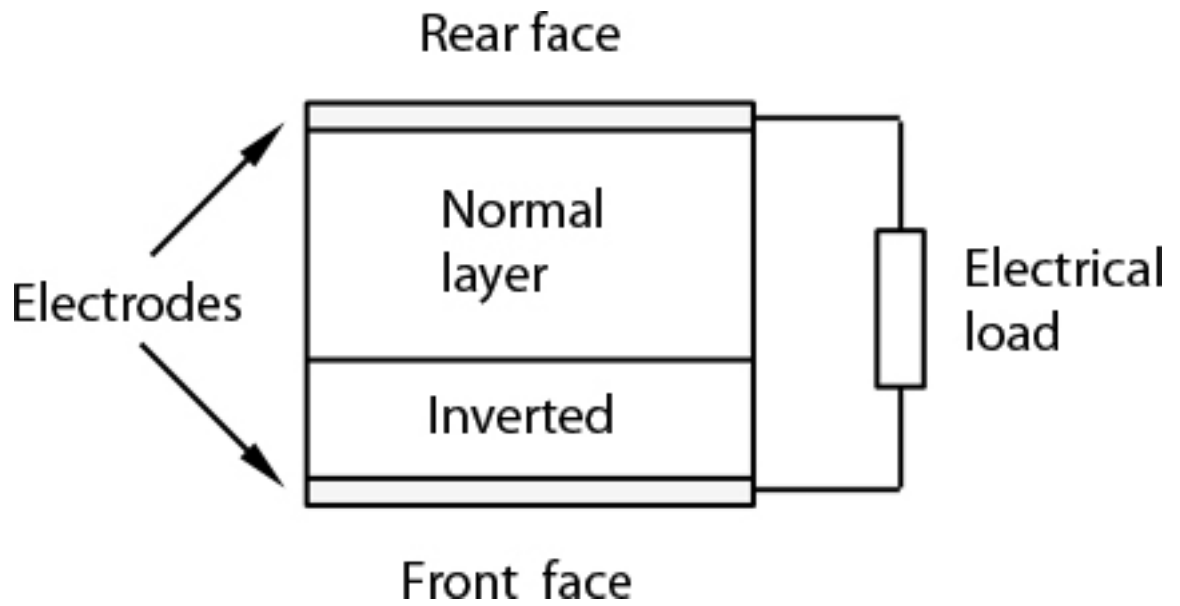
(a) FFIL transducer in receive operation
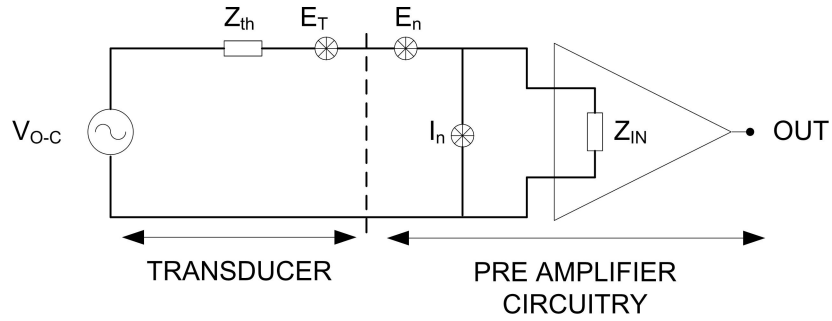
(b) Thevenin equivalent electrical equivalent for the FFIL receiver

Figure 5.4: A front face inversion layer (FFIL) receive transducer and its Thevenin equivalent electrical noise model
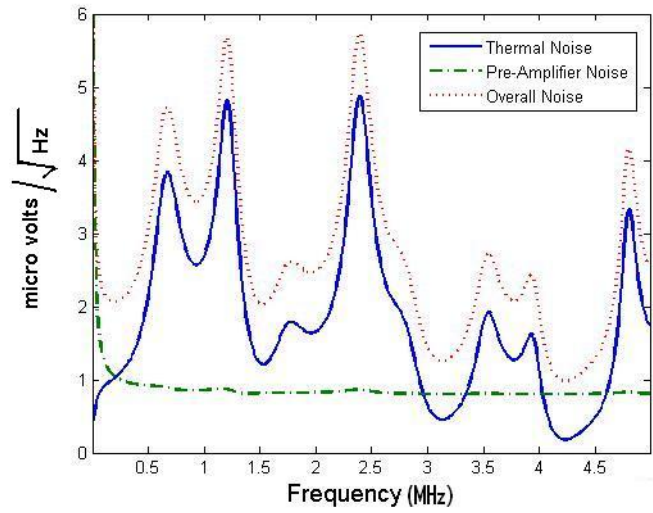
(a) Equivalent input noise voltages within a FFIL receiver
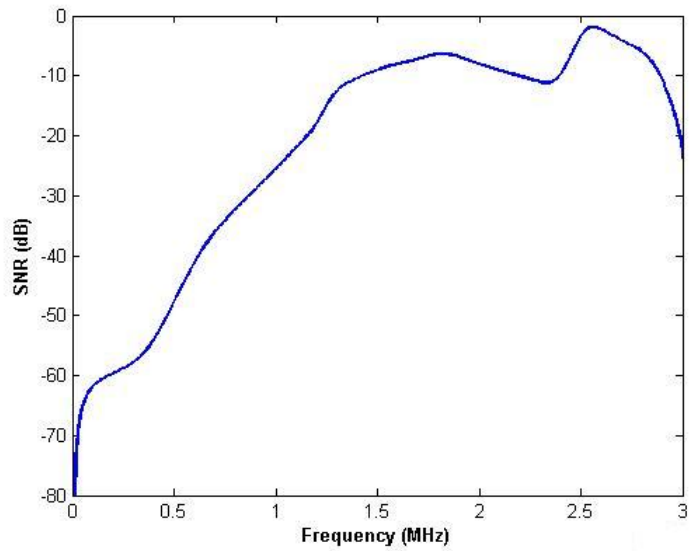
(b) Simulated FFIL receiver SNR

Figure 5.5: Simulated noise mechanism within a front face inversion layer (FFIL) receiver and its signal to noise ratio (SNR) plot

5.3.3 SPICE analysis using circuit simulation programs

The noise model developed in analytical form as described in the previous Section, is useful to carry out comprehensive investigation into all the noise sources within the transducer system. However, the requirement to separate the sources of noise and performing the overall noise analysis is difficult, particularly in the case of complex circuitry involving many elements.

One solution to this problem is to perform the noise analysis of the transducer using the systems model and combine the result with the circuit noise analysis result imported from a SPICE circuit simulation. In order to do this, firstly, the transducer noise should be determined using a systems model. As mentioned in the preceding section, an earlier study by Banks [76] indicated that transducer noise power spectral density (PSD) is equivalent to the thermal noise produced by the resistive portion of the transducer operational impedance, and can be simulated easily from the linear systems model for a variety of thickness mode transducer configurations, as indicated in the previous example.

For any electrical circuit to be used with a transducer, the total output noise voltage (reffered to as $\hat{E}$(onoise) in PSPICE syntax), is calculated by summing the mean square values of all the noise contributions within a given circuit. Similarly, the noise referred to any input port ($\hat{E}$(inoise)), can be worked backwards from $\hat{E}$(onoise), by dividing the output noise voltage by the circuit gain. Figure 5.6 shows a noise model calculated at the output or input of a given circuit. SPICE circuit simulation software packages can be used to calculate both $\hat{E}$(onoise) and $\hat{E}$(inoise) using the *.NOISE* command in PSPICE, used in conjunction with AC analysis.

Consider a sample pre-amplifier circuit as shown in Figure 5.7(a), the V(onoise) and V(inoise) simulated using LTSPICE software is shown in 5.7(b). The simulation is carried out in this case over a wide frequency range and the noise voltage peaking at

high frequency is due to decoupling of the two stages in the amplifier design used. Note that it is not critical, as the primary aim of this simulation is to illustrate the fact that it is possible to carry out such simulations using a hypothetical, yet realistic amplifier design. V(inoise) expressed usually as $V/\sqrt{Hz}$ (alternatively as $A/\sqrt{Hz}$, if expressed as a noise current source), can be exported from LTSPICE and added to the thermal noise predicted by the transducer design software to analyse the overall system SNR.

(a) Total RMS noise voltage measured at the output of a circuit

(b) Total noise voltage referred to an input of a circuit
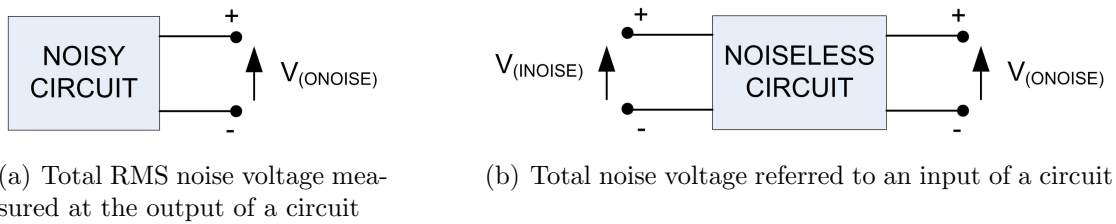
Figure 5.6: Noise measurement for a electrical circuit

Electrical and electronic device parameters vary due to manufacturing tolerances and also due to aging of components. Consequently, the ability to investigate the effect of device parameters on the overall system performance is essential. Performing noise analysis of the actual preamplifier circuit in the SPICE environment allows more complex analysis such as Monte-Carlo Analysis (MCA), sensitivity and Worst-Case Analysis to test circuit tolerances [71]. For example, consider the preamplifier configuration shown in Figure 5.7(a), and the effect of manufacturing tolerance on device fundamental resonance frequency (nominally 1MHz in this case), are presented in Figure 5.8. It is clear from these simulations the variations in the total noise present in the circuit, directly as a result of variation in component parameters is minimal. Appendix D shows the SPICE circuit file used for MCA analysis on the sample preamplifier circuit, shown previously. The upper and lower confidence level (say, for example, the two sided at 95% interval) can calculated easily from the above MCA simulated population using the formula shown below:

$$\text{MCA output mean } \pm 1.96 * \text{stdErr} \tag{5.4}$$

131
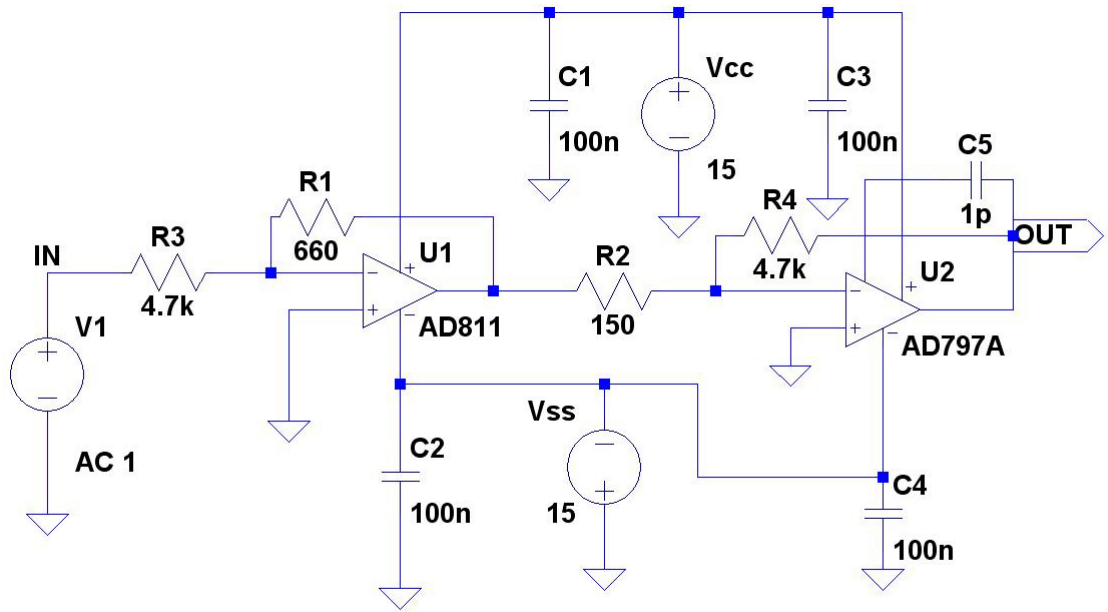
(a) A sample electrical circuit used to perform noise analysis
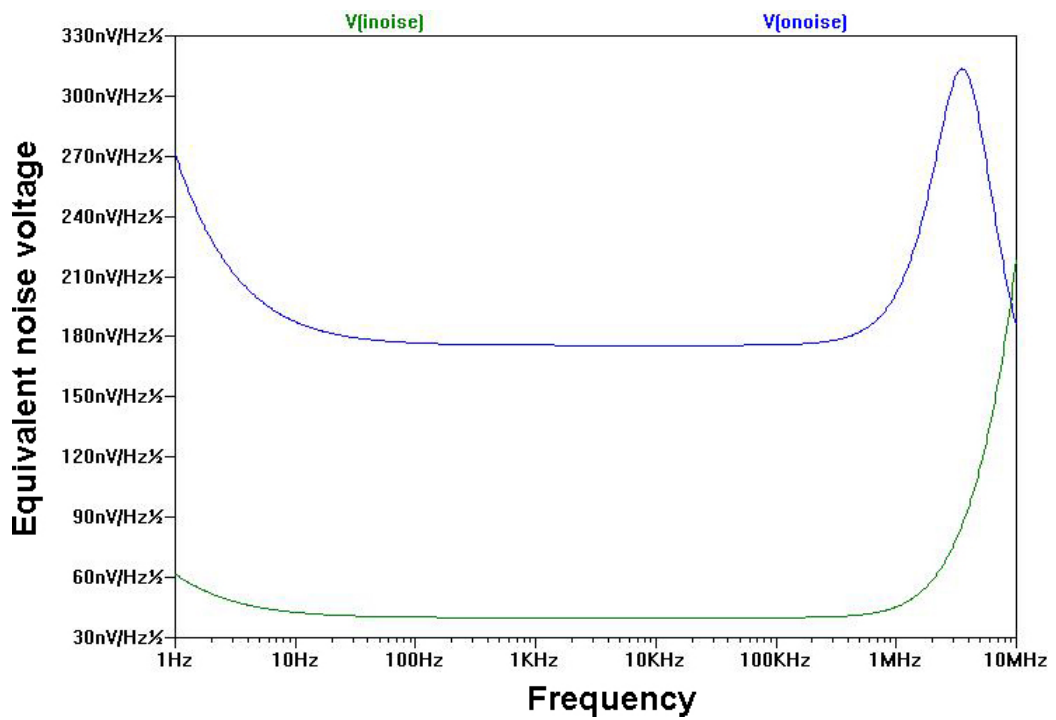
(b) V(onoise) and V(inoise) simulated using LTSPICE

Figure 5.7: Noise power spectral density plot for the above preamplifier electrical circuit, simulated using SPICE circuit simulation software LTSPICE

where stdErr is the mean error in the MCA output calculated using (MCA output standard deviation)$/\sqrt{n}$, and n is the total number of MCA simulations.
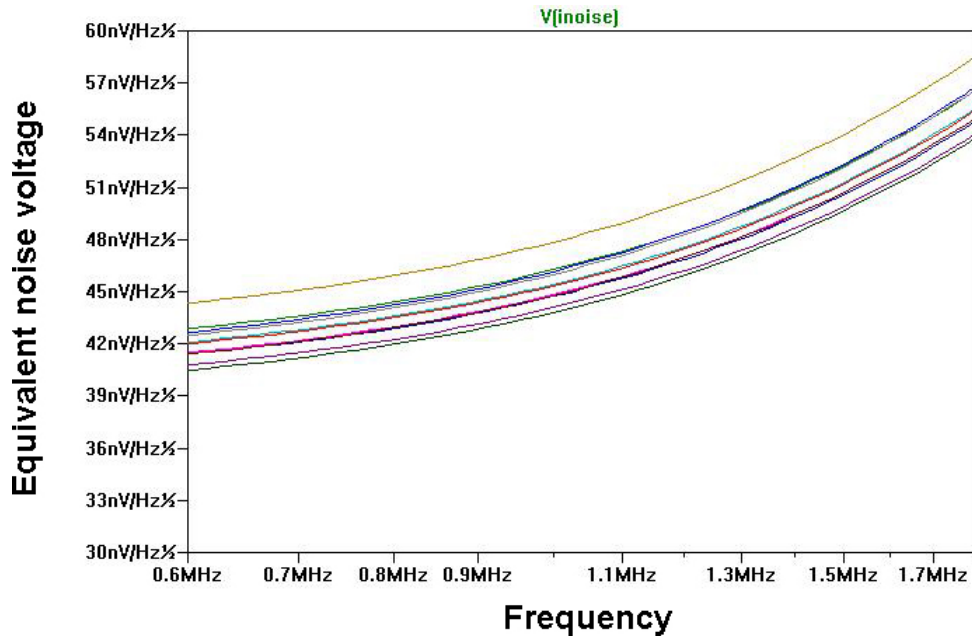
Figure 5.8: Monte-Carlo Analysis on a sample pre-amplifier circuit to investigate the effect of circuit component manufacture on preamplifier noise

An alternative approach to noise analysis is to perform the transducer system design together with the associated electronics in the circuit simulation software. The most straight forward way to achieve this is by using an electrical analogy of transducer behaviour, that can be implemented directly in the circuit simulation software. For example, consider the equivalent circuit model of Mason's thickness mode transducer model adopted by Redwood [10]. The model consists of a capacitance C_0, a negative capacitance $-C_0$, an ideal transformer and a transmission line, and can be implemented easily in any circuit simulation program which could model transmission lines and linear dependent sources. This provides a powerful simulation option to optimise transducer design along with electrical matching circuits and the associated drive and receive electronics.

The use of transformers in the above model could lead to unrealistic impedance values, and negative capacitance. This could be easily avoided by using controlled

source models [82], the analysis and implementation of which are more intuitive in circuit simulation programs.

Among the two strategies discussed so far, using an electrical analogy for transducers has many distinct advantages, and provides a powerful tool to simulate thickness mode transducers with variety of electrical and acoustical loading conditions. However, such equivalent models must be derived for every transducer type and cannot be easily developed for more complex transducer configurations such as inversion layer transducers (ILT) and stacked thickness mode devices.

Alternatively, a more general strategy to integrate the systems model and circuit models would be to use a Thevenin equivalent circuit to model transducers [8]. The Thevenin equivalent electrical analogy for any transducer in reception mode is easy to understand and simulate. For example, for any linear transducer, in order to find its Thevenin equivalent circuit analogy, one needs to calculate the open circuit voltage response (V_{O-C})and the device electrical impedance (Z_{Th}). Both V_{O-C} and Z_{Th}, can be simulated in MATLAB using an appropriate linear systems model. This will provide a table of voltage and impedance data as a function of frequency over the device operational bandwidth. The next key challenge is to write an automated code to convert this frequency dependent voltage and impedance data, to a format suitable to use in SPICE circuit simulation programs, to allow integration of the two packages.

In order to achieve translation of the data into a format suitable for SPICE, a novel modelling strategy is proposed. Firstly the V_{O-C}, the time domain signal obtained by inverse Fourier transforming the frequency domain open circuit Thevenin voltage, is exported as a comma separated variable file. This can be achieved using the delimited write command (dlmwrite) in MATLAB. Then using the piece wise linear (PWL) voltage source in SPICE could be used to read the Thevenin voltage into a

SPICE circuit program, and the syntax is as shown below,

PWL Node1 Node2 Voc.txt (5.5)

where, Node1 and 2 denote the node labels for positioning the voltage source in a SPICE circuit file, and Voc.txt is a comma separated Thevenin voltage time domain response simulated in the MATLAB environment.

The Thevenin impedance, however, cannot be loaded directly in SPICE. However, arbitrary behavioral sources (B-sources) in LTSPICE and analogue behaviour models (ABM) in PSPICE can be used to model such complex elements. A code snippet for B-Source syntax is shown below,

Bxxx n1 n2 V $=<$ expression $>$ [[units] Freq $=<$ valuelist $>$ [delay $=<$ value $>$]](5.6)

Where the transfer function of the frequency circuit element is specified by an ordered list of points of freq, mag and phase as follows:

$< (f1, m1, p1)[(f2, m2, p2)...] >$ (5.7)

where fi, mi, and pi stand for the ith frequency, magnitude, and phase values in the list

The following unit specifiers may optionally precede the 'Freq' keyword in the syntax: "rad"=radians, "mag"=non dB, and "ri" to use real and imaginary in place of magnitude and phase.

Perl script, a common cross platform open source programming language, is used to convert the impedance list to an abstract behaviour model B source in LTSPICE (G_{freq} in PSPICE), and is presented in Appendix E. Both V_{O-C} and Z_{Th} can be

```
.SUBCKT xdr N1 N2
Thevenin equivalent spice model sub circuit
PWL 1 N1 Voc.txt
G11 1 N2 FREQ V(10,3)=
+( 1.000000e+8,-1.085478e+001, 1.614900e+001)
+( 2.000000e+8,-9.670879e+000,-3.863000e+000)
+( 3.000000e+8,-9.655554e+000,-1.727700e+001)
.....
.ENDS
```

made automatically exported into a SPICE subcircuit (say txdrThevenin.txt) using the MATLAB script as shown below,

The above SPICE subcircuit text file can be included in any SPICE circuit file (alternatively known as a netlist) using an *.INCLUDE* spice command as shown below,

```
...
.include txdrThevenin.txt
X1 20 30 xdr
...
```

Where X1 is an instance of the Thevenin equivalent model subcircuit used in PSPICE, and can be easily extended to other SPICE based behaviour model sources, if needed.

This novel modelling strategy presented is extremely important, as it presents an integrated approach combining the strong features of industry standard software MATLAB and LTSPICE, to model transducer system noise behaviour. In which, MATLAB can be used to perform transducer simulation (using linear systems approach) and the resulting device noise characteristics can be exported to LTSPICE environment to perform an in depth noise analysis. Also, in theory it would be possible to combine both MATLAB and LTSPICE simulations with a generic optimisation program, to optimise around system SNR during the transducer design stages.

However, this will be a memory intensive operation, requiring multiple instances of both MATLAB and LTSPICE run simultaneously, which is often prohibitive in typical windows operating system found in a desktop computer.

5.4 Summary

Detailed understanding of the effect of system electronics on a transducer's performance is essential for the following reasons:

1. Accurate modelling of transducer's transmit and receive response and

2. Effective noise analysis in some applications

In other words, a circuit design simulation that complements transducer design is essential while designing transducer systems with optimal overall signal to noise ratio. Conventionally, while designing a transducer/array, a 50 Ohms electrical load is assumed and an electrical matching network is used to achieve this while connecting the device electronics.

This Chapter has presented several approaches to improve upon this and analyse noise performance of a transducer and related electrical circuits. Two general strategies to interface an open source version of the SPICE circuit simulator, LTSPICE, were presented. Firstly, a method to perform noise analysis of transducer design using MATLAB was described. This systems noise analysis approach requires to model each noise source, both intrinsic to the transducer and the electrical circuit, which is rather cumbersome for complicated transducer design.

An alternative is to perform the noise analysis in circuitry in LTSPICE, and one way to achieve this is to model the transducer in SPICE using an electrical analogy. However, the need to model specific electrical analogies for each transducer type, makes this technique not ideal. A novel, more general strategy was proposed to simulate a Thevenin equivalent model of a transducer [8] in MATLAB and export the appropriate data to LTSPICE for noise analysis. Analogue source models LTSPICE are used to represent such equivalent models in LTSPICE, and this approach could

be extended easily to similar analogue source models in other circuit simulation programs, if required.

All the methods described in this chapter provide means of modelling circuitry associated with a transducer system to be modelled along with the transducer systems model, and could be applied effectively to improve overall system design. However, the main disadvantage in all the approaches developed during the course of this thesis is the necessity to invoke external third party programs such as PSPICE/LT-SPICE many times during design optimisation process. This is necessary as the device transfer function, calculated using the linear system model changes dramatically when a parameter within the model is varied during the optimisation process. Consequently, source and load impedances need to be adjusted simultaneously, in order to match the varying transducer electrical characteristics. At the present form, the only way to achieve this in the proposed software is to implement a iterative batch processing program, which would slowdown the optimisation process greatly. Details of how this could be improved further by considering a wholistic model of the transducer and electronics is presented as a suggestion for future work, in Chapter 8. The next chapter presents the expert system and optimiser module development for the proposed transducer design software.

Chapter 6

Design of expert system and control of optimisation process

This chapter presents the design and development of a prototype expert system for the proposed transducer design software. The implementation of an expert system and optimisation algorithm, and the strategy of bringing together both parts, is discussed in this chapter. The most appropriate choice of optimiser, based on the particular characteristics of the transducer design problem space is discussed. Also, a selection of typical results is included to illustrate the expert system driven transducer design and optimisation approach.

6.1   Optimisation problem and the need for an expert system

The transducer design optimisation problem is a multidimensional problem with many key interdependent and dependent parameters. Even while designing a relatively straight forward thickness mode transducer, with simple optimisation param-

eters, the problem space is not simple, with many local minima in the search space, making the optimisation process more challenging. The problem complexity grows directly in proportion to the number of parameters used in the optimisation process and also the appropriate selection of optimisation algorithm is key for obtaining consistent results.

Secondly, the design of an ultrasonic transducer for different application areas can differ greatly. For example, the measure of overall round-trip efficiency or insertion loss [64] is not significant while designing an ultrasound transducer or array for sonar applications. However, insertion loss is a critical parameter for bio-medical probe design. Therefore, application specific design knowledge is another key factor for successful and efficient design of ultrasound systems. In the proposed software tool, a powerful genetic algorithm based optimiser is used to find the optimum design parameter(s) and a rule based expert system is used to capture expert knowledge and guide the whole design optimisation problem.

Ever since the acceptance of knowledge based approaches from the 1970s [46], many commercial expert systems have been developed and used successfully to solve different problems. These include expert systems such as DENDRAL to interpret chemical spectrograms, MYCIN to diagnose illness, and DIPMETER to analyse geological data. The main usefulness of the expert system approach in the proposed design software is that it assists the user by providing valuable advice on key design aspects, which in the present scenario could include selecting the parameters to optimise, and provide recommendations on materials for use in manufacturing. Especially, input in constraining the optimisation process is very useful as this will avoid having to run a comprehensive search or optimisation routine on the complete list of design parameters, which can take a considerable amount of computational time, often with little improvement on the results.

141

6.2 Expert system overview

In its simplest form, an expert system [47]–[51] consists of the expert knowledge organised into a collection of rules, and an inference mechanism. In the proposed software tool, a simple rule based deduction algorithm, based on an open source program *expert1* [52] is used to build the expert system. The *expert1* program, a forward chaining model (i.e. to start with the available data and use inference rules to extract more data until a goal is reached [47]), is chosen primarily because it is similar to the expert system shell CLIPS [53]. CLIPS stands for C language interpreted production system, and is a multi paradigm program shell written in C programming language. CLIPS supports rule based, object oriented and procedural programming, and has been used widely in many commercial expert systems. Furthermore, if it is required to develop a fully fledged design package in low level programming languages such as C for speed and portability, it is easy to migrate the knowledge base from *expert1* to CLIPS.

The *expert1* deduction algorithm implemented in a MATLAB environment uses propositional logic [86],[87] and follows the normal rules of classical logic in symbolic form. The knowledge base comprises a set of propositions and the description of what is known about a proposition uses a two variable logic process that could conveniently represent unknown, inconsistent, partly true and partly false, as well as true and false cases [52]. The deduction algorithm is applied to an expert system (in MATLAB) where there are multiple rules and information on different propositions is supplied as the initial data for deduction. A graphical user interface (GUI) for the expert system is developed and is accessed from the expert system menu in the overall program. The main purpose of the GUI development is to make the expert system user friendly, so the knowledge engineering aspect can be readily implemented in the future. The detailed description of the deduction engine and the expert system is presented in the following sub sections.

6.2.1 Knowledge representation using propositions and rules

The knowledge representation is a key factor in designing an expert system as it affects the development, efficiency, portability and maintenance of the system. The transducer design tool knowledge base is made up of a set of propositions, which are considered to be simple, indivisible statements. For example, ILT can be a proposition, which could mean *an inversion layer transducer.* Propositional logic largely involves studying logical operators such as 'AND' and 'OR', and the use of such operators to connect multiple simple propositions. In classical logic, the propositions are assumed to be simple, i.e. they can be either true or false, but a deduction engine needs also to be able to support the fact that the status of a proposition is unknown and inconsistent. In fact, most propositions will start from the unknown state. Also, it is possible that rules and/or facts supplied can give inconsistent information about a proposition, and hence it is desirable to also be able to detect and report this situation. Thus, the logic needed to implement a deduction algorithm needs to be quadruple valued, with the following states: unknown, true, false, and inconsistent.

A convenient way of expressing the status of knowledge about a proposition is to use two variables, one giving the extent to which the proposition is known to be true, and the second giving the extent to which the proposition is known to be false. If expressed as %true and %false and the percentages are restricted to either 0% or 100% a quadruple logic results as shown below in Table 6.1:

State	%True	%False
True	100	0
False	0	100
Unknown	0	0
Inconsistent	100	100

Table 6.1: Four Valued Logic

Different ranges for the state variables can be chosen if desired, to extend the quadruple logic to a multi valued logic procedure. In the current implementation, propositions are indivisible units and the state of what is known about a proposition during each design process is described by the two state variables ILT^T and ILT^F, where the superscript T and F denote %True and %False, as described earlier and ILT stands for the proposition 'Inversion layer transducer'.

Rules, in the case of an expert system, represent the domain specific expert knowledge by providing the known relations between the propositions. They are generally developed and understood in the following form:

$$\text{If } \{U \ \& \ V \ \& \ \dots\dots W\} \text{ Then } Z \tag{6.1}$$

where U, V,...Z are simple propositions

In other words, rules link propositions by logical operators such as 'OR' and 'AND', and are used to make deductions about the propositions, typically using initial values for some of the propositions.

6.2.2 Deduction engine implementation

The rules described using the familiar IF THEN structure are transformed to a symmetric form according to the usual rules of classical logic [55]–[58] for the deduction engine. Deduction then relies on the rules and a simple transformation to %true and %false state variables [52]. For example, the rule "**IF** even harmonic sensitive **AND** thickness mode device **THEN** recommend inversion layer device" can be written in symmetric form as "$EHS^F|CTD^F|ILT^T$", where EHS, CTD and ILT are the propositions, which stand for even harmonic sensitivity, thickness mode device and inversion layer transducer, respectively and the superscripts (T or F) denote the

corresponding %true or %false state variable. Deduction in *expert1* is performed by evaluating the AND and OR operators that occur between the IF and THEN part in a rule, using the rules used in fuzzy set theory [83]–[85] as follows:

a and b is evaluated as min(a,b)

a or b is evaluated as max(a,b)

Using such rules for deduction is very useful as they are simple to apply in a program and also can be applied multiple times [52]. The second advantage is specially useful in implementing the deduction engine, as applying rules repeatedly will not alter the results and hence rules can be applied in any order.

6.2.3   Prototype expert system

This section presents an example to illustrate the working of the deduction engine used in the proposed transducer design tool. To begin with, let us consider the following propositions to be present in the knowledge base.

ILT : An inversion layer transducer

FFIL : Front face ILT

BFIL : Back face ILT

EHS : Even harmonic sensitive

CTD : Thickness mode device

ONEDARRAY : 1D Array

MML : Multiple matching layer

MBL : Multiple Backing layer

EBW : Enhanced bandwidth

Some sample rules about these propositions are shown below:

145

IF EHS & CTD **THEN** ILT

IF CTD & EHS & EBW **THEN** MML

IF CTD & EHS & EFFICIENCY **THEN** MML

These rules are converted to symmetrical OR format in the MATLAB program as follows:

$$\text{EHS}^\text{F}|\text{CTD}^\text{F}|\text{ILT}^\text{T} \tag{6.2}$$

$$\text{CTD}^\text{F}|\text{EHS}^\text{T}|\text{EBW}^\text{F}|\text{MML}^\text{T} \tag{6.3}$$

$$\text{CTD}^\text{F}|\text{EHS}^\text{T}|\text{EFFICIENCY}^\text{F}|\text{MML}^\text{T} \tag{6.4}$$

The data available for deduction (facts) is obtained from the user specification and is EHS:true and CTD:true. The state variables corresponding to these facts are $\text{EHS}^\text{T} = 100$ and $\text{CTD}^\text{T} = 100$. The deduction is carried out by applying rules (Equation 6.2–6.4) repeatedly in order, until there are no further changes in the state variables. Thus by running the deduction algorithm with the limited transducer world gives the results shown in Table 6.2. This sample expert system example illustrate how by supplying the requirement (EHS and CTD) a new design recommendation is deduced (i.e. ILT in this case).

Proposition	[%True %False]
CTD	[100 0]
EHS	[100 0]
ILT	[100 0]
EBW	[0 0]
MML	[0 0]
EFFICIENCY	[0 0]

Table 6.2: Results from a limited transducer world

The final results displayed to the user will be the description of all the propositions that have the state variables with some numerical value other than zero. For the example described so far the results are as shown in the Table 6.3.

Proposition	%True	Description
CTD	100	The transducer is a conventional thickness mode device
EHS	100	The transducer has even harmonic sensitivity
ILT	100	The transducer is an inversion layer device

Table 6.3: Result for a four valued logic procedure

As mentioned earlier in the thesis, the expert system can be extended easily by passing values between 0 to 100 for the facts, instead of a four valued logic. This would allow the user to implement a confidence factor into the system, allowing presentation of several possible solutions with different degrees of confidence. For example, if passing the state variables $ehs^T = 70$ and $ctd^T = 100$ in the previous example, results in the output detailed in Table 6.4.

Proposition	%True	Description
CTD	100	The transducer is a conventional thickness mode device
EHS	70	The transducer has even harmonic sensitivity
ILT	70	The transducer is an inversion layer device

Table 6.4: Result for a multi-valued logic procedure

6.2.4   Knowledge engineering

Knowledge engineering, the methodology for developing the expert system in a timely manner, is crucial. An open ended, iterative approach is proposed in acquisition and building of knowledge into the transducer design software system, due to time constraints. Figure 6.1 illustrates the methodology used for the transducer design tool project. The important stage in the design of an expert system is to decide about the knowledge representation. As heuristics or 'Rules of thumb' are

often used by human experts, it is not easy to capture such a fuzzy and complex chain of reasoning in an procedural algorithm. The proposed software uses rule based knowledge mainly because of its suitability for easy knowledge acquisition, incremental development, and portability with other commercial expert system shells such as CLIPS. More importantly the rule based system can be developed with less effort and time than an algorithm.

A series of interviews were carried out with transducer design experts, mainly Prof. Gordon Hayward (Head, The Centre for Ultrasonic Engineering, University of Strathclyde)and Mr. Victor Murray (Managing Director, Alba Ultrasound, UK). This initial discussions indicated clearly that it is important to capture the key application specific constraints, assumptions and requirements for the desired transducer.

Consequently, the expert system is designed with a two stage approach. A high level application specific details knowledge base, and a low level design specific technical knowledge. The main high level classification is based on the application domain such as SONAR, NDT, and Biomedicine, as transducer design requirements and criteria, as they vary significantly across different application areas. A sample questionairre (Appendix A) has been prepared as a result of these discussions, to assist knowledge acquisition exercise in future.

A sample representation of the design heuristics that will result from data acquisition is shown in Figure 6.2.This prototype system consist of rules and propositions for a limited SONAR world to illustrate the knowledge based approach, which can be appended and refined throughout the development and use of this software. As it is illustrated in the Figure. 6.2, the high level specification such as application, load medium, and design requirement such as bandwidth, sensitivty is obtained from the user during the initial stages. This will then fire the relevant rules to make recommendations based on the user input. The user can choose to accept or ignore

the recommendations while deciding about the low level design specifications, next. Typical low level designs include details such as material volume fraction (in case of composites), matching and backing layer specifications. Once all the low level input parameters are finalised, the simulation and optimisation tasks can be carried out. The proposed software also allows saving final design in a text file, to be loaded directly later if required.
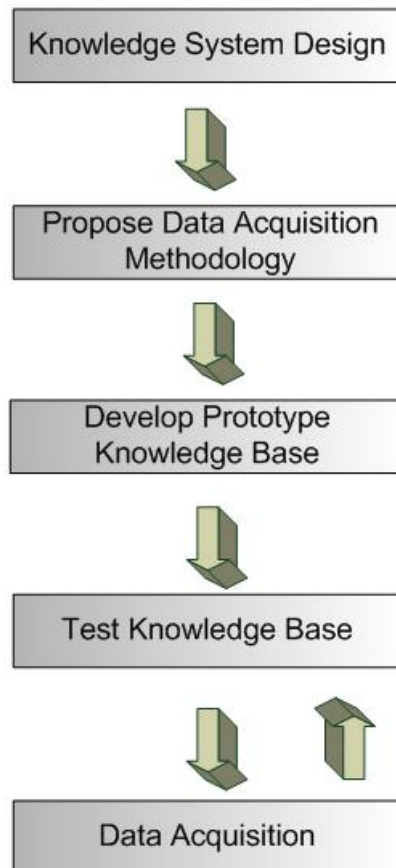
Figure 6.1: Knowledge engineering methodology
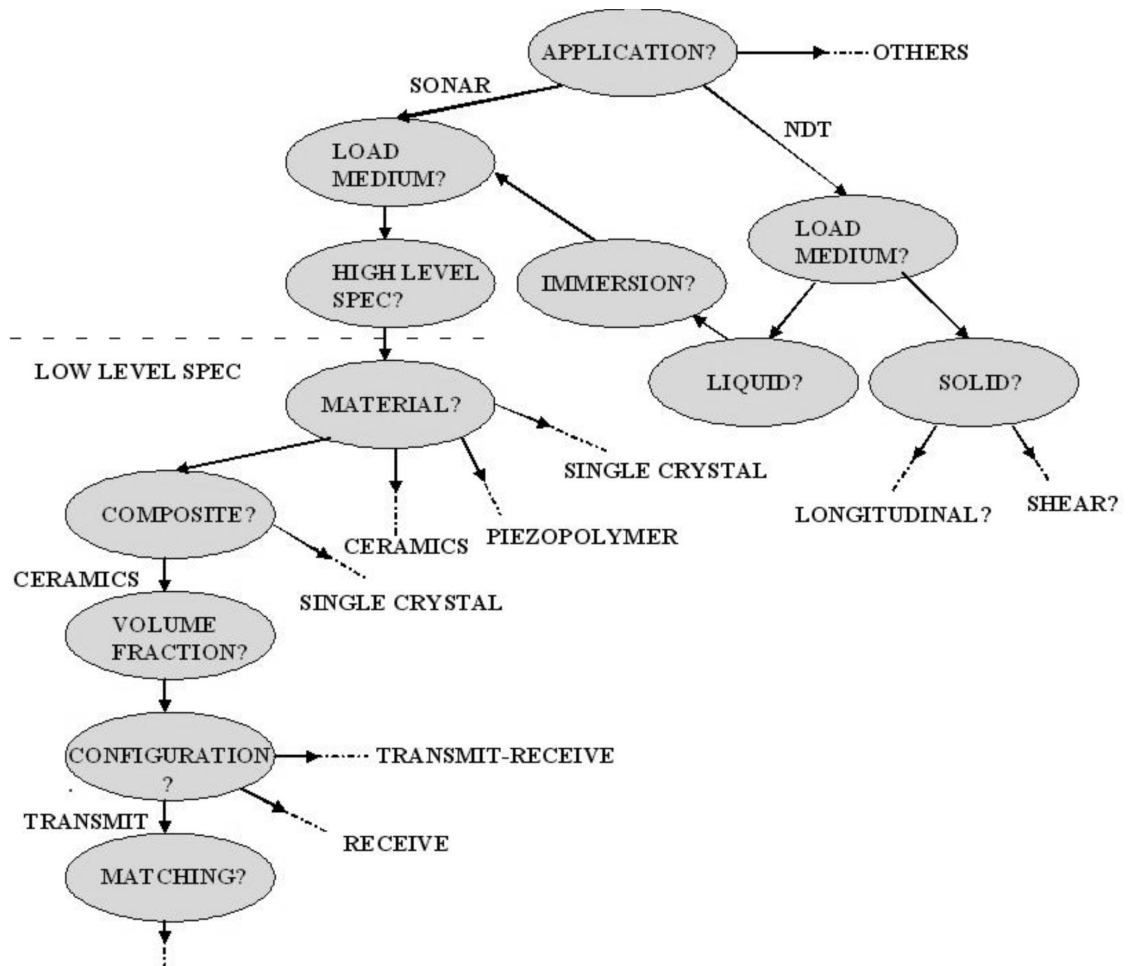
Figure 6.2: Sample transducer design heuristics

6.3 Choice of optimisers

The main aim of an optimiser is to steer a process towards a particular goal. The optimiser accepts a set of input parameters, which are varied in order to produce an output as close as possible to the stated goal function. The goal function may be any output parameter or a combination of output parameters of the numerical simulation model in the software. Examples include single values, such as device bandwidth, efficiency, gain bandwidth product, or a collection of values such as an impulse response spectrum. In other words, optimisation can be considered as an iterative process as illustrated in Figure 6.3, in which the optimiser controls the simulation process, deciding upon input parameters and evaluating output cost functions to determine appropriate changes to the input for the next iteration. The process continues until the output is sufficiently close to the goal function.
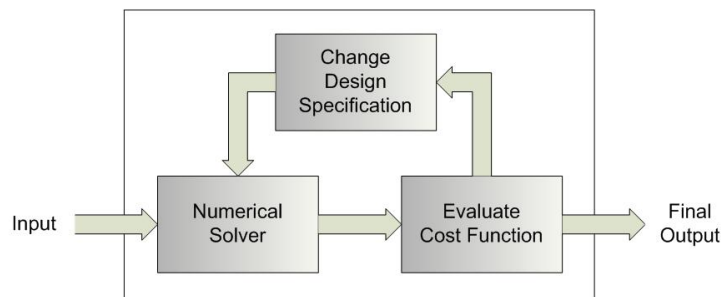
Figure 6.3: Optimisation process overview

A number of general techniques have been developed and used effectively in global optimisation problems in the past. These includes methods such as brute force search, gradient methods, iterated search, simulated annealing, genetic algorithm and pattern search [1]–[6]. A brief discussion of some of these general search techniques and the reason for choosing a genetic algorithm approach for the current work is presented in this section.

The most basic or fundamental way to implement an optimiser is to perform a *brute force search* in the whole problem space. The search itself could be implemented in a random or in a systematic manner. However, this approach is the most inefficient in terms of computational time required and grows directly in proportion to the problem. The classical way to solve an optimisation problem is to use some kind of a *gradient method* [59]. The gradient search techniques such as steepest descent/ascent method and Newton's method work very well for unimodal, continuous problems. However, when the problem is discrete and/or the problem space has lots of local minima, as in most practical cases, the gradient approach will fail and tend to iterate towards, local minima. One way to overcome this problem is to combine the above two techniques and use a *iterated search approach*. Essentially, a gradient search is performed randomly in many points in the problem space, and the final or global optimum is deduced by comparing all the outcomes. Even though this approach goes some way towards exploring the problem space for a gradient based approach, the method is computationally intensive, and it is difficult to obtain the right balance between the two techniques used. Furthermore, this approach is not guaranteed to find the global optimal solution.

Another variant of the iterated search approach is the *simulated annealing* method proposed in [60]. Simulated annealing is a stochastic optimisation technique inspired by the annealing process in metallurgy. In a physical annealing process, a high temperature melt is cooled slowly. Initially, when the temperature is high, the atoms in the melt are free to move, allowing it to explore the whole problem space in an attempt to find a state of low energy (the global optimum for the atom). As the temperature gradually decreases, the movements are restricted and at final cooling temperature the global optimum will be achieved. The local minima are avoided by the ability of the process to jump out or exit at early stages of the evaluation. Consequently, the cooling schedule (or the rate of decrease of temperature) is crucial

to make the annealing technique work. If the melt is cooled rapidly the atoms tend to crystalise or freeze at a local minimum without exploring the complete problem space for an global optimum. A search technique is implemented by taking the probability of the fitness function and a global parameter (temperature, T), to decide whether or not to depart from the local minimum and the global parameter T changes throughout the optimisation process. That is, to begin with, T is large and the process is almost random, but as T reduces, the problem becomes increasingly local in nature. However, in simulated annealing there is no information passed between each iteration, and consequently this knowledge of the problem space cannot be used to guide the optimisation process, which is very valuable in most scenarios.

While the choice of optimiser influences the ability to perform global optimisation efficiently, it does not mean that the other optimisation techniques mentioned earlier are unsuitable for the problem at hand. The Genetic Algorithm (GA) approach is selected over the other optimisation techniques for the proposed software because of the inherent suitability of the algorithm to perform well in discontinuous, and demanding optimisation problems that cannot be solved using conventional methods. GA overcomes most of the problems suffered by other global search techniques. The introduction of a GA optimisation algorithm along with a description of the hybrid genetic algorithm routine implemented in the software program is presented in the following section.

6.3.1 Genetic algorithm based optimisation techniques

6.3.1.1 Introduction to Genetic Algorithms

The Genetic algorithm is a stochastic search technique, invented by Holland [1] and is a part of evolutionary computing that is based on Darwin's theory of evolution.

Genetic Algorithms (GAs) solve optimisation problems by mimicking the principles of gene combination in biological reproduction. GAs [2]–[6] have received considerable attention as a novel optimisation technique, because of the following main advantages.

- GAs can handle any kind of objective function and any kind of constraints (linear or non linear) defined on discrete, continuous or mixed search spaces

- The ergodicity of the evolution operator makes genetic algorithms very effective at performing global searches.

- GAs work on the coding space, not on the solution itself

- GAs use payoff information (fitness function), not any other auxiliary knowledge of the underlying process

- GAs inherent nature suits parallel processing

Figure 6.4 shows the general structure of a genetic algorithm. GAs presume that the potential solution to any problem is an individual (*chromosome*) and can be represented by a set of parameters (*genes* of a chromosome). It is an iterative approach and begins with a random set of solutions (chromosomes) called *population*. Holland worked primarily with binary strings to represent chromosomes, but any data structures (arrays, trees, lists, or any other object) can be used. In each cycle, genetic operations are performed on the present population to produce new offspring. The GA optimisation algorithm can be implemented as a 'simple' or 'steady state' method. The simple genetic algorithm [4] is a generational algorithm in which the entire population is replaced in each generation. In the steady state genetic algorithm, only a few individuals are replaced each 'generation'. This type of replacement is often referred to as overlapping populations. Typically the ge-

netic operations at each iteration involve three operations; selection, crossover and
mutation.
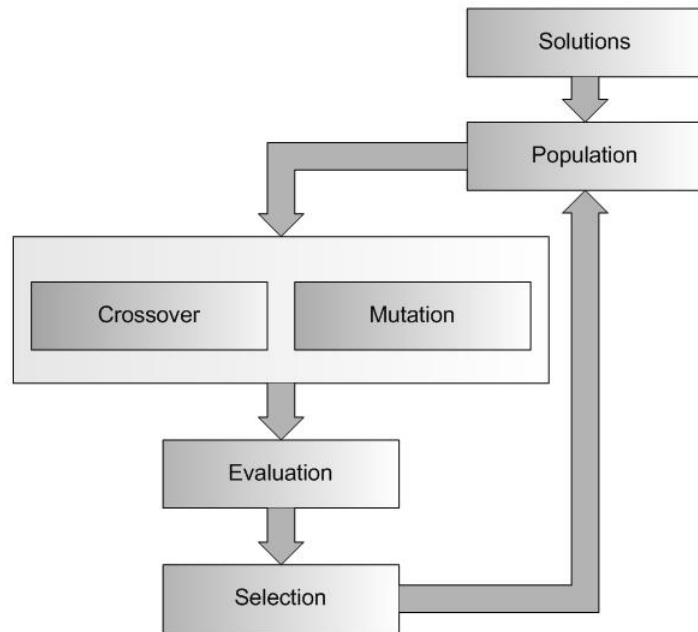
Figure 6.4: Genetic Algorithm (GA) overview
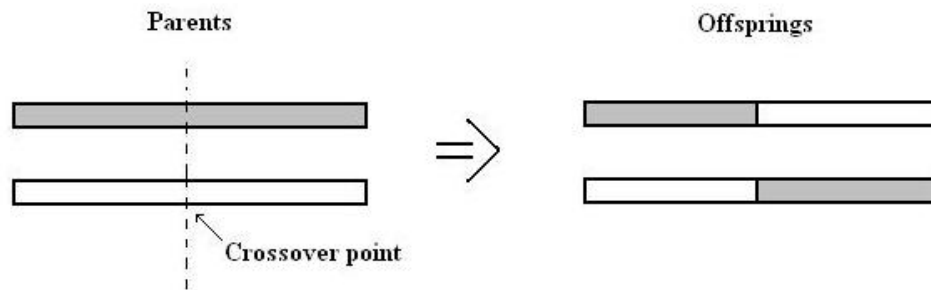
Figure 6.5: Crossover genetic operation

Crossover is the most important genetic operator. It operates on two chromosomes,
the offspring here is a combination of both chromosomes involved. The simplest way
to perform crossover is to take a random cut point in both the parent chromosomes
and then swapping as illustrated in Figure 6.5. The performance of GA depends, to
a great extend on the performance of the crossover operator.

Mutation is a background operator which produces spontaneous random changes in chromosomes. A simple way to achieve mutation is by altering one or more genes in a chromosome. It can help the search find solutions that crossover alone might not encounter.

The principal driving force behind the GA is essentially the *selection* process. It pressurises the population to yield better offspring in each cycle. At each step, some offspring are selected to be the parents in the next cycle. Some of the more common selection methods include roulette wheel selection (the likelihood of picking an individual is proportional to the individual's score), tournament selection (a number of individuals are picked using roulette wheel selection, then the best of these is (are) chosen for mating), and rank selection (pick the best individual every time) and threshold selection. The key consideration in the selection process is to find good individuals and also to maintain diversity, to ensure that the population does not converge quickly to the best individual in a population. In other words, the selection process should be biased toward better individuals, but should also pick some that are not quite as good (but hopefully have some good genetic material in them).

Two of the most common methods for maintaining diversity are DeJong-style crowding and fitness scaling [4].

1. In DeJong-style crowding, when new offspring are created, they replace the individuals in the population that are most similar to them.

2. Fitness scaling derates the objective score of individuals that are less unique than others in the population. By derating the scores of similar individuals, less similar individuals are more likely to be selected for mating.

156

During the iterative process, at each generation relatively good chromosomes (solutions) are produced and the relatively bad ones die. Over successive generations, the population "evolves" toward an optimal solution.

6.3.2 Hybrid optimisation routines

The GA optimisation routine is implemented in the proposed software by using the MATLAB [37] genetic algorithm tool box. The MATLAB GA tool box provides a graphical user interface shown in Figure 6.6 to set up and solve global optimisation problems. The supplied GUI cannot be compiled to generate a stand alone executable along with user programs. However, the GA tool can be invoked as a function within the user programs. The GA function has the format as shown below:

$$[x, fval, reason, output, population] = ga(fitnessfun, nvars, options)$$

where the **fitnessfun** is a pointer variable (commonly refered to in the software literature as a function handle) to the fitness function program, **nvars** is the number of independent variables to optimise; options is a structure containing options for the genetic algorithm; **x** and **fval** are the results returned by the GA function; reason is the reason the algorithm terminated; output is a structure containing information about the performance of the algorithm at each generation; and population is the final population.

The GA function can be invoked with different options, multiple times from within a user defined M-file function, and the returned results can be analysed and presented to the user. The fitnessfun is an M-file, which accepts the parameters to be optimised as a vector. Within the fitness function, first the numerical simulation of the transducer using the user design specification (loaded from a file) and the optimisation parameter (passed as input) is performed. Then the cost function parameter is

extracted from the simulation results. The fitness function does not plot any results as this will slow down the optimisation process greatly. However, when the optimisation procedure terminates, the GA function returns the final result which can be presented to the user as a plot. Also, during the optimisation it is possible to plot various trends within the population at each iteration, by specifying what to plot in the options parameter passed to GA function. This is useful in monitoring the performance of the optimisation process and make necessary changes to the functions option to further improve the process. For example, while running the optimisation process, if there is no marked improvement in the result after a certain number of generations, while rerunning it the stopping criteria can be changed in such a way that the GA optimisation stalls at a particular generation.

GAs have proved to be a versatile and effective approach for solving optimisation problems. Nevertheless, there are many problems in which a genetic algorithm alone is not the best way to go about obtaining a solution. Many hybrid models have been proposed in the past to solve these problems. One of the most common hybrid genetic algorithms is to incorporate local optimisation as an add-on to the simple GA. Because of the complementary properties of GA and conventional heuristics, this method often outperforms either method operating alone. Hybrid optimisation routines can be performed easily by specifying a particular option while invoking the command line GA function. For example, the program can be made to run local minimisation MATLAB functions (such as fminunc, fminsearch, pattersearch ...etc). This will make the program first run the genetic algorithm to find a point close to the optimal point and then uses that point as the initial point for the local search functions in an attempt to improve the value of the fitness function further.
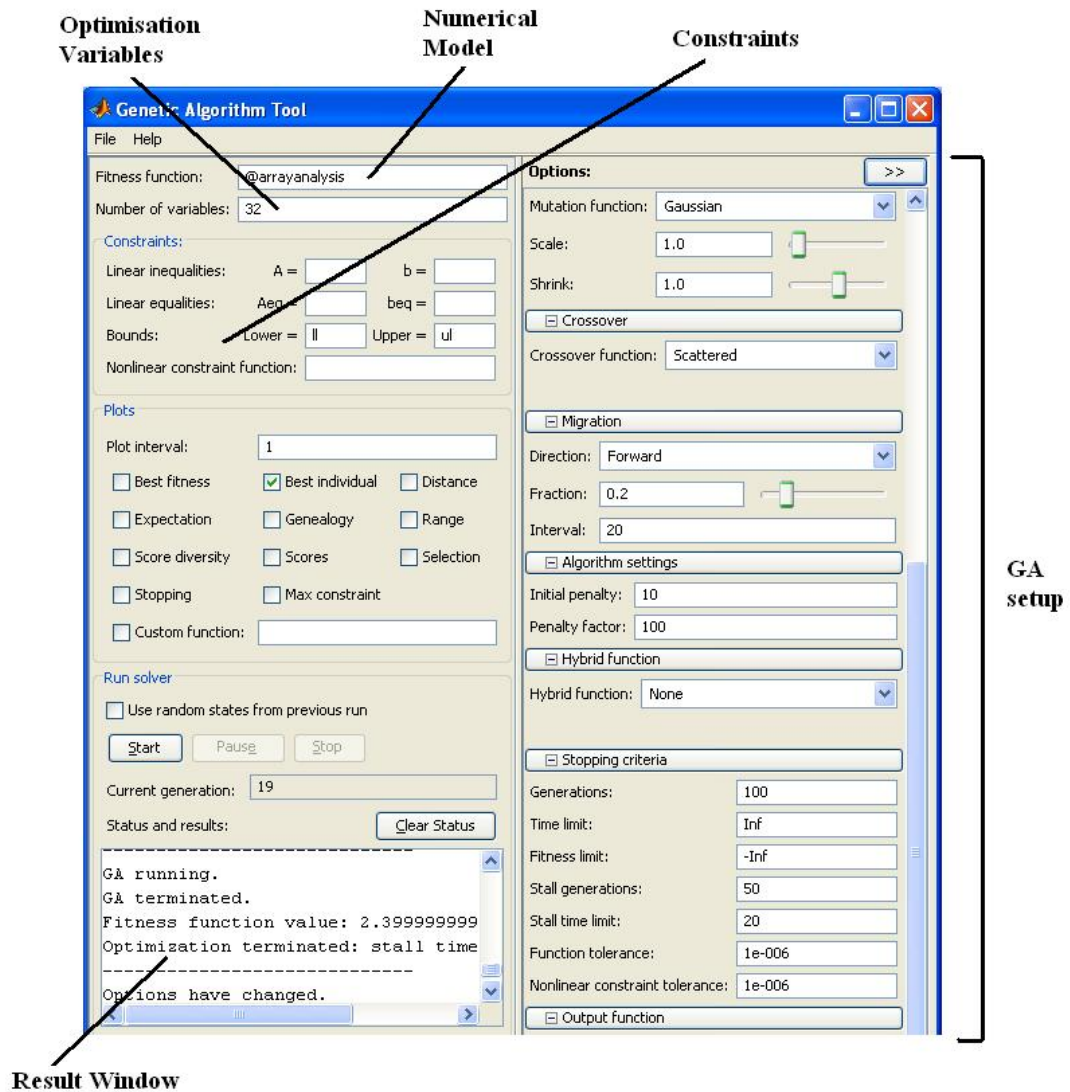
Figure 6.6: The MATLAB GA toolbox graphical user interface

6.4 Results

In order to illustrate the use of an optimiser in a practical situation, and the necessary considerations, some results are presented in this section. To show that the knowledge based approach will facilitate an effective solution in terms of manufacturing complexity and cost, a relatively straightforward thickness mode design was considered, followed by an IL device, intended to maximise bandwidth. The design specification for the first example was to create a 400 kHz device, operating into

159

water, with high sensitivity and a fractional transmission bandwidth greater than 55%. No constraints were placed on the electrical interface and mode purity was required across the band. The expert system produced a solution in the form of an air backed, 70% volume fraction composite (PZT5H/Hardset Epoxy [44]) with a single matching layer, operating directly into the water load. The optimiser was then invoked to refine the design of the matching layer. For illustration purposes, a layer of specific acoustic impedance equivalent to the geometric mean of the two media on either side was selected as a starting point. The matching layer thickness was set as the variable parameter for the optimiser. Equation 6.5 shows the figure of merit used for the optimisation. Other cost functions or figures of merit can be used, depending on the design requirement.

$$\text{Cost Function} = - (f_U - f_L) * 100/f_{peak} \qquad (6.5)$$

where, f_U, f_L are the upper and lower 3dB frequencies, respectively and f_{peak} is the center frequency.

Figure 6.7 shows the frequency response of the transducer at the optimum layer thickness predicted by the optimiser. The optimiser prediction is verified by a slow iterative process of running the modelling program with a range of thickness values, starting from zero and in steps of 0.1mm increasing up to the transducer thickness. Figure 6.8 shows the cost function value for different trials.

To illustrate a more complex transducer configuration, a device with a fundamental operating frequency of 500 kHz and intended for a non-linear, immersion application, was specified. In this case, a strong second harmonic response was required, with a -6db degree of flatness across the band. Such input is termed as the high level design specification. The expert system then conducts an interactive dialogue with the user to define the low level design parameters. During this interview process

160
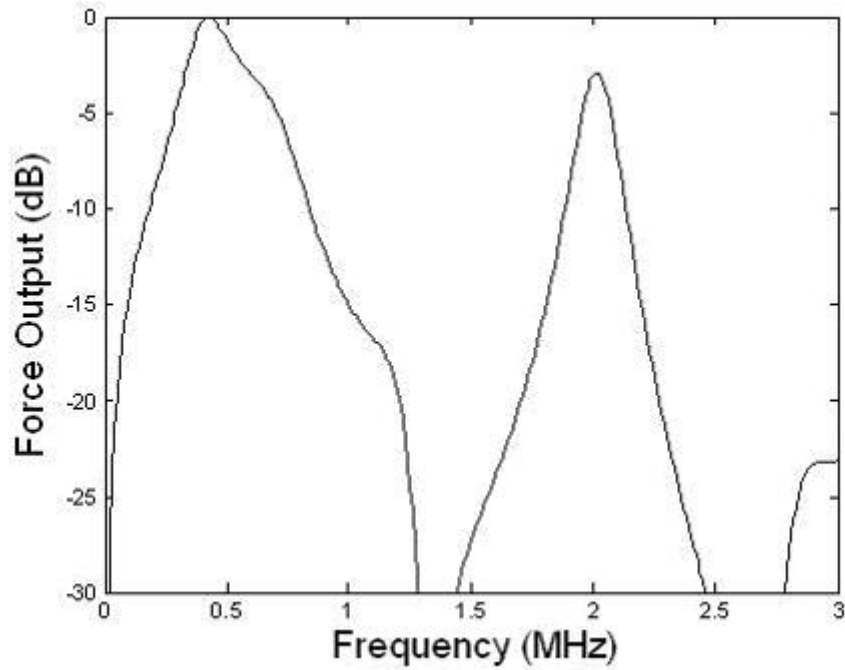
Figure 6.7: Relative Transmit Sensitivity with matching layer thickness predicted by the optimiser.

the transducer configuration and key optimiser parameters are identified. In this particular case, the process resulted in an IL, 1-3 composite (PZT-5H/Mediumset polymer, 50% Volume Fraction) thickness mode device, with a fundamental frequency of 500 kHz. The material database is then interrogated queried to help select appropriate material properties. An additional 'in house' program CompD, based on [61], is used to predict practical parameters useful for modelling and manufacture (this includes pitch, thickness, acoustic impedance and bulk capacitance). At this stage, the expert system recommends a front face inversion layer device with one matching layer, with the matching layer thickness being the parameter to optimise. However, the user can override the recommendation with alternative (and/or additional) parameters.

The materials database is queried again to select a matching layer. Initially, a material whose specific acoustic impedance is close to the geometric mean of the
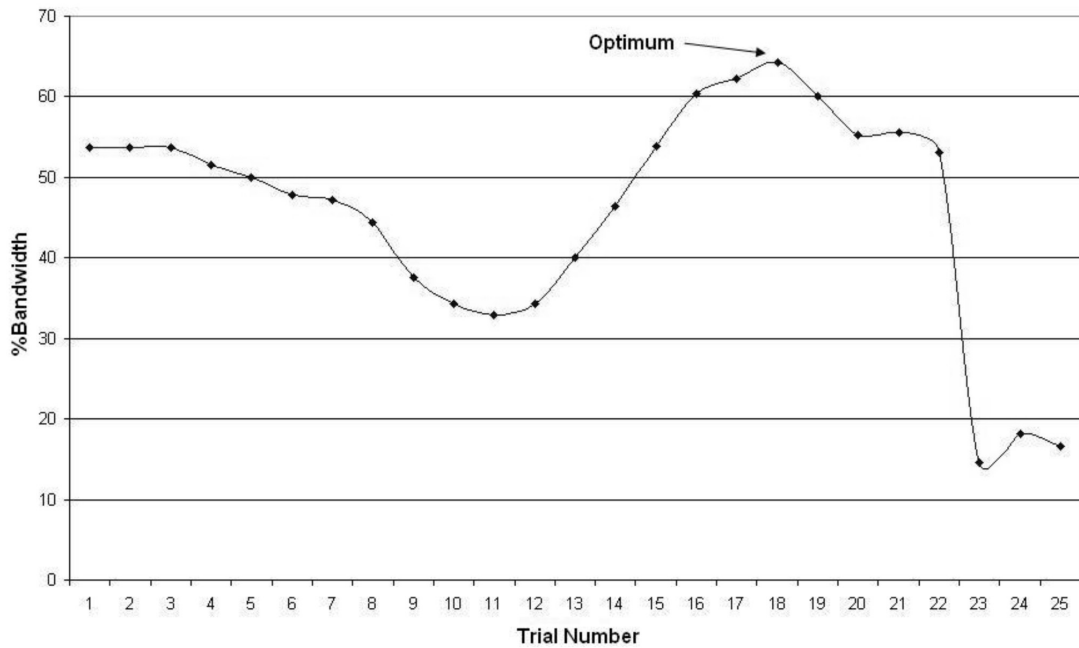
Figure 6.8: Manual optimisation around quarter wavelength.

water load and the transducer is chosen and the initial thickness of matching layer was $\lambda/4$ at 750 kHz.

Once a transducer model and key optimisation parameters are identified, the optimiser then works within this boundary to obtain a best configuration to match the user design specification. A genetic algorithm optimisation procedure was invoked, with the matching layer thickness as the single optimiser parameter. In this example, the cost function was selected to reduce peaking at the fundamental and second harmonic frequencies, in order to promote a relatively flat response. The relative normalized sensitivity for the predicted matching layer thickness is shown in Fig. 6.9. It should be noted that the result obtained is not necessarily the optimum configuration, due to the constraints placed on the optimisation process by the knowledge base. Further improvement is usually possible by including more key optimisation parameters and using a more complex cost (or fitness) function for the optimisation process.
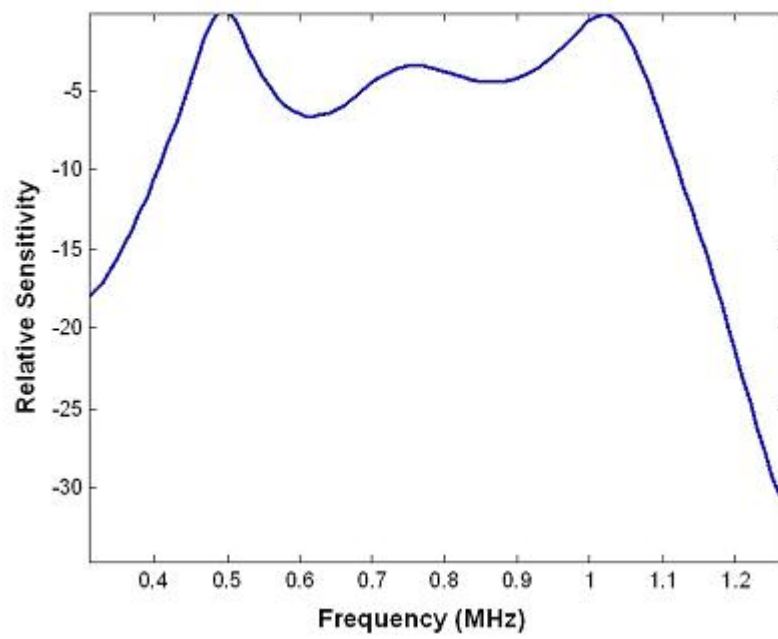
Figure 6.9: Relative Sensitivity with matching layer thickness predicted by the optimiser.

6.5   Summary

This Chapter presented the implementation of an expert system and optimisation algorithm, and the strategy of bringing together both parts in the proposed transducer design software. The brief review of expert system theory and the choice of optimiser available, based on the particular characteristics of the transducer design problem is also introduced. Finally, a typical optimisation example was included to illustrate the expert system driven transducer design optimisation approach. A selection of practical design optimisation and manufacture examples, to help confirm the modelling success, is presented in the next Chapter.

Chapter 7

A selection of design examples

This chapter presents a selection of design and optimisation results, to help confirm the modelling success. The first of these relates to the design optimisation of multiple matching layers, designed to promote bandwidth and sensitivity in relatively straightforward thickness mode applications. This is followed by the design of a more complex inversion layer transducer (ILT). Finally, beam modelling to optimise the structure of a one-dimensional array in order to minimise the number of elements required to achieve the desired directivity profile is presented.

7.1 150kHz conventional thickness mode transducer design example

The design requirement is to construct a thickness mode transducer for immersion probe applications, centered around a nominal frequency of 150 kHz, with four quarter wavelength matching layers at the front face and air (or) very light backing layer. No specific constraints are placed on the device operational bandwidth and sensitivity requirements.

CERAMIC PARAMETERS:	PHYSICAL CHARACTERISTICS:
Ceramic Material: PZT5H	Calculation method: Fm
c_{11}^E: 1.340000e+011	Type: Circular
c_{12}^E: 8.970000e+010	Dimensions: 92 mm Diameter
$c_{13:8.570000e+010}^E$	Transducer Area: 6647.6
$c_{33:1.090000e+011}^E$	Volume Fraction: 0.500
e_{31}: -5.06	Transducer Thickness: 11.471
e_{33}: 21.20	Saw Width: 0.500
Density: 7780	Saw Pitch: 1.912
Attenuation: 0.92	Aspect Ratio: 0.118
EPOXY PARAMETERS:	**FREQUENCY PARAMETERS:**
Epoxy Material: CY208	k_t: 0.69
c_{11}: 4.710000e+009	f_e: 113137.99
Attenuation: 10.00	f_m: 150000.00
Density: 1150.00	c_{33}^D: 5.288003e+010
	h_{33}: 2.052720e+009
	Attenuation: (dB/cm @ 1MHz) 3.29
	Density: 4465.0
	Acoustic Impedance (MRayls): 15.37
	Capacitance: 3.502000e-006
	Thickness Velocity: 3441.40

Table 7.1: 150 kHz conventional thickness mode transducer active layer specification

The first stage in the design process is calculating the active piezoelectric layer specification. For this purpose, an in house program CompD, which is based on [61] is integrated into the proposed design software. A sample first cut design specification of the 1-3 microstructure of an active piezoelectric layer using the CompD simulation program for this device is presented in Table 7.1. The simulated and measured device operational impedance of the active layer in air is shown in Figure 7.1. It is clear from these simulations that the device has a mechanical resonance frequency of 150 kHz to satisfy the required design specification. Please note that a 50 Ohm electrical load is considered in all simulations in this section, unless otherwise stated.

A classical quarter wavelength matching layer is choosen for this design. For a piezoelectric composite (approximately 15 MRayl in this case) radiating to water (1.5 MRayl), the approximate impedance values for the four front face matching
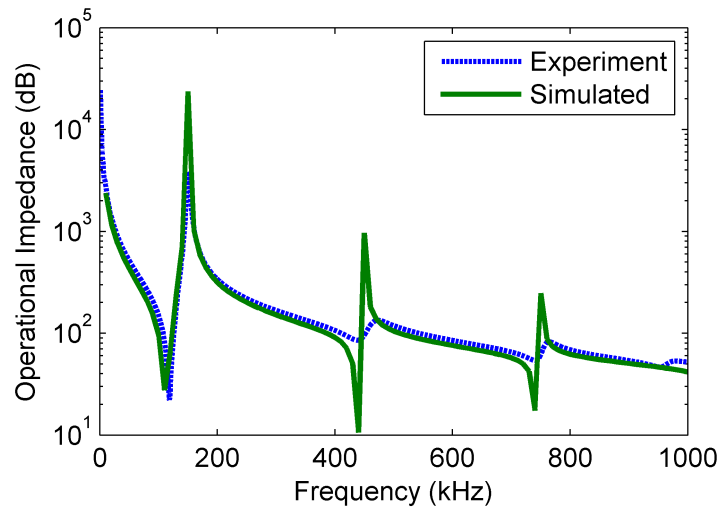
Figure 7.1: Simulation and predicted operational impedance of the 150kHz composite, without matching and backing layers

	Impedance (MRayl)	Density (Kg/m3)	Length (mm)	Velocity (m/s)
Layer 1	12.7	7848	2.7	1621
Layer 2	7.2	4376	2.72	1634
Layer 3	3.3	1183	4.6	2774
Layer 4	1.8	722	4.2	2538

Table 7.2: Manufactured matching layer materials properties for the the four matching layers

layers calculated using the approach followed by Desilets et al. [12] are 12.5 MRayl, 7 MRayl, 3 MRayl and 15 MRayl, respectively. The materials database is then queried to obtain real material parameters, matching as closely as possible to the requirements and salient data are listed in Table 7.2. Further simulations were carried out with these realistic materials data and are presented in Figure 7.2, together with the measured pulse echo results from the manufactured prototype transducer.
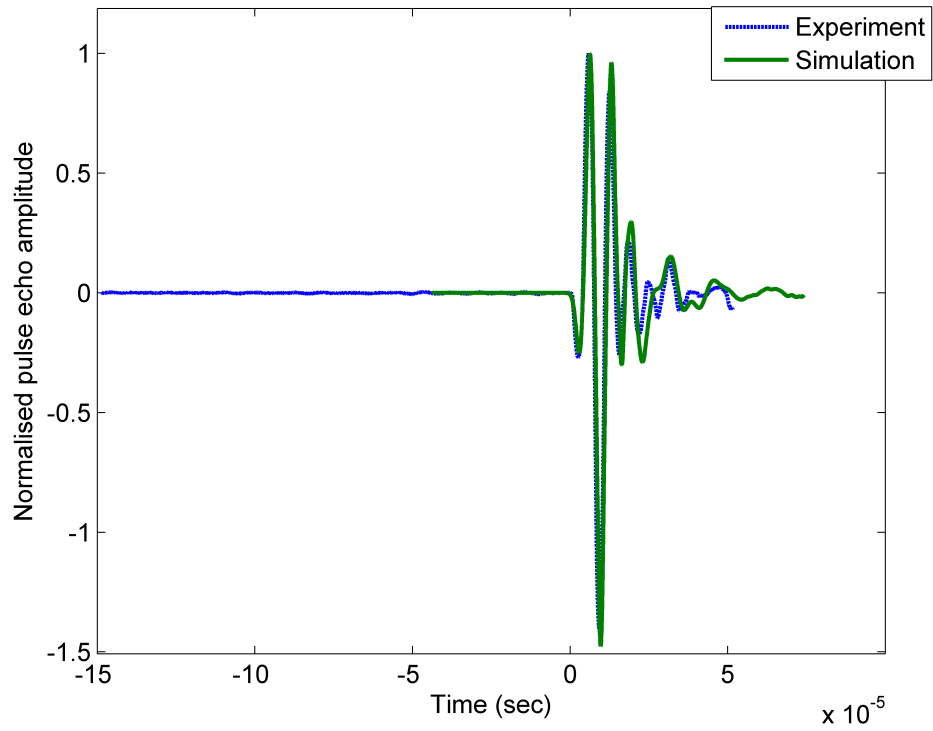
(a) Pulse echo time domain impulse response plot
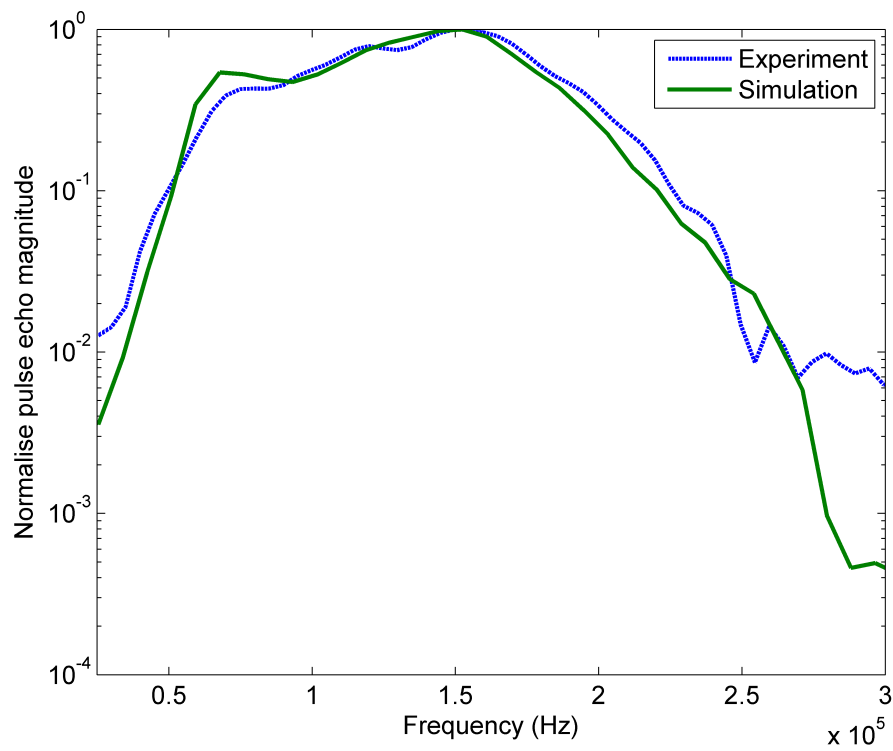
(b) Pulse echo frequency domain impulse response plot

Figure 7.2: (a) Time and (b) frequency domain pulse echo response comparison results of the 150 kHz thickness mode transducer with four matching layers radiating into a water load, and air backing

168

CERAMIC PARAMETERS:	PHYSICAL CHARACTERISTICS:
Ceramic Material: PZT5H	Calculation method: Fe
c_{11}^E: 1.210000e+011	Type: rectangular
c_{12}^E: 7.540000e+010	Dimensions: 30 mm by 30 mm
c_{13}^E:7.520000e+010	Transducer Area: 900 mm^2
c_{33}^E:1.110000e+011	Volume Fraction: 0.4
e_{31}: -5.4	Transducer Thickness: 1.149 mm
e_{33}: 15.8	Saw Width: 0.500
Density: 7750	Saw Pitch: 0.43
Attenuation: 0.84	Aspect Ratio: 0.186
EPOXY PARAMETERS:	**FREQUENCY PARAMETERS:**
Epoxy Material: CY1301	k_t: 0.64
c_{11}: 7.504000e+009	f_e: 999.61
Attenuation: 5.00	f_m: 1245.91
Density: 1140.00	c_{33}^D: 4.9e+010
	h_{33}: 2.6e+009
	Attenuation: (dB/cm @ 1MHz) 2.37
	Density: 3763.5
	Acoustic Impedance (MRayls): 13.59
	Capacitance: 1.9e-006
	Thickness Velocity: 3609.89

Table 7.3: 1 MHz Invertion layer transducer active layer specification

7.2 Inversion layer transducer design

Using the mathematical model described earlier in Section 3.1.2, a FFIL receiver, denoted device B, with a nominal fundamental thickness mode of 1MHz, comprising 40% volume fraction PZT5A (Ferroperm, Kvistgard, Denmark) and CY1301/HY1300 epoxy (Vantico Ltd, Duxford, UK) was designed. Table 7.3 lists the detailed specification of the active layer design for device B. To help confirm the mechanical behaviour of the active layer manufactured, impedance analyser measurement is taken at this stage. Figure 7.3 shows a comparison of simulated and measured active element operational impedance. It can be seen clearly that the presence of the inverted layer promotes the even harmonic activity in the device, and by carefully selecting a matching scheme, a transducer with much improved operational bandwidth and sensitivity can be achieved.
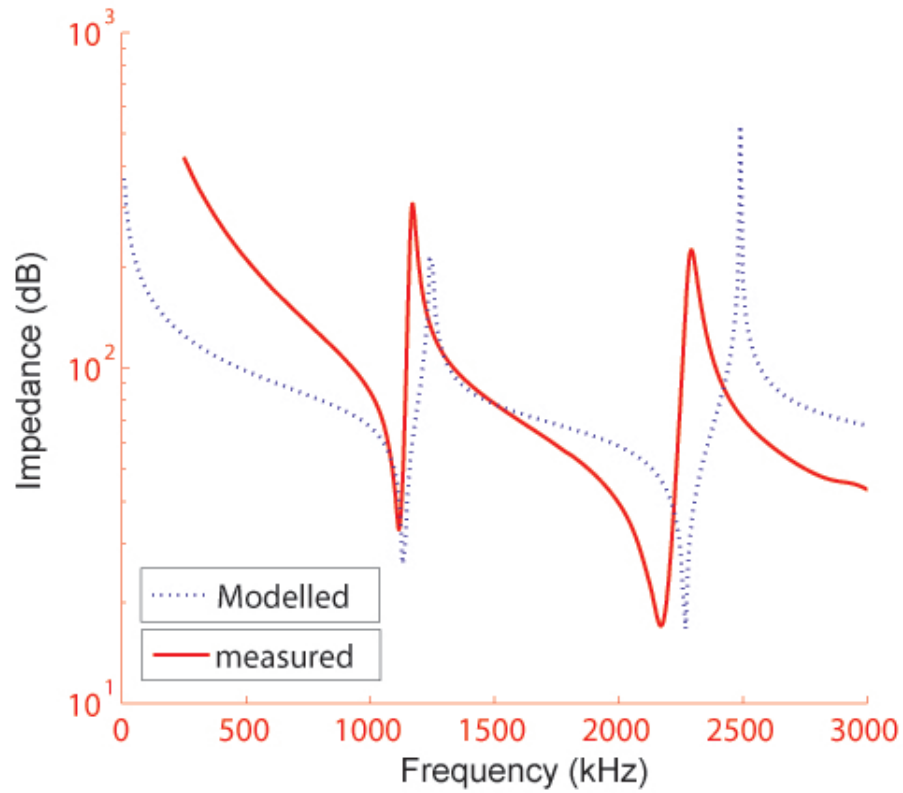
Figure 7.3: Active layer operational impedance profile measured using an impedance analyser (solid line) compared with predicted model (dotted line)

Various acoustic matching schemes were derived to match the impedance of the above transducer (13.6MRayl) to water load (1.5MRayl), using well established filter design techniques [19], described earlier in Chapter 4 . Two examples, one giving a maximally flat and a second exhibiting equal-ripple transducer bandwidth are shown in Table 7.4. The predicted impulse response profile of a four layer, matched FFIL transducer (equal-ripple scheme #1 in Table 7.4) is shown in Figure 7.4.
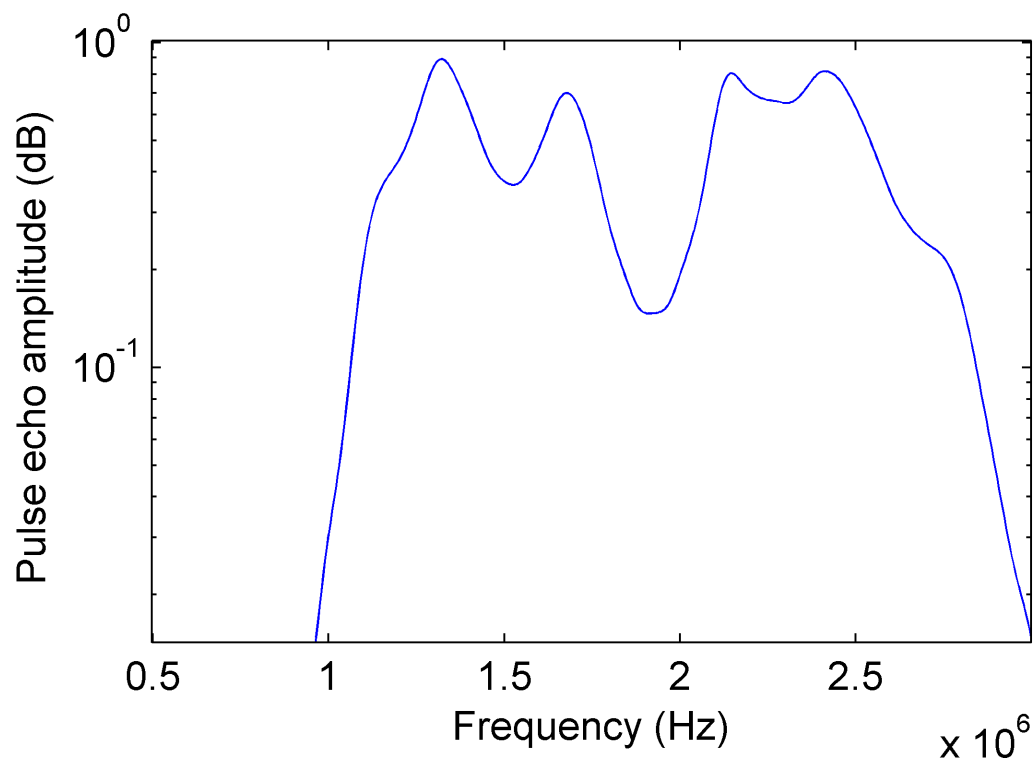
Figure 7.4: Simulated FFIL impulse response of device B in pulse echo mode of operation

device B was manufactured using the Chebyshev equal-ripple scheme 2 detailed in Table 7.4. The salient properties of the matching layer materials used in manufacture, measured at 500kHz are shown in Table 7.5. Figure 7.5 show the experimental results, and Figure 7.6 shows the picture of finished device B in a water tight container together with a schematic describing the casing. A comparison of both the simulated and measured pulse echo impulse response spectrum is presented in Figure 7.7, and the results compare well in identifying the peaks in the response. However, the peak amplitude does not match well, and this is due to the accuracy of the damping model used for simulation purposes. It is clearly evident that ITL devices due to its even harmonic sensitive nature can be used to manufacture broadband transducers by choosing an appropriate matching layer scheme.
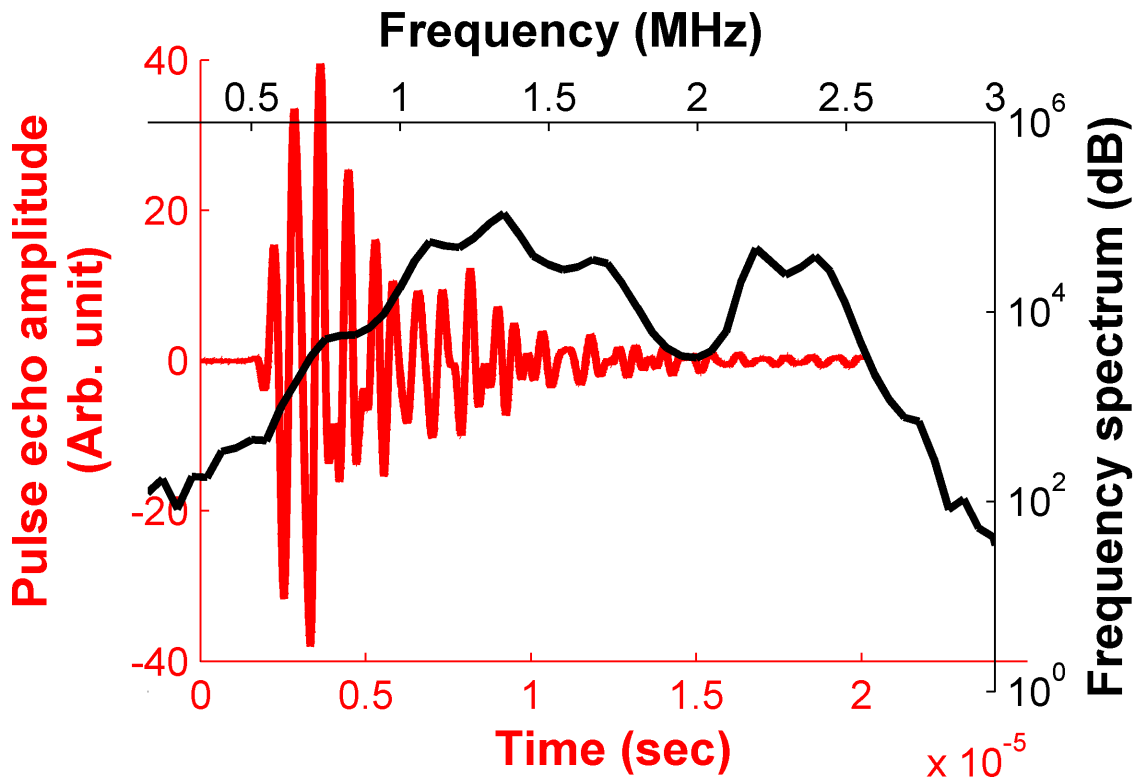
Figure 7.5: Experimental pulse echo response of device B in water

Layer	1	2	3	4
Binomial/Maximally flat	11.96	6.88	3	1.72
Chebyshev/Equal-ripple scheme 1	10.19	6.15	3.34	2.01
Chebyshev/Equal-ripple scheme 2	6.46	5.1	4	3.15

Table 7.4: Theoretical matching impedance(MRayl) calculated using the filter design technique, for a four layer design

	Z(MRayl)	Density (Kg/m3)	Velocity (m/s)	Thickness (mm)
Layer 1	6.26	2487	2519	0.63
Layer 2	5.16	2039	2532	0.61
Layer 3	4.13	1829	2257	0.56
Layer 4	3.03	1178	2568	0.64

Table 7.5: Matching Layer Material Properties measured at 500kHz

(a) Completed ILT (device B) in a watertight housing
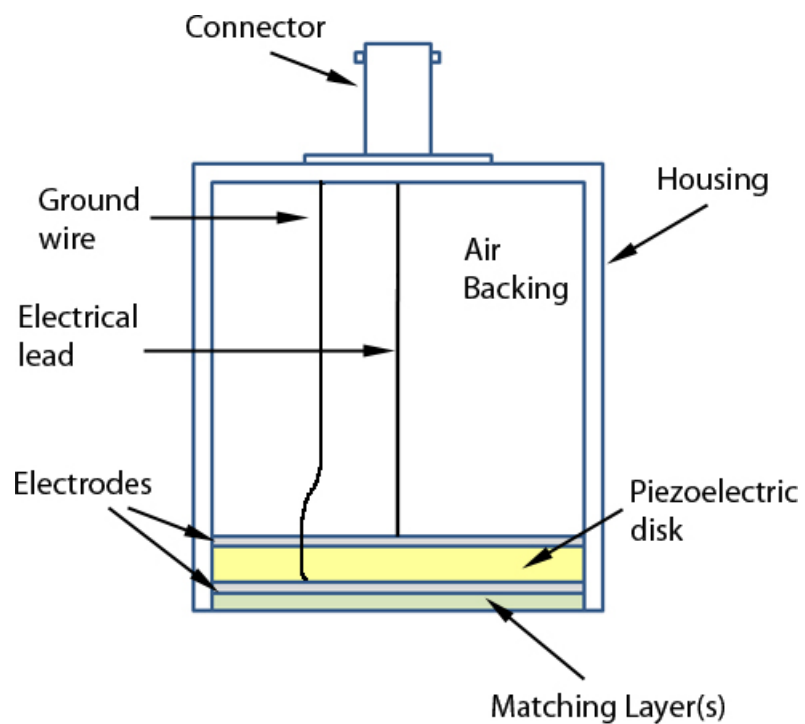
(b) A schematic showing the transducer construction

Figure 7.6: Final manufactured device picture and a schematic showing its construction
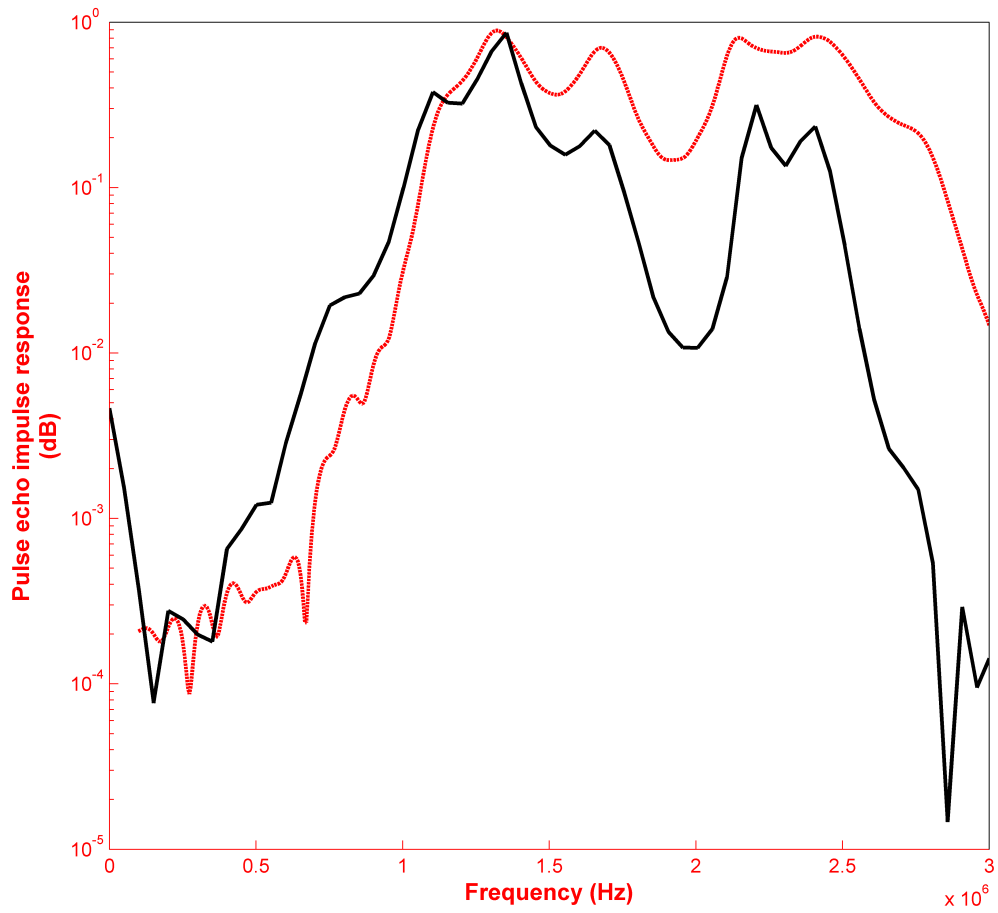
Figure 7.7: Comparison of simulated (red dotted) against experimental (black solid) pulse echo impulse response spectrum of device B, operating in water

7.3 Transducer array design

The final design optimisation example is of the structure of a one-dimensional transducer array in order to minimise the number of elements required to achieve a desired directivity response. A key requirements in ultrasonic arrays is spatial resolution, and this is directly dependent on the array apperture size. Figure 7.8 shows a simulation illustrating the effect of array beamwidth as a function of array aperture size.
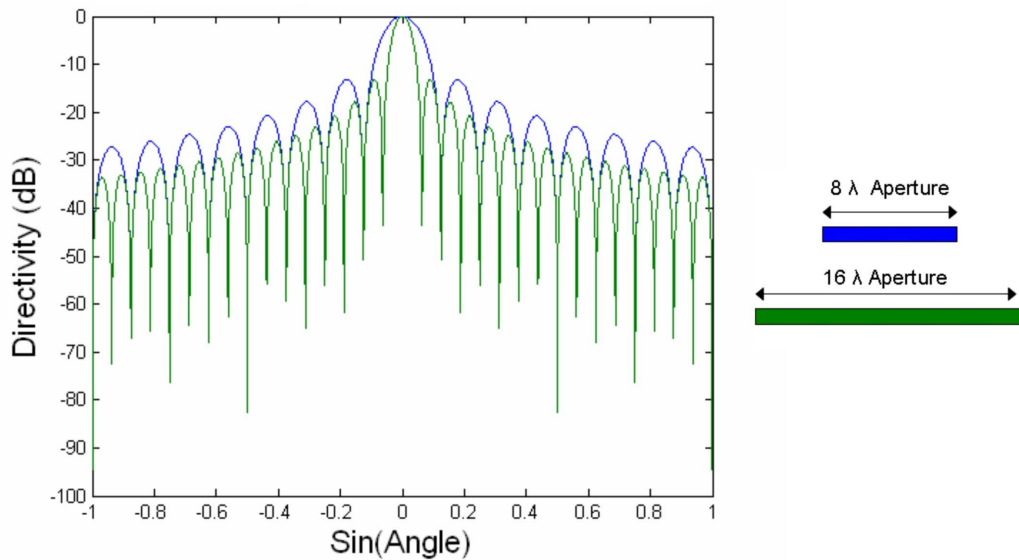
Figure 7.8: Effect of array aperture on beamwidth

There is a desire to minimise the number of elements in an array, as more elements mean more array controller channels and increases manufacturing complexity, increasing expense of the device. Increasing the element spacing in an array would minimise the element count. However, it introduces undesirable grating lobes, a form of aliasing caused by the periodic spacing of the array elements occurs, when the element pitch is greater than $\lambda/2$. Figure 7.9 shows the effect of greating lobe introduced in the array field profile as a result of having larger element spacing instead to $\lambda/2$ spacing.
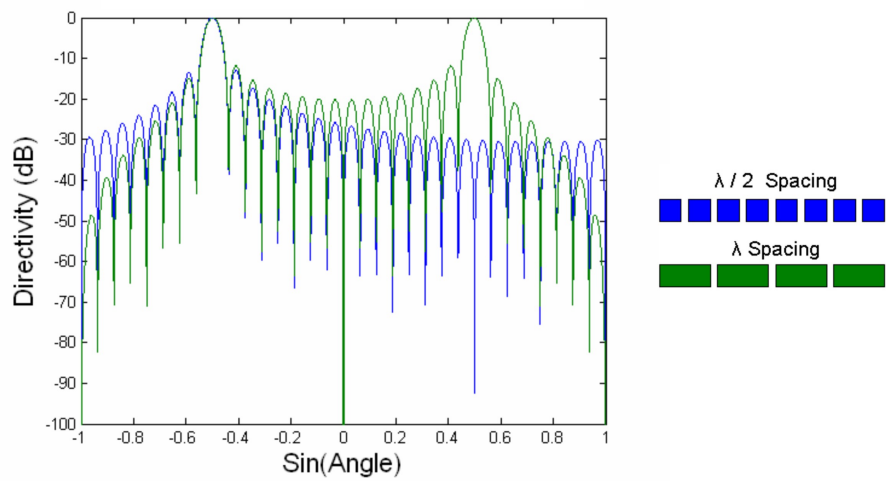
Figure 7.9: An example to illustrate grating lobes in array directivity profile

An array optimisation program in MATLAB to use was established. The genetic algorithm optimisation algorithm was used to find the optimum design for a given number of elements i.e. achieve desired beamwidth and minimise sidelobe level to an acceptable level. In each design optimisation simulation, a user specifies the high level design criteria, such as, target beamwidth, maximum steering angle, and maximum aperture. Simulations were then performed using a resolution of 10 transducer points per wavelength, and an angular resolution in the field of 0.1 degrees. Firstly, the design tool was used to optimise a 16-element array which was required to achieve a steering range of ± 30 degrees. The target beamwidth at this angle was 5.1 degrees, which is equivalent to that of a 24-element array with $\lambda/2$ spacing steered at -30 degrees. The maximum allowed aperture was 14 λ. The result was an aperiodic array with a maximum sidelobe height of -11.24 dB that achieves the target beamwidth. Furthermore, the total active width of the array is 8λ, which is the same as a conventional 16-element array. The directivity of the optimised array is shown in Figure 7.10, compared with a 16 element periodic array with a 12λ aperture. The evenly spaced array has a grating lobe at -4.36 dB, meaning the optimised array has achieved a 6.88 dB improvement in the worst-case sidelobe level.

The optimiser was also used to investigate the relationship between the number of elements and the maximum sidelobe level. The target beamwidth was 3.4 degrees, the steering range was ± 20 degrees, and the maximum allowable aperture was 18λ. The results are shown in Figure 7.11 along with a 32 element $\lambda/2$ spaced array for comparison. All arrays achieved the target beamwidth expect the 20 element design, which achieved a beamwidth of 3.5 degrees. The optimised results indicate a linear relationship between the number of elements and the minimum achievable maximum sidelobe height. The results also highlight the flexibility this method affords. The sidelobe level of a 32-element array can be reduced by 5 dB through

178

optimisation. Alternatively, the sidelobe level can be maintained whilst reducing the number of elements to 20, which would significantly reduce the burden on the array manufacture.
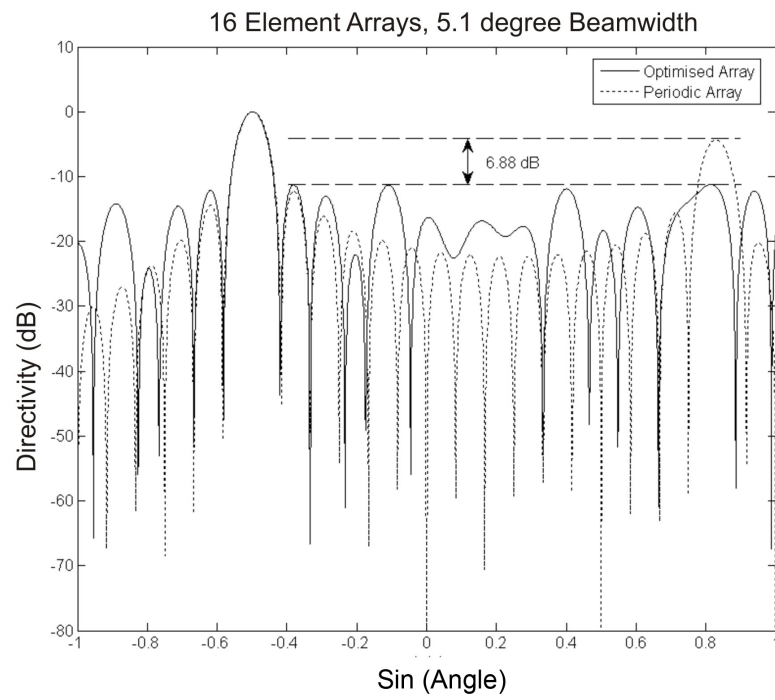
Figure 7.10: Comparison of optimised and conventional array beam profile.
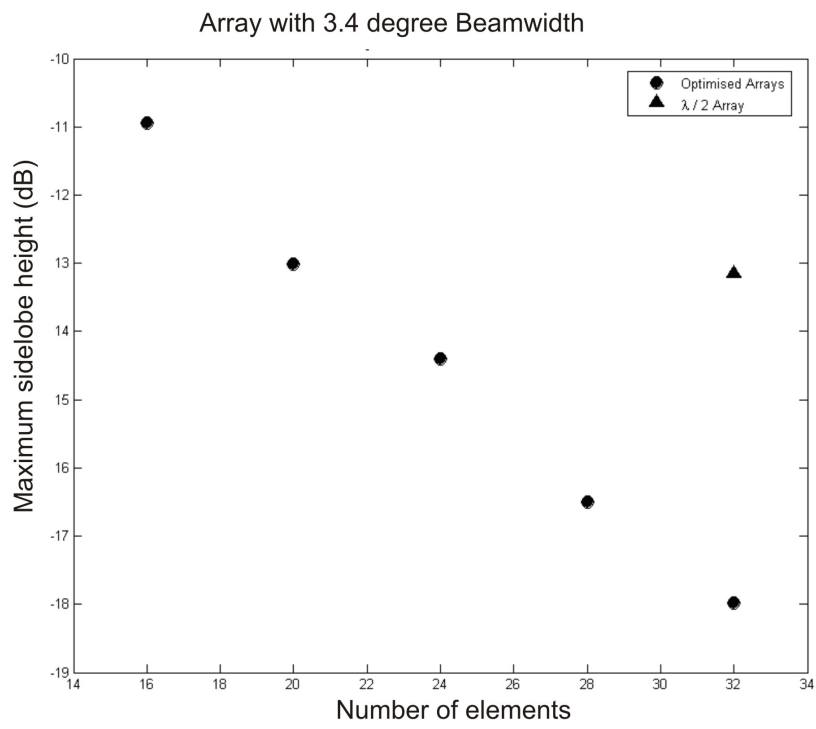
Figure 7.11: Relationship between maximum sidelobe levels and number of elements

7.4 Summary

Three design examples have been provided to exemplify optimisation of transducer design with the proposed tool. The first two examples relate to the implementation of an multiple passive matching scheme to thickness mode devices, and the final being a one dimensional sparse array design optimisation. The simulation results indicate clearly that a knowledge based approach is clearly a fast, efficient and cost effective way to design complex transducer systems, provided comprehensive coded expert knowledge, suitable simulator and complex application specific cost functions are available. The next chapter presents a critical appraisal of the work carried out within the scope of this thesis and some recommendations for future work.

Chapter 8

Conclusions and suggestions for future work

This chapter presents a detailed critical appraisal of the work undertaken and summarises the successes and failures, progress and opportunites/prospects. A section on suggestions for further work, to be undertaken by someone following on from the thesis is also included.

8.1   Concluding Remarks

A new approach for design and optimisation of ultrasonic transducers and arrays has been presented in this thesis. In developing this strategy, the aim is to overcome some of the main difficulties in designing complex ultrasonic systems. The key contribution of this thesis is the development of the design software bringing together an expert knowledge, optimisation programs, mathematical transducer models and external commercial circuit simulation programs in an efficient way. The work can be divided into the following key areas:

- A suite of analytical models were developed to simulate a variety of thickness mode transducer structures.

- A rule based expert system to capture expert knowledge and guide the design and optimisation process was implemented. The expert system also forms an intelligent front-end for the software program by permitting interactive and flexible user dialogue. An incremental approach to perform knowledge acquisition is suggested to build expert knowledge base, due to time constraints.

- A genetic algorithm based optimisation or search procedure was used for design optimisation of complex transducer systems.

- A comprehensive materials database was collected to aid transducer design and optimisation process.

- Ways to integrate the transducer models with electronic simulation environments such as PSPICE and LTSpice were investigated, and an automated system to export equivalent transducer models into a format suitable for SPICE environment is implemented in the proposed software.

- A graphical user interface (GUI) in MATLAB to unite various key aspects of the project, and demonstrate the feasibility of such an integrated approach was also presented.

Work to date indicates that such an integrated approach provides a fast, efficient and cost effective way to design complex transducer systems, provided that appropriately coded expert knowledge, the device simulation environment and application specific cost functions are available. The following section presents some of the recommendations for future work that will help in extending the proposed philosophy.

8.2   Suggestions for further work

For illustration purposes, mainly simple thickness mode devices and one dimensional arrays are considered within the scope of this work. For the software design program to be of significant use, it needs to be able to include many more types of devices. Due to the modular nature of the software architecture, the software can be easily extended to include different types of transducer, such as electrostatic devices, and multi-element arrays, subject to the availability of appropriate simulators. Also, it is essential these new analytical models be verified against Finite Element Modelling tools and experiments, prior to adding to the existing collection of models. The remainder of this chapter highlights some of the further work opportunities arising from this work.

8.2.1 Tapered transmission line technique based graded matching layers for thickness mode piezoelectric transducers

Conventionally, in order to match thickness mode piezoelectric transducer impedance to that of a load medium, multiple quarter wavelength (QWL) matching layers are often used at the front face of the device. During the course of this work such multiple matching layers have been succesfully manufactured for both conventional and complex inversion layer transducers, which resulted in an improved sensitivity and operation bandwidth characteristics of these devices. However, the change in impedance level in this case is obtained in a number of (often 3 or 4) discrete steps, which provides impedance matching with limited bandwidth characteristics.

This work could be extended to develop a continuously varying characteristic matching impedance profile, and tapered transmission line filter theory (commonly used in microwave circuits [19]) would be ideal for creating such broadband matching layers for ultrasonic applications. The filter design GUI implemented in the transducer design tool developed within the course of the research, contains only preliminary filter types such as binomial transformation and Chebyshev techniques, and supports design of only limited number of layers (taking into account the current manufacturing capability). More complex filter design techniques such as graded filters [93]–[94] can be added to the existing collection, to make it more versatile. The theory to calculate the reflection and transmission coefficients of such tapered impedance profiles with exponential, triangular and Chebyshev taper could be studied along with the effect of filter design parameters such as 'tolerance' on device operational characterisitcs. Comparison analysis of various graded matching layer devices; along with conventional QWL matching layers would be very useful.

While the theory and benefit of using such graded matching profiles to solve the impedance mismatch problem is readily understood, the problem of making such thin

graded matching layers would be more challenging. Novel methods to both produce thin layers directly onto a transducer/array substrate and the use new composite materials/structure for matching layers should be investigated, to manufacture thin matching layer structures.

8.2.2 Quantifying mismatch error in matching layer characterisation experimental setup

It was shown in Chapter 3, that it is possible to develop a procedure to test the matching layer integrity before attaching it to a transducer, by processing the through test data obtained from a characterisation tank experimental set. Some further work is required to extend this approach, especially, in processing the captured experimental data:

1. Develop advanced signal processing techniques that could extract features from the experimental data and the part simulated data, to relate to bond line thickness in the target.

2. Quantify or score the difference between the two data sets (experimental and simulated) and relate to quality of bonding.

For the preliminary investigation in Section 4.4.1, Fourier spectral analysis was employed to analyse the captured test data. The underlying assumption here is that the system is both linear and stationary. However, real world signals, such as this, are usually of finite duration, non-stationary and from systems that are frequently nonlinear (either intrinsically or through interactions with imperfect probes or numerical schemes). Consequently, it is necessary to further this study using advanced signal processing techniques such as empirical mode decomposition [97] or wavelet analysis [98].

8.2.3 An improved integrated approach to model transducer and associated electronics in multiphysics environment

Chapter 5 presented different strategy to interface commercial SPICE circuit simulation environment, such as PSPICE and LTSPICE, with the proposed transducer design tool. In the proposed transducer design tool, noise analysis is addressed by installing a facility to export a Thevenin equivalent circuit representation of the transducer, which enables to combine the result with the circuit noise analysis within a SPICE environment. A possible alternative approach to perform comprehensive noise analysis would be to include an electrical analogy of the transducer/array directly in the SPICE environment along with its associated electronics.

However, these two approaches are cumbersome to operate with design optmisation programs in the proposed design tool written using MATLAB. The main difficulty is the necessity to invoke external third party programs such as PSPICE/LTSPICE many times. This is necessary as the device transfer function, calculated using the linear system model, changes dramatically when a parameter within the model is varied during the optimisation process. Consequently, source and load impedances need to be adjusted simultaneously, in order to match the varying transducer electrical impedance. In its present form, the only way to achieve this in the proposed software is to implement a iterative batch processing program, which slows the optimisation process greatly.

An alternative and integrated approach would be to study in detail all the parameters within an ultrasonic system using a Multiphysics modelling environment. Figure 8.1 shows how COMSOL [96], a commercial multiphysics package with an inbuilt SPICE circuit simulation engine, can be used to model a complete transduction system. Mechanical modelling of a wide variety of transducers, including electrostatic devices, could be built (manually or import CAD drawings) easily in the COMSOL
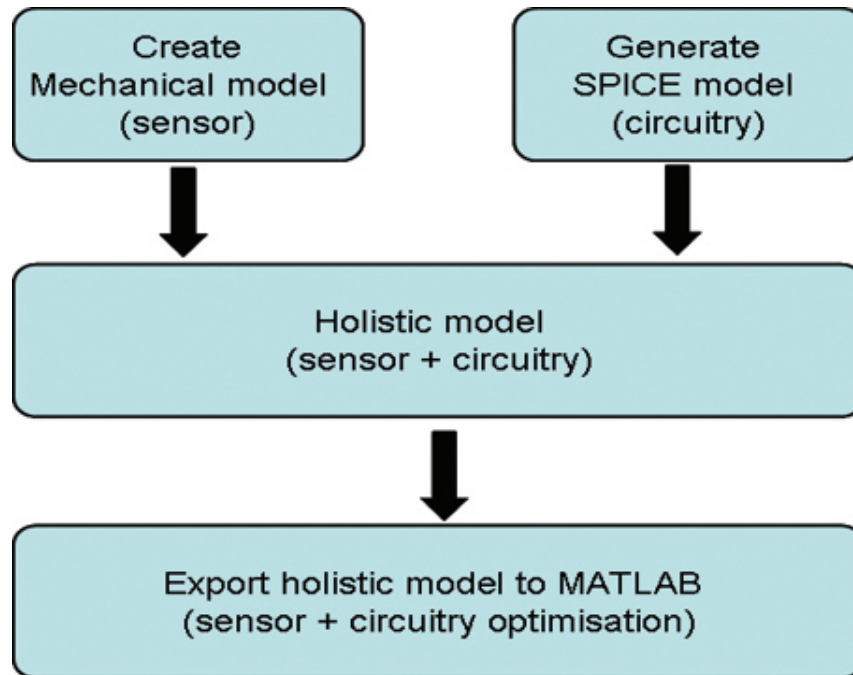
Figure 8.1: Using COMSOL multiphysics to model transdcuer and electronics

Multiphysics (CM) environment. CM has its own inbuilt SPICE engine, which allows to import SPICE models of the electronics circuitry that are generated using external commercial products such as PSPICE/LTPICE softwares. The imported SPICE circuits are included in CM as set of ODEs, global expressions, and global variables to produce an output equivalent of the actual system. This is a significant advantage as it allows to export and post-process the CM simulation problem, into simulation environments such as MATLAB, taking advantage of its powerful toolboxes for various design optimisation tasks.

8.2.4 Modelling to include manufacturing tolerances

Understanding the effect of manufacturing tolerance is vital while designing any sensor, as it has a direct influence on its quality and cost. While modelling transducer behaviour during the design phase, one of the simplest ways to address this problem would be to use computational algorithms such as "Monte carlo methods (MCC)"

[99]. MCC allows defining inputs to a model with a set of values. Deterministic computation using randomly selected inputs are then performed and the final aggregated results are presented to the user, instead of a single prediction. Use of statistical simulation methods such as MCC, utilising sequences of random numbers to perform the simulation, have been used widely in many applications to quantify uncertainity in a system. However, while studying systems with a large number of coupled degrees of freedom, such as a transducer/array design, MCC is not ideal. More sophisticated and faster realistic models for the transducer should be developed to address this issue. One possible solution to this problem would be to use an interval arithmetic approach [100]-[101]. This allows to code uncertainity into the analytical model itself as all influencing factors are considered as an interval, which can fluctuate within bounds.

8.2.5 Further code developments for the proposed design tool

MATLAB software is used to develop the prototype transducer design software presented in this thesis, and text or excel file formats are used to store data, including design specification, material properties and results. Although MATLAB is useful to demonstrate a prototype software system, having a complete product developed in MATLAB is not an ideal solution. Especially, the GUI in MATLAB is not very versatile, to handle large complex applications, such as the proposed transducer design software. An ideal solution is to code programs in MATLAB to verify working, and then develop all the modules using a low level language optimised for computational speed and code distribution. Dynamic link library files written within C programing language would be ideal for this task, as this would allow use of an advanced development environment such as C and C++ to be used to build a versatile GUI for the transducer design software.

189

8.2.5.1 Using optimisation paradigms

A Genetic algorithm (GA) approach based optimisation technique was used in the prototype software. GA is more robust when compared to most other optimisation techniques such as simulated annealing, and gradient methods. However, many new algorithms are available, such as differential evolution optimisation, direct search, and particle swarm optimisation. Performance of such new global optimisation techniques could be added to the software, to compare the suitability for transducer design optimisation problem. While they offer potential design improvement, there is no guarentee to arrive at the global optimum.

8.2.5.2 Improving material database and adding content based design input

Knowledge Engineering, the methodology for developing the expert system in a timely manner, is crucial. An open ended, iterative approach is proposed in acquisition and building of knowledge into the transducer design software system, due to time constraints. Having a prototype expert system developed and proven, now a dedicated knowledge acquisition activity needs to be carried out to build a working knowledge base.

Also, there is a need for storing all the design specifications, model parameters and results in a database to facilitate content based redsign of devices. Consequently, there is a need for an unified database interface to the software.

Bibliography

[1] John H. Holland,"Adaptation in natural and artificial systems : an introductory analysis with applications to biology, control, and artificial intelligence", MIT Press, 1992.

[2] L. Davis, "Handbook of Genetic Algorithms", Van Nostrand Reinhold, 1975.

[3] M. Gen and R. Cheng, "Genetic Algorithms and Engineering Design", John Wiley & Sons, 1997.

[4] David E. Goldberg, "Genetic Algorithms in Search, Optimization and Machine Learning", Addison-Wesley, 1989.

[5] K. F. Man, K. S. Tang, S. Kwong and W. A. Halang,"Genetic Algorithms for Control and Signal Processing", Springer, 1975.

[6] P. Bouchilloux and K. Uchino, "Application of Genetic Optimization Method to Design of Ultrasonic Motors", *Proceedings of SPIE*, Vol. 4693, 2002.

[7] W.P.Mason, "Electromechanical Transducers and wave filters", *Van Nostrand Inc.*, 1948.

[8] R.W.Martin and R.A.Sigelmann, "Force and electrical Thevenin equivalent circuits and simulations for thickness mode piezoelectric transducers", *J. Acoust. Soc. Am*, vol. 58, no. 2, pp. 475-489, October 1974.

[9] R. Krimholtz, D. A. Leedom and G. L. Matthaei, "New Equivalent Circuit for Elementary Piezoelectric Transducers", *Electron Letters*, Vol. 6, pp. 398-399, 1970.

[10] M.Redwood, Transient performance of piezoelectric transducer, *J. Acoust. Soc. Am*, vol. 33, no. 4, pp. 527-536, April 1961.

[11] G. K. Lewis, "A matrix technique for analyzing the performance of multi-layered front matched and backed piezoelectric ceramic transducers", *J. Acoust. Soc. Am*, pp. 395-416, 1980.

[12] C. S. Desilets, J. D. Fraser and G. S. Kino, "The deisgn of effecient broadband piezoelectric transducers", *IEEE Transactions on sonics and ultrasonics*, vol SU-25, no. 3, May 1978.

[13] H. Chang, S. Lee, J. Kim and J. Jeong,"Design of tapered transmission lines with arbitrary reflection characterisitics", *Jpn. J. Appl. Phys*, vol 41, pp.2289-2294, April 2002.

[14] G. Hayward, C. J. MacLeod and T. S. Durrani, "A systems model of the thickness mode piezoelectric transducer", *J. Acoust. Soc. Am*, vol. 76, no. 2, pp. 369-382, 2004.

[15] G. Hayward and J. A. Hossack, "Unidimensional modeling of 1-3 composite transducers", *J. Acoust. Soc. Am*, vol. 88, no. 2, pp. 599-608, August 1990.

[16] J. A. Hossack and G. Hayward, "Finite-Element Analysis of 1-3 Composite Transducers", *IEEE Trans. on Ultrasonics, Ferroelectrics and Frequency Control*, vol. 38, no. 6, pp. 618-629, 1991.

[17] G.S.Kino, "Acoustic waves", *Prentice-Hall,Inc*, 1987.

[18] Kinsler, Frey, Coppens and Sanders, "Fundamentals of acoustics", *John Wiley and Sons*, 1982.

[19] R. E. Collins, "Foundations of Microwave Engineering", McGraw-Hill, 1966.

[20] A. Trog, A. R. Mackintosh, D. Hayward, A. J. C. Kuehne and R. A. Pethrick, "Kinetic of Photopolymerisation of Polyfunctional Epoxy Based Resins Using Photo-Differential Scanning Calorimetry", (submitted to Polymer International).

[21] A. Trog, R. L. O'Leary, G. Hayward and R. A. Pethrick, "Acoustic properties of Epoxy resin blends and filled resins for acoustic matching layer applications", (submitted to Ultrasonics)

[22] A. Trog, " A new range of ultrasonic transducers", *PhD Thesis*, University of Strathclyde, 2007

[23] R. L. O'Leary, "An investigation into the passive materials utilized in the construction of piezoelectric composite transducers", *PhD thesis*, University of Strathclyde, Glasgow, 2003.

[24] M. G. Grewe, T. R. Gururaja, T. R. Shrout and R. E. Newnham,"Acoustic Properties of Particle/Polymer Composites for Ultrasonic Transducer Backing Applications", *IEEE Trans. on Ultrasonics, Ferroelectrics and Frequency Control*, Vol. 37, No. 6, pp. 506-514, 1990.

[25] H. Wang, T. A. Ritter, W. Cao, and K. K. Shung, "High Frequency Properties of Passive Materials for Ultrasonic Transducers", *IEEE Trans. on Ultrasonics, Ferroelectrics and Frequency Control*, Vol. 48, No. 1, pp. 78-84, 2001.

[26] K-Bar Hand Applicator, R K Print and Coat Ltd, Lillington, Royston Herts., SG8 0QZ.

[27] K. Nakamura, K. Fukazawa, K. Yamada and S. Saito, "Broadband Ultrasonic Transducers Using a LiNbO3 Plate with a Ferroelectric Inversion Layer", *IEEE Trans. on Ultrasonics, Ferroelectrics and Frequency Control*, vol. 50, no. 11, pp. 1558-1562, November 2003.

[28] S. Miyazawa, "Ferroelectric domain inversion in Ti-diffused LiNbO3 optical waveguide", *J. Appl. Phys*, 50(7), pp. 4599-4603, July 1979.

[29] Y. Estanbouli, G. Hayward and J. C. Barbenel, "A Study of Inversion Layer Transducers", *Proceedings of IEEE Ultrasonics Symposium*, pp. 1322-1325, October 2003

[30] Y. Estanbouli, G. Hayward, S. N. Ramadas and J. C. Barbenel, "A Block Diagram Model of the Thickness Mode Piezoelectric Transducer Containing Dual, Oppositely Polarised Piezoelectric Zones", *IEEE Trans. on Ultrasonics, Ferroelectrics and Frequency Control*, vol. 53, no. 5, pp. 1028-1036, 2006.

[31] S. N. Ramadas, G. Hayward, R. L. O'Leary, T. McCunnie, A. J. Mulholland, A. Troge, R. A. Pethrick, D. Robertson and V. Murray, "A Three-Port Acoustic Lattice Model for Piezoelectric Transducers Containing Opposing Zones of Polarization", *Proceedings of 2006 IEEE Ultrasonics Symposium*, (in press).

[32] T. R. Gururaja, A. Shurland and J. Chen, "Medical ultrasonic transducers with switchable frequency bands centered about f0 and 2f0", *Proc. 1997 IEEE Ultrasonics Symposium*, pp 1659-1662.

[33] P.E.Bloomfield, "Multilayer Transducer Transfer Matrix Formalism", *IEEE Trans. on Ultrasonics, Ferroelectrics and Frequency Control*, vol. 49, no. 9, pp. 1300-1311, September 2002.

[34] J. A. Hossac, P. Mauchamp and L. Ratsimandresy, "A high bandwidth transducer optimised for harmonic imaging", *Proc. 2000 IEEE Ultrasonics Symposium*.

[35] Xerox History Page, *http://www.parc.xerox.com/about/history/default.html*

[36] Apple History Web Page, *http://www.apple-history.com/*

[37] The MathWorks, *http://www.mathworks.com/*

[38] Phased Array Tutorial - Olympus NDT, *http://www.olympusndt.com/en/ndt-tutorials/phased-array/*.

[39] D. A. Hutchins and G. Hayward, "Radiated Fields of Ultrasonic Transducers", in Physical Acoustics, Vol XIX (Academic Press, NY, R.N. Thurston and A.D. Pierce, eds., 1990), pp. 2-80.

[40] G. Cardone, G. Cincotti, "Optimization of Wide-Band Linear Arrays", *IEEE Trans. on Ultrasonics, Ferroelectrics and Frequency Control*, vol. 48, no. 4, pp. 943-952, july 2001.

[41] S. Holm, B. Elgetun, and G. Dahl, "Properties ofthe beampattern of weight- and layout-optimized sparse arrays", *IEEE Trans. on Ultrasonics, Ferroelectrics and Frequency Control*, vol. 44, no. 5, pp. 983-991, 1997.

[42] A. Trucco, "Thinning and Weighting of Large Planar Arrays by Simulated Annealing", *EEE Trans. on Ultrasonics, Ferroelectrics and Frequency Control*, vol. 46, no. 2, pp. 347-355, march 1999.

[43] C. Huang, V. Z. Marmarelis, Q. Zhou and K. K. Shung, "An Analytical Model of Multilayer Ultrasonic Transducers with an Inversion Layer", *IEEE Trans. on Ultrasonics, Ferroelectrics and Frequency Control*, vol. 52, no. 3, pp. 469-479, March 2005.

[44] CUE Materials Database, http://www.cue.ac.uk/download.html

[45] Ferroperm, "www.ferroperm-piezo.com"

[46] J. Giarratano and G. Riley, "Expert Systems, Principle and Programming", *PWS Publishing company*, 1998.

[47] P. Jackson, "Introduction to Expert Systems", Addison Wesley, 1998

[48] N. Ford, "Expert systems and artificial intelligence", *Library Association Publishing Limited*, 1991.

[49] http://www.cee.hw.ac.uk/ alison/ai3notes/all.html

[50] http://www.aaai.org/AITopics/html/expert.html

[51] http://www.expertise2go.com/webesie/tutorials/ESIntro/

[52] W. Whiten, "Expert1: An opensource deduction engine code for expert system", *http://www.mathworks.com/matlabcentral/fileexchange/*

[53] CLIPS expert system shell, *http://www.ghg.net/clips/CLIPS.html*.

[54] S. J. Russell and P. Norvig; "Artificial Intelligence: A Modern Approach", *Pearson Education Ltd: London*, 2003.

[55] M. Ben-Ari; "Mathematical Logic for Computer Science", *Springer: London*, 2004.

[56] S. K. Langer; "An introduction to symbolic logic", Dover, 1953.

[57] L .P. Edward, "Applied symbolic logic", A Wiley - Interscience publication, 1980.

[58] G. J. Massey; "Understanding symbolic logic", Harper and row, 1970.

[59] E. W. Weisstein; "Method of Steepest Descent." From MathWorld–A Wolfram Web Resource, http://mathworld.wolfram.com/MethodofSteepestDescent.html

[60] S. Kirkpatrick, C. D. Gellat and M. P. Vecchi; "Optimisation by simulated annealing", Science, Vol. 220, no. 4598, pp. 671-680, 1983.

[61] W. A. Smith and B. A. Auld, "Modeling 1-3 composite piezoelectrics: thickness-mode oscillations", *IEEE Trans. on Ultrasonics, Ferroelectrics and Frequency Control*, Vol. 38, No. 1, pp. 40 - 47, Jan. 1991.

[62] M. N. Jackson, "Simulation and control of thickness mode piezoelectric transducers", *PhD Thesis*, University of Strathclyde, 1984

[63] G. Hayward and M. N. Jackson, "A Lattice Model of the Thickness - Mode Piezoelectric Transducer", *IEEE Trans. on Ultrasonics, Ferroelectrics and Frequency Control*, vol. 33, no. 1, pp. 41-50, 1986.

[64] T. L. Szabo, "Diagnostic Ultrasound Imaging", *Elsevier Academic Press*, 2004.

[65] H. N. Norton, "Handbook of transducers", *Prentice Hall*, 1989.

[66] G. Hayward, "Time and frequency domain modelling of the piezoelectric transducer", PhD Thesis, University of Strathclyde, 1982.

[67] J. A. Hossack, "Modelling techniques for 1-3 composite transducers", PhD Thesis, University of Strathclyde, 1990.

[68] W. Galbraith, "Development of a PVDF membrane hydrophone for use in air coupled transducer calibration", PhD Thesis, University of Strathclyde, 1997.

[69] P. J. Fish, "Electronic noise and low noise design", *Macmillan Series*, 1993.

[70] C. D. Motchenbacher and J. A. Connelly; "Low noise electronic system design", *Wiley-Interscience Publication*, 1993.

[71] J. O. Attia; "Pspice and Matlab for electronics: An integrated approach", *CRC Press*, 2002

[72] J. A. Connelly and P. Choi; "Macromodelling with Spice", Prentice Hall, 1992.

[73] P. W. Tuinenga, "SPICE: A guide to circuit simulation and analysis using Pspice", *Prentice Hall*, 1995.

[74] M. H. Rashid, "SPICE for circuits and electronics using Pspice", *Prentice Hall*, 1990.

[75] M. E. Herniter, "Schematic capture with Cadence Pspice", *Prentice Hall*, 2001.

[76] G. Hayward, R. A. Banks and L. B. Russell, "A Model for Low Noise Design of Ultrasonic Transducers", *Proc. IEEE Ultrasonics Symposium*, pp. 971-974, 1995.

[77] R. A. Banks, "An investigation of intrinsic noise in piezoelectric receiver systems", *MPhil Thesis*, University of Strathclyde, 1996.

[78] Cadence Design Systems Inc., "http://www.cadence.com"

[79] LTSpice Circuit Simulation Software, "http://www.linear.com/"

[80] Cybernet Systems Co. Ltd., "http://www.cybernet.co.jp/slps/"

[81] S. A. Morris and C. G. Hutchens, "Implementation of Mason's model on circuit analysis programs", *IEEE Trans. on Ultrasonics, Ferroelectrics and Frequency Control*, Vol. 33, No. 3, pp. 295-298, 1986.

[82] W. Leach, "Controlled source analogous circuits and SPICE models for piezoelectric transducers", *IEEE Trans. on Ultrasonics, Ferroelectrics and Frequency Control*, Vol. 41, No. 1, pp. 60-66, Jan 1994.

[83] T. Masters; "Practical neural network recipes in C++", *Morgan Kaufmann*, 1993.

[84] J. F. Baldwin; "Fuzzy logic", Wiley, 1996.

[85] H. J. Zimmermann, "Fuzzy set theory–and its applications", *Boston : Kluwer Academic Publishers*, 1991.

[86] S. G. Paris; "Propositional logical thinking and comprehension of language connectives : a developmental analysis", Mouton, 1975.

[87] J. Krajicek; "Bounded arithmetic, propositional logic and complexity theory", Cambridge University Press, 1995.

[88] R.N.Thorston and A. D. Pierce, "Ultrasonic measurement methods (Physical acoustics series)", Academic Press, 1990.

[89] Harry. L. Van Trees, "Optimum Array Processing", Wiley Interscience Publications, 2002.

[90] E. Campbell, "The Design and Modelling of Capacitive Micromachined Ultrasonic Arrays for Imaging Applications", First Year Project Report, Centre for Ultrasonic Engineering, University of Strathclyde, 2003.

[91] S. N. Ramadas, A. Tweedie, R. L. O' Leary, G. Hayward, "A Rule Based Design Optimisation Tool for Ultrasonic Transducers and Arrays", Proceedings of International congress on ultrasonics (ICU2007), 2007, (in press).

[92] Douglas Elliot, "Handbook of Digital Signal Processing", Elsevier Academic Press, 1987

[93] X. Wang and H. Masumoto, "'Design and experimental approach of optical reflection filters with graded refractive index profiles", J. Vac. Sci. Technol. A, Jan/Feb 1999, pp 206 - 211.

[94] H. Chang, S. Lee, J. Kim and J. Jeong,"Design of tappered transmission lines with arbitrary reflection characteristics", Jpn. J. Appl. Phys, Vol. 41, 2002, pp 2289 - 2294

[95] K. E. Parsopoulos, M. N. Vrahatis, "Recent approaches to global optimisation problems through particle swamp optimisation", Neural Computing, Vol. 1, 2002, pp 235 - 306.

[96] COMSOL Inc., "http://www.comsol.com/"

[97] N. E. Huang1, Z. Shen, S. R. Long, M. C. Wu, H. H. Shih, Q. Zheng, N. Yen, C. C. Tung and H. H. Liu, "The empirical mode decomposition and the Hilbert spectrum for nonlinear and non-stationary time series analysis", Proceedings of Royal Society of Lond. A, 454, 903-995.

[98] R. Polikar, Fundamental concepts and an overview of the wavelet theory, "http://users.rowan.edu/ polikar/WAVELETS/WTpart1.html"

[99] K. Binder, D. W. Heermann,"Monte Carlo simulation in statistical physics", Springer-Verlag, 1988.

[100] J. C. Burkill, "Functions of intervals.", Proceedings of the London Mathematical Society, 22:375-446, 1924.

[101] T. Sunaga, "Theory of an Interval Algebra and its Application to Numerical Analysis.", Gaukutsu Bunken Fukeyu-kai, Tokyo, 1958.

Appendix A

Knowledge Aquisition Questionnaire

Centre for Ultrasonic Engineering

Transducer Design Questionnaire

(1) Rank the design issues on a scale of 1-10 in order of importance

	1	2	3	4	5	6	7	8	9	10
Sensitivity (Insertion Loss)	☐	☐	☐	☐	☐	☐	☐	☐	☐	☐
Bandwidth	☐	☐	☐	☐	☐	☐	☐	☐	☐	☐
Electrical Matching (Power Matching)	☐	☐	☐	☐	☐	☐	☐	☐	☐	☐
Efficiency	☐	☐	☐	☐	☐	☐	☐	☐	☐	☐
Beam Pattern	☐	☐	☐	☐	☐	☐	☐	☐	☐	☐
Transmit Voltage Response (TVR)	☐	☐	☐	☐	☐	☐	☐	☐	☐	☐
Receive Sensitivity	☐	☐	☐	☐	☐	☐	☐	☐	☐	☐
Signal to Noise Ratio (SNR)	☐	☐	☐	☐	☐	☐	☐	☐	☐	☐
Impedance or Admittance	☐	☐	☐	☐	☐	☐	☐	☐	☐	☐
Other Issues – Please Specify and Rank	☐	☐	☐	☐	☐	☐	☐	☐	☐	☐
	☐	☐	☐	☐	☐	☐	☐	☐	☐	☐
	☐	☐	☐	☐	☐	☐	☐	☐	☐	☐
	☐	☐	☐	☐	☐	☐	☐	☐	☐	☐
	☐	☐	☐	☐	☐	☐	☐	☐	☐	☐
	☐	☐	☐	☐	☐	☐	☐	☐	☐	☐
	☐	☐	☐	☐	☐	☐	☐	☐	☐	☐
	☐	☐	☐	☐	☐	☐	☐	☐	☐	☐
	☐	☐	☐	☐	☐	☐	☐	☐	☐	☐

(2) For the list shown previously, please classify each parameter under an application heading

SONAR	
Biomedicine	
NDE	
Industrial Process Control	
Others	

(2) List of some general questions about transducer design process

The questions below are prepared specific to SONAR application and will be generalized later to suit other application areas. Please feel free to use the blank sheets at the end of this report, should you require more space.

a) What are the main factors that control the SONAR transducer design process?

b) Criteria for material selection in transducer, including passive backing & matching layers?

c) How does pressure rating affect material selection in SONAR transducer design?

d) Given a transducer specification, how to decide the transducer type (composite, single crystal...etc)?

e) If composites, how to decide type (2-2, 1-3...etc) and volume fraction?

f) What are the main issues in deciding the electrical interface of the transducer?

g) Please refer to useful sonar equations and rules that is used during the transducer design process; this will help us to build an application specific cost function for the software to perform design optimisation?

h) Typical design specification that the company receive from customer?

i) Typical design specification that is handed to a design engineer in a company?

Appendix B

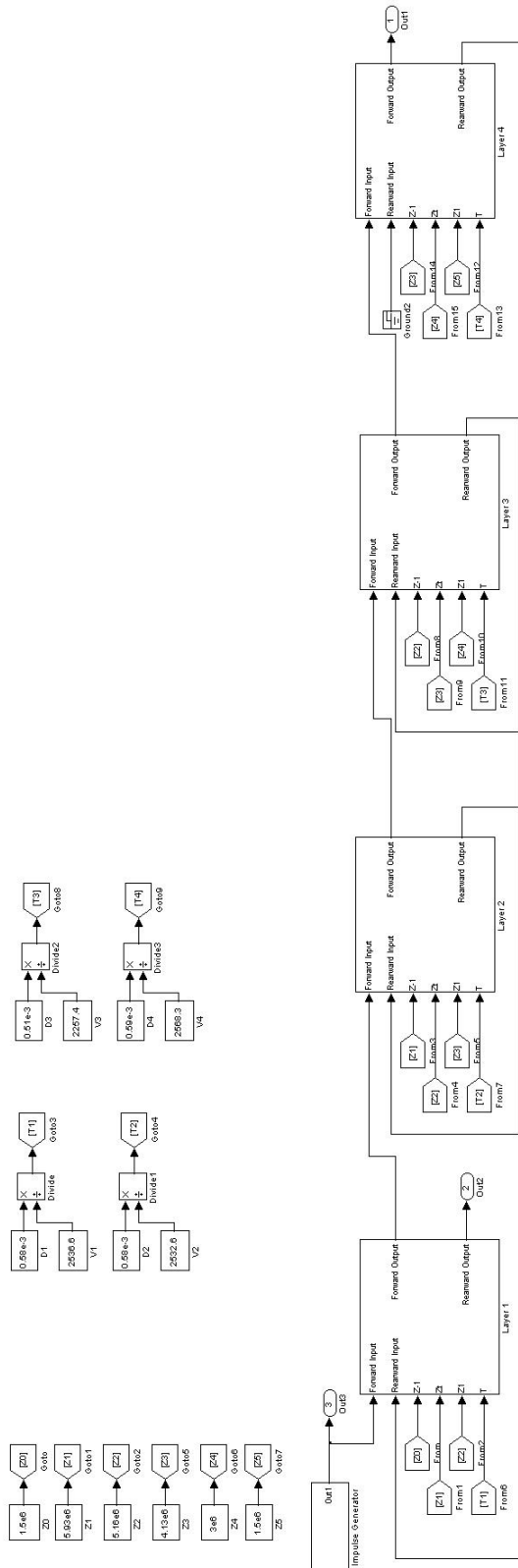# SIMULINK model to simulate impulse response of a four passive matching layer system

Figure B.1: SIMULINK model to calculate matching layer impulse response

Appendix C

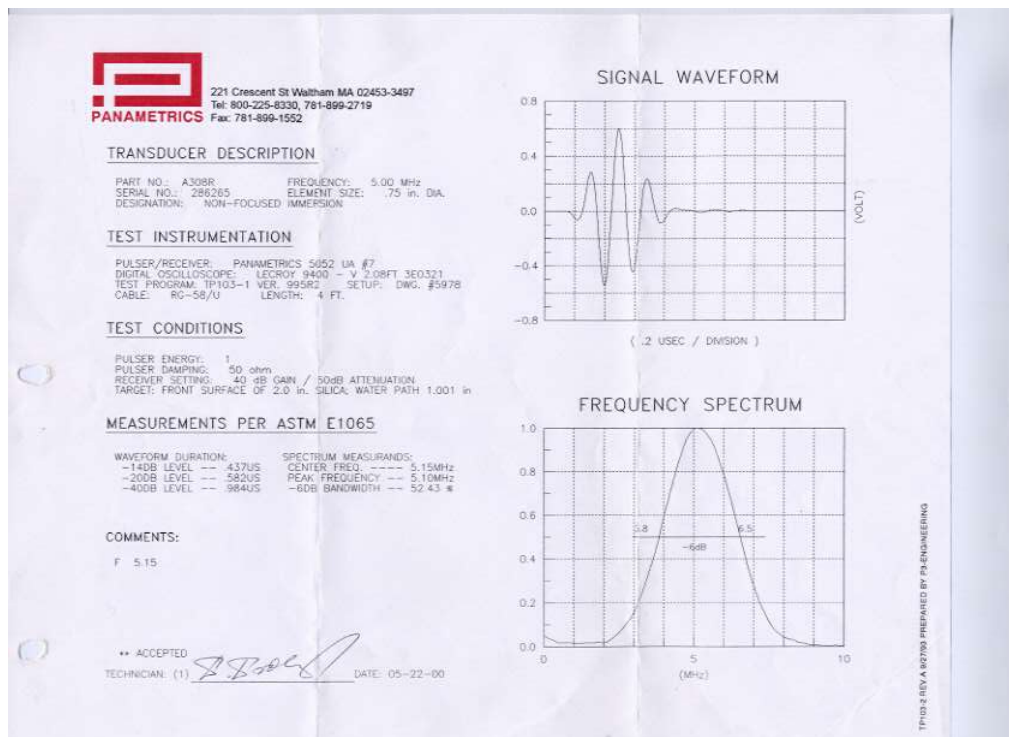# 5MHz immersion probe specfication data sheet

Figure C.1: Specification of the commercial 5MHz immersion probe used in the matching layer study

Appendix D

Monte Carlo Analysis SPICE code

XU1 0 N005 N001 N006 N003 AD811

C2 N006 0 100n

R1 N003 N005 mc(660,tol)

R3 N005 IN mc(4.7k,tol)

V1 IN 0 AC 1

Vcc N001 0 15

C3 N001 0 mc(100n,tol)

C1 N001 0 mc(100n,tol)

R2 N004 N003 mc(150,tol)

R4 OUT N004 mc(4.7k,tol)

C4 N006 0 mc(100n,tol)

ss 0 N006 15

C5 OUT N002 mc(1p,tol)

XU2 0 N004 N001 N006 OUT N002 AD797A

.noise V(OUT) V1 dec 100 1 10Meg

.lib mylib/AD797A.lib

.lib mylib/ad811.lib

step param X 0 20 1 ; a dummy paramter to cycle Monte Carlo runs

.param tol=.05 ; +/- 5% component tolerance

* Monte Carlo Simulation in LTspice

* mc(val, tol) is a function that uses a random number generator

* to return a value between val-tol*val and val+tol*val

* Other functions of interest:/n /nflat(x): a function that uses a random number generator

* to return a value between -x and x;

* gauss(x): a function that uses a random number generator

* to return a value with a Gaussian distribution and sigma x.

.end

Appendix E

Perl script to convert MATLAB variables to SPICE

Perl script to convert MATLAB variables to SPICE

```perl
#!/usr/bin/env perl
#
#
#   Program: csv2net.pl
#   Description: Reformat CSV file containing FREQ,VAL1,VAL2 into a
SPICE netlist.
#

open(FH, $ARGV[0]) or &syntax("File Error");
($ARGV[1] =~ /DB|MAG|R_I/i) or &syntax("Format Error");
($ARGV[2] =~ /^E/i) or &syntax("Source Error");
($#ARGV eq 4) or &syntax("Parameter number error: $#ARGV");

($out = $ARGV[0]) =~ s/.csv$//;
$out.= ".net";
if(-f $out) {
     print "$out exists. Press Ctrl-C if you do NOT want to overwrite.
";
     $bla=<STDIN>;
}
open(OUT, ">$out");

print OUT $ARGV[2]." ".$ARGV[3]." ".$ARGV[4]." FREQ {V(1,0)}=
".$ARGV[1]."\n";
while(<FH>) {
     s/[\r\n]*//g;
     my($freq,$mag,$ang)=split(/\,/, $_);
     print OUT "+($freq, $mag, ".($ang?$ang:"0").")\n";
}

sub syntax($) {
     my $x = shift(@_);
     print "[$x]\n Syntax: $0 Input.csv <Format>  <EName> <Node1>
<Node2>\n";
     print "Output format must be one of DB, MAG, R_I, and must equal
input format!\n";
     print "<EName> must begin with an E!\n\n";
     exit 254;
}
```